

**Mechanisms of loss of high energy protons from the bunched
beams in storage rings**

Dissertation

zur

Erlangung des akademischen Grades

Doktor-Ingenieur (Dr.-Ing.)

der Fakultät für Ingenieurwissenschaften
der Universität Rostock

vorgelegt von

Ilya Agapov
aus Moskau

Rostock
2004

Gutachter der Dissertation: Prof. Dr. Ursula van Rienen, Universität Rostock
Dr. Ferdinand Willeke, DESY Hamburg

Preface

This work is dedicated to the analysis of some aspects of long term beam behavior in a storage ring when random perturbations are present. The techniques discussed are fairly general and can be applied to a wide range of problems, but here we will concentrate on the study of synchrotron motion of bunched beams of heavy particles like protons or ions. This study is motivated by the coasting beam production observed in the HERA proton accelerator, which was found to contribute to background in the detectors. We study the evolution of the longitudinal bunch distribution under the influence of two kinds of random perturbations: jump processes and continuous fluctuations. The first type models scattering processes like the Touschek effect and gas scattering, the second models processes such as RF field noise. The question we want to answer is which role do these phenomena play in the longitudinal tail buildup and coasting beam production. The physics of these processes is well understood at present, but, to our knowledge, the effect of nonlinearity on the tail evolution and on the escape rate has not been fully studied. Appropriate methods are discussed and simulations are compared to experimental observations at HERA.

Contents

1	Introduction	1
2	Probability background	5
2.1	Random variables and Markov chains	5
2.2	Continuous random processes	6
3	Discrete random perturbations and the Touschek effect	13
3.1	The Touschek effect and the intra-beam scattering	13
3.2	Kinetic equations	17
3.3	Averaging of the kinetic equations	18
3.4	The diffusion (Fokker-Planck) approximation	20
3.5	Reduction to a linear integro-differential equation	22
3.6	Solution of the Boltzmann equation (method of self-consistent chains).	22
3.6.1	Self-consistent chains	22
3.6.2	Computation procedure	25
3.6.3	Results for HERA	26
3.7	Summary	27
4	RF noise	33
4.1	Randomly perturbed synchrotron oscillations	33
4.2	The averaged Fokker-Planck equation	38
4.3	Effect of coherence	49
4.4	Solving the Fokker-Planck equation	51
4.4.1	A two-point boundary value problem	52
4.4.2	The system of equations with coupled boundary values arising from averaging of stochastic systems with complicated phase space where branching can occur	54
4.4.3	On the mechanism of separatrix crossing	55
4.4.4	On numerical solution of the coupled system	56
4.5	Impact on synchrotron motion	59
4.5.1	Bunch diffusion - rough estimates	59
4.5.2	Escape from the stable bucket	60
4.5.3	On effects of noise spectral density	60
4.5.4	Estimates for HERA	60
4.6	Summary	62

5	Some experimental observations	71
5.1	Backgrounds and longitudinal bunch evolution	71
5.2	Bunch manipulations with amplitude and phase modulations	73
5.3	Summary	75
6	Epilogue	77
6.1	Noise in nonlinear systems	77
6.2	Conclusion	78
A	Particle motion in a storage ring	79
A.1	Equations of motion	79
A.2	Action-angle variables	82
B	Sketch of the proof of proposition 1	87
C	On the precision of the 'self-consistent chains' method	91

Some frequently used symbols

e	electron charge
$\varepsilon_{x,y}$	vertical and horizontal emittances
$\beta_{x,y}$	vertical and horizontal beta functions
β, γ	relativistic factors
$\sigma_{x,y,s}$	r.m.s. beam sizes
ω_{RF}	frequency of an RF cavity resonator
$k(\tau)$	the autocorrelation function
ξ_t	a equivalent to $\xi(t)$
$S_\xi(\omega)$	spectral power density of a random process ξ
$p_{i,j}$	transition probabilities of a Markov process
W_t	the Wiener process
dW_t	white noise
$H(q,p)$	the Hamiltonian

Chapter 1

Introduction

For modern collider physics experiments, like those installed at HERA, beams of high intensity are needed, so that the luminosity is high and there are sufficient physics event statistics. HERA is a lepton-proton storage ring at DESY Hamburg (see figure 1.1) , with the following experiments operating

- The experiments designed to understand proton structure by colliding a proton beam with an electron beam - H1 and ZEUS
- Nucleon spin study by colliding polarized electrons/positrons with a fixed target of polarized nucleons - HERMES
- Study of heavy C- and B- quark production and CP violation using a fixed wire target - the HERA-B experiment.

Table 1.1: Main parameters of the HERA ep collider

circumference	6355m
proton energy	920 GeV
lepton energy	27.5 GeV
number of colliding bunches	174
design p bunch intensity N_p	$1 \cdot 10^{11}$
design e current I_e	60mA
longitudinal e spin polarization	50-70%
design peak luminosity	$7 \cdot 10^{31} cm^{-2} s^{-1}$
proton envelope function at IP's $\beta_{z,x}$	18cm, 2.45m
typical proton emittances $\varepsilon_{z,x}$	5nm
lepton beam size at the IP's $\sigma_{z,x}$	30, 114 μ m
proton bunch length	200mm
lepton bunch length	8mm

For ep bunched beam collisions the luminosity (per collision, Gaussian beams) is

$$\mathcal{L} = R \frac{I_e N_p}{2\pi e \sqrt{(\sigma_{x,p}^2 + \sigma_{x,e}^2)(\sigma_{z,p}^2 + \sigma_{z,e}^2)}} \quad (1.1)$$

with R being a reduction factor, which depends on the β function at the interaction point, the p bunch length¹ and the crossing angle [11]. With nonzero crossing angle and bunched beams high luminosity is achieved by creating bunches with small transverse and longitudinal dimensions and bringing them properly into collision. Beams of high intensity can produce high background rates at the detectors, so that the detector components suffer from radiation damage and data cannot be taken.

High background has been a substantial problem for experiments at HERA. Its potential sources are

- Direct synchrotron radiation
- Backscattered synchrotron radiation
- Bremsstrahlung and lepton background produced by leptons scattered at the residual gas
- Proton halo
- Protons scattered at the desorbed gas in the interaction regions

All these can, in principle, be controlled by beam steering, by putting masks and absorbers in the critical regions and by providing a good vacuum pressure around the detectors.

In addition a connection between the background and the coasting beam observed at HERA-p has been suggested. The coasting beam is formed by particles that leave the stable RF buckets and drift in the longitudinal direction along the ring. The synchrotron radiation losses are no more compensated for such particles and they constantly lose energy. Due to dispersion they will have a large transverse offset and form the beam halo. The chromatic tune shift due to large momentum offset also introduces a threat of hitting a resonance. The beam-beam force has a much stronger impact on off momentum particles (see [16],[59] for details). Due to all these effects the coasting beam particles are likely to escape the aperture limitations rather quickly. Although the collimation system is designed to shield the detectors [54], some portion still ends up there and causes the background. In a superconducting accelerator it is difficult to collimate off-momentum particles effectively. The collimator system has two stages: the first collimator deflects a proton which then hits the secondary collimator. In the regions with high dispersion, the arcs, superconducting magnets are installed and putting a collimator next to one of such magnets may cause a quench. Thus particles with momentum offset cannot be collimated efficiently. The collimation of the coasting beam may also be performed by introducing transverse kicker magnets acting in the gap between the bunches. The timing of the kicks must be very precise. Therefore, it is technically difficult to produce a short clean rectangular kick since a signal with extremely large bandwidth would be required.

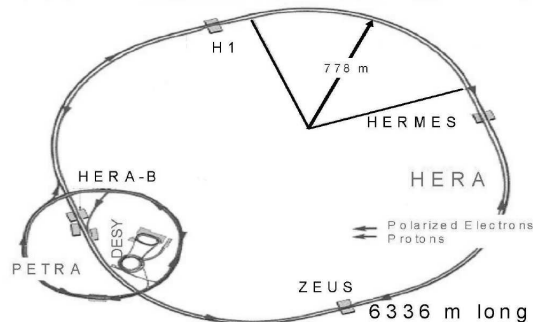
The observation of the coasting beam was first performed at the HERA-B experiment by analyzing the scattering rates of the proton beam on the target wires [19]. Its existence has also been confirmed by measuring the difference between the bunched and unbunched currents and the results indicated that the accumulated coasting current (up to $2mA$ of approximately $100mA$ initial total current) must be considerably reduced to allow the experiments to operate. The coasting beam has also been observed at other machines such as RHIC [64].

High coasting beam current can have other consequences. For example, the particles filling the abort gap between the bunch trains can prevent a safe beam dump. This, for example, is expected to play a role at the LHC.

There could be several possible causes for the production of the coasting beam. These could possibly be longitudinal particle instabilities arising from the coupling of synchrotron and betatron motion, wake fields, noise in the radio frequency cavities, parasitic collisions and many others. Since the transverse proton beam lifetime observed in HERA was satisfactory, we focused on the study of the escape mechanisms from the stable RF buckets due to the following phenomena: the Touschek effect (or intra-beam scattering) and

¹this is the hourglass effect

Figure 1.1: Schematic overview of the HERA ep collider and its accelerator chain



noise in the radio-frequency system. Both processes may be considered to be small random perturbations. Deterministic perturbations to synchrotron motion are also taken into consideration to some extent.

The particles in a bunch experience collisions with each other, at high energies collisions may lead to large momentum jumps, which in turn lead to bunch size growth and to particle loss from the bunch. This process was recognized by B. Touschek in 1963 on a small e^-e^+ storage ring [7] and later studied by many, including A. Piwinski [49], [50]. It is to be taken into account for high intensity beams like those stored in HERA-p.

Noise is always present in the accelerating RF fields. Since the effect of radiation damping on the proton motion in stable RF buckets is weak, even extremely small perturbations can accumulate and influence the motion on large time scales. This influence was observed in all proton machines (such as SPS and HERA). The question arises: to what extent is the RF noise responsible for producing the coasting beam?

Deterministic perturbations also have a considerable influence on bunch motion. The major source of such perturbations is assumed to come from the longitudinal impedances arising in beam-cavity interactions. As far as nonlinear single-particle motion is concerned, a deterministic perturbation will cause a complicated effect, the so-called nonlinear resonance [12]. Under certain conditions it can lead to particle loss. The interplay of resonance with noise can also lead to interesting phenomena [25].

Synchrotron oscillations in HERA are of quite complicated nature due to the presence of two radio frequency (RF) systems. The first, at 52 MHz, dominates at the injection energy of 40 GeV while the second, at 208 MHz, provides shorter bunches and dominates when the beam is stored at 920 GeV. It is technically complicated to turn off the 52MHz system and the accelerating field seen by the beam is produced by a two frequency system. For details see Appendix A. A simple analytical treatment of both the Touschek effect and the RF noise problem is generally not possible for the bunch tail particles which exhibit nonlinear behavior (which is the case for all RF systems as soon as the bunch size is of the order of an RF wavelength). This motivated us to study the motion of nonlinear oscillating systems under the influence of various kinds of random perturbations more carefully, taking into account issues specific to synchrotron motion in a storage ring and to develop appropriate simulation techniques.

The presentation has the following structure:

In Chapter 2 basic facts from probability theory are briefly given for reference.

In Chapter 3 modeling of the Touschek effect (or intra-beam scattering) is discussed [49], [9], [18]. Here the nonlinearity of the RF potential introduces a difficulty. The statistical characteristics of a scattering event are expressed by some averaged functions over the particle trajectory taking into account the bunch density. For the tail particles it is too complicated to calculate calculating these averages analytically and computer simulations must be made. The tail distribution is important when the escape problem is concerned. The approaches to such simulations are discussed and calculations based on the “chain method” are presented.

In Chapter 4 issues concerning simulation of the influence of RF noise on the synchrotron oscillations are presented. So far only the sinusoidal RF voltage has been treated carefully [17], [32]. Obtaining and solving a Fokker-Planck equation for the case of a double RF system is perhaps principally the same, but technically more elaborate. The following technical issues are discussed: averaging the Fokker-Planck equation, calculating the diffusion coefficient by perturbation techniques, solving the equation when the phase space includes separatrices and estimating the effect of noise coherence.

In Chapter 5 the corresponding observations in HERA-p are presented.

Apparently, the major source of the coasting beam at HERA has been the influence of the RF noise whereas the contribution of intra-beam scattering appears to be weak.

In the last chapter we indicate other possible applications of the methods discussed as well as bottlenecks arising in generalizing these techniques and some open questions.

Chapter 2

Probability background

This section shortly summarizes some well-known facts and definitions from the theory of probability and random processes following [21], [55] and can be skipped by those who are familiar with them. A good introduction to the theory of random processes and stochastic differential equations may be found in [21], [24], [55], more rigorous treatment is given in [22], [28], [29], [35].

2.1 Random variables and Markov chains

A random variable $\xi(\omega)$ is a measurable function defined on the space of elementary events Ω . The moments of a random variable are

$$\begin{aligned}\langle \xi \rangle &= \int_{\Omega} \xi(\omega) d\omega \\ \langle \xi^2 \rangle &= \int_{\Omega} (\xi(\omega) - \langle \xi \rangle)^2 d\omega \\ &\dots\end{aligned}\tag{2.1}$$

The characteristic function is

$$\theta(u) = \langle e^{iu\xi} \rangle\tag{2.2}$$

The simplest special case of a random process is the Markov chain. A Markov chain is given by the space of states (say, a subset of integers) and the transition probabilities from state i to state j in time t $p_{ij}(t)$ satisfying

1. $0 \leq p_{ij}(t) \leq 1$
2. $\sum_j p_{ij}(t) = 1$
3. $\forall t > 0, s > 0 \quad p_{ij}(t+s) = \sum_k p_{ik}(t)p_{kj}(s)$ (Chapman-Kolmogorov equation)
4. $\lim_{t \downarrow 0} p_{ij}(t) = \delta_{ij}$ (stochastic continuity)

Then it can be shown that the following limits exist

$$a_{ij} = \lim_{t \downarrow 0} \frac{p_{ij}(t) - \delta_{ij}}{t}$$

If $i \neq j$ then the limits are always bounded. Therefore, the transition probabilities satisfy the Kolmogorov system of equations

$$\frac{d}{dt}p_{ij}(t) = \sum_k a_{ik}p_{kj}(t) \quad (2.3)$$

The system possesses a unique solution if $a_{ij} \geq 0$, $a_{ii} \leq 0$, $\sum a_{ij} = 0$, $\sup |a_{ii}| < \infty$ and the solution satisfies the initial conditions $p_{ik}(0) = \delta_{ik}$. These conditions are usually met in practice. The matrix a_{ij} is the discrete analogy of an infinitesimal generator of a Markov process and will be called the infinitesimal generator matrix.

2.2 Continuous random processes

A random process $\xi(t)$ is in general a random function taking values in an appropriate functional space. Assume that this is the space of all real-valued functions. A random process is defined if for every set t_1, \dots, t_n the joint probability density of random variables $\xi(t_i)$ $f_n(x_1, \dots, x_n, t_1, \dots, t_n)$ is given, such that

$$\int f_n(x_1, \dots, x_n, t_1, \dots, t_n) dx_1 \dots dx_n = 1 \quad (2.4)$$

$$f_n(x_1, \dots, x_n, t_1, \dots, t_n) \geq 0 \quad (2.5)$$

$$\begin{aligned} f_n(x_1, \dots, x_i \dots x_j \dots, x_n, t_1 \dots t_i \dots t_j \dots t_n) = \\ f_n(x_1, \dots, x_j \dots x_i \dots, x_n, t_1 \dots t_j \dots t_i \dots t_n) \end{aligned}$$

and

$$f_n(x_1, \dots, x_n, t_1, \dots, t_n) = \int f_{n+k}(x_1, \dots, x_{n+k}, t_1, \dots, t_{n+k}) dx_{n+1} \dots dx_{n+k}$$

One also writes ξ_t instead of $\xi(t)$ and $f(x_{t_1} \dots x_{t_n})$ or $f(x_1 \dots x_n)$ instead of $f_n(x_1, \dots, x_n, t_1, \dots, t_n)$ for brevity. One defines the moment function of order n

$$m_n(t_1, \dots, t_n) = \langle \xi_{t_1} \dots \xi_{t_n} \rangle \quad (2.6)$$

with the usual notation $\xi_t = \xi(t)$. The random process is defined by an infinite series of moment functions of all orders. The physical significance of a moment function decreases with the increase of its order. In applications it is often sufficient to know only the first two functions $m_1(t)$ and $m_2(t_1, t_2)$. Equivalent to the knowledge of moment functions is the knowledge of the correlation functions

$$k_n(t_1 \dots t_n) = \mathbf{K}[\xi(t_1) \dots \xi(t_n)]$$

where \mathbf{K} is the correlation between random variables. The second order correlation is

$$\mathbf{K}[\xi_1 \xi_2] = \langle \xi_1 \xi_2 \rangle - \langle \xi_1 \rangle \langle \xi_2 \rangle \quad (2.7)$$

and the correlation of arbitrary order is given by

$$\mathbf{K}[\xi_1 \dots \xi_n] = \frac{1}{i^n} \frac{\partial \ln \Theta(u_1 \dots u_n)}{\partial u_1 \dots \partial u_n} \Big|_{u_1 = \dots = u_n = 0} \quad (2.8)$$

where

$$\Theta(u_1 \dots u_n) = \langle \exp\{i(u_1 \xi_1 + \dots u_n \xi_n)\} \rangle \quad (2.9)$$

The process is called stationary (strict sense) if the moment functions (or correlation functions) are invariant under time shifts

$$\begin{aligned} k_1(t) &= m_1(t) = m \\ k_2(t_1, t_2) &= k_2(0, t_2 - t_1) = k(t_2 - t_1) \end{aligned}$$

...

and so on. For a stationary process one defines the correlation time and the process intensity

$$\begin{aligned} \tau_{cor} &= \frac{1}{k(0)} \int_0^\infty |k(\tau)| d\tau \\ K &= \int_{-\infty}^\infty k(\tau) d\tau \end{aligned}$$

The spectral density of a stationary process is

$$S_\xi(\omega) = 2 \int_{-\infty}^\infty e^{i\omega\tau} \langle \xi_t \xi_{t+\tau} \rangle d\tau = 4 \int_0^\infty \cos(\omega\tau) \langle \xi_t \xi_{t+\tau} \rangle d\tau \quad (2.10)$$

for a process with zero mean

$$S_\xi(\omega) = 2 \int_{-\infty}^\infty e^{i\omega\tau} k(\tau) d\tau \quad (2.11)$$

for a process with mean $\langle \xi \rangle = m$

$$S_\xi(\omega) = 2 \int_{-\infty}^\infty e^{i\omega\tau} k(\tau) d\tau + 4\pi m^2 \delta(\omega) \quad (2.12)$$

for instance (see also figure 2.1)

$$\begin{aligned} k(\tau) = e^{-\gamma\tau} &\Rightarrow S(\omega) = \frac{4\gamma}{\omega^2 + \gamma^2} \\ k(\tau) = e^{-\gamma\tau} \cos(\omega_0\tau) &\Rightarrow S(\omega) = 4\gamma \frac{4\omega^2 + \omega_0^2 + \gamma^2}{(\omega^2 - \omega_0^2 - \gamma^2)^2 + 4\gamma^2\omega^2} \end{aligned} \quad (2.13)$$

For a multidimensional process $(\xi_1(t), \xi_2(t))$ one defines cross-correlation function

$$k_{12}(t_1, t_2) = \mathbf{K}[\xi_1(t_1), \xi_2(t_2)]$$

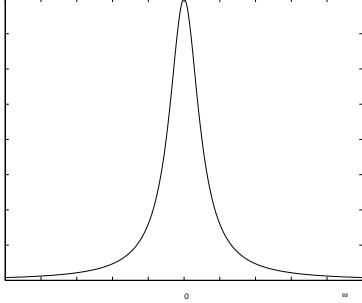
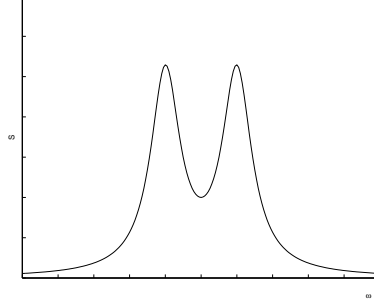
and cross-spectral density

$$S_{\xi_1 \xi_2}(\omega) = 2 \int_{-\infty}^\infty e^{i\omega\tau} \langle \xi_{1,t} \xi_{2,t+\tau} \rangle d\tau$$

The spectral density has to be distinguished from the random spectrum of the random process which is a Fourier transform of a particular process sample

$$Y(\omega) = \frac{1}{\sqrt{2\pi}} \int_{-\infty}^\infty e^{-i\omega t} \xi(t) dt \quad (2.14)$$

Figure 2.1: Sample spectral densities

(a) Spectral density of a process with $k(\tau) = e^{-\gamma|\tau|}$ (b) Spectral density of a process with $k(\tau) = e^{-\gamma|\tau|} \cos(\omega_0\tau)$

This integral diverges for stationary random processes and has to be understood as a generalized function. The spectral density has a meaning of the averaged noise spectrum. It has a meaning only if we consider the noise signal passed through a narrow band filter with $\Delta\omega \sim |\omega - \omega_0|$ instead of a random spectrum.

$$Y(\omega_0, t_0) = \int_{-\infty}^{\infty} G(t_0 - t)\xi(t)dt \quad (2.15)$$

$$G(t_0 - t) = \frac{1}{\sqrt{2\pi}} \int_{-\infty}^{\infty} e^{i\omega(t_0-t)} g(\omega)d\omega \quad (2.16)$$

with $g(\omega)$ a pulse located in the interval $\Delta\omega$ around ω_0 and

$$\int_{-\infty}^{\infty} g(\omega)d\omega = 1 \quad (2.17)$$

the connection between so filtered signal and the spectral density is

$$\langle (Y(\omega_0, t_0)^2) \rangle = \frac{1}{2} S_{\xi}(\omega_0) \int_{-\infty}^{\infty} |g(\omega)|^2 d\omega \quad (2.18)$$

As has been mentioned, the first two moments already contain the most significant information about the random process and the higher order moments are mostly responsible for extremal behavior. It is then natural to consider a class of stationary processes with only the first two moments different from zero. Such processes are called second order processes. Their statistical properties are completely defined by the correlation function $K(\tau)$.

A random process with $K(\tau) = K\delta(\tau)$ is called a delta-correlated process or *white noise* with intensity K . It is an abstraction of a physical process with negligible correlation time. It has the advantage that it is a Markov process (see below), but it has infinite intensity and cannot be physically realized. A random process with arbitrary $K(\tau)$ is also known as *colored noise*.

An important role is played by *Markov random processes*, or processes without after-effect. Let $\xi(t)$ be a random process and $t_n > t_{n-1} > \dots > t_1$. The conditional probability density of $\xi(t_n)$ with $\xi(t_{n-1}) \dots \xi(t_1)$ given is

$$f(x_n|x_{n-1} \dots x_1) = \frac{f_n(x_n \dots x_1)}{f_{n-1}(x_1 \dots x_{n-1})} \quad (2.19)$$

A process $\xi(t)$ is called Markov if the conditional probability 2.19 depends on x_{n-1} only, i.e.

$$f(x_n|x_{n-1} \dots x_1) = p_{t_{n-1}t_n}(x_{n-1}, x_n) \quad (2.20)$$

$p_{t_1t_2}(\xi_1\xi_2)$ is called the transition probability of the Markov process. Markov processes possess a remarkable property, namely their transition probabilities satisfy the *Chapman-Kolmogorov equation*

$$p_{t_1t_3}(x_1, x_3) = \int p_{t_1t_2}(x_1, x_2)p_{t_2t_3}(x_2, x_3)dx_2 \quad (2.21)$$

The Chapman-Kolmogorov equation is what makes Markov processes so significant. It provides a method of calculating the evolution of probability density in time. For more general classes of random processes such methods do not normally exist and they are usually treated by approximating them with an appropriate Markov process. The probability density $f(x, t)$ describes the probability of finding the random process at point x at time t and, in case of a Markov process, satisfies

$$f(x_1, t_1) = \int p_{t_1t_2}(x_1, x_2)f(x_2, t_2)dx_2 \quad (2.22)$$

which is proved by integrating 2.21 over x_3 . Equation 2.21 can be reduced to a differential equation.

$$\dot{f}(x) = \sum_{n=1}^{\infty} \frac{(-1)^n}{n!} \left(\frac{\partial}{\partial x} \right)^n [K_n(x)f(x)] \quad (2.23)$$

with

$$K_n(x) = \lim_{\tau \rightarrow 0} \frac{\langle (x_\tau - x)^n \rangle}{\tau} \quad (2.24)$$

If the series 2.23 can be truncated at the second term then we get the *Fokker-Planck* or diffusion equation

$$\dot{f}(x) = -\frac{\partial}{\partial x} [K_1(x)f(x)] + \frac{1}{2} \frac{\partial^2}{\partial x^2} [K_2(x)f(x)] \quad (2.25)$$

This possibility is equivalent to some regularity requirements on the paths of the random process (like continuity). The coefficients K_1 and K_2 are called the drift and diffusion coefficients. The *Wiener process* or standard Brownian motion is a diffusion process with zero drift and unit diffusion. The trajectory of a Wiener process is continuous but nowhere differentiable. One can however define the derivative of the Wiener process dW_t which happens to be the white noise process.

In applications physical processes are often given as solutions of differential equations. To be able to treat equations with r.h.s. containing random processes one has to take advantage of the theory of Brownian motion and stochastic differential equations. Suppose we are given a differential equation with a random r.h.s.

$$\dot{x} = g(x, t, \omega)$$

then it is natural to say that a solution is a function $x(t)$ satisfying the integral equation

$$x(t) = x(0) + \int_0^t g(x(s), s, \omega)ds \quad (2.26)$$

But for many important random processes (like white noise) this integral does not exist in the usual Riemann-Stieltjes sense. The theory of stochastic differential equations based on special integral definition was developed by Ito and Stratanovich. One starts with equations with white noise in the r.h.s

$$\frac{dx}{dt} = a(x) + b(x) \frac{dW_t}{dt}$$

which is usually written in the form

$$dx = a(x)dt + b(x)dW_t$$

The solution is formally a random process satisfying the corresponding integral equation

$$x(t) = x(0) + \int_0^t a(x(s))ds + \int_0^t b(x(s))dW_s \quad (2.27)$$

The first integral is understood in the usual sense. The second one is an integral over a path of a Wiener process and doesn't exist in the usual sense [29]. It is defined in the following way. Let Π be a partition of interval $[a, b]$ with points $\{s_i\}_{i=1, n}$ and $\|\Pi\| = \max_{i=1, n-1} |s_{i+1} - s_i|$, then

$$\int_a^b g(W)dW_s = \lim_{\|\Pi\| \rightarrow 0} \sum [\varepsilon g(W_{s_i}) + (1 - \varepsilon)g(W_{s_{i+1}})] [W_{s_{i+1}} - W_{s_i}] \quad (2.28)$$

Such an integral is called the *stochastic integral*. It exists for a large class of integrands and 2.27 admits a solution. For different ε this defines different random processes. When $\varepsilon = 0$ the integral is in Ito's sense, when $\varepsilon = 0.5$ Stratanovich's. When a stochastic differential equation has a solution in Stratanovich's sense, then there exists a corresponding equation having the same solution in Ito's sense. Ito's integral could be defined for a somewhat broader class of integrands. Some important properties of stochastic integrals are shown below

Ito

$$\begin{aligned} \langle \int_0^\tau dW_s \rangle &= 0 \\ \langle (\int_0^\tau dW_s)^2 \rangle &= \tau \\ \langle \int_0^\tau W_s dW_s \rangle &= \frac{1}{2} W_\tau^2 + \tau \\ f(W_t) &= f(W_0) + \int_0^t f'(W_s)ds + \frac{1}{2} \int_0^t f''(W_s)dW_s \end{aligned}$$

Stratanovich

$$\begin{aligned} \langle \int_0^\tau dW_s \rangle &= 0 \\ \langle (\int_0^\tau dW_s)^2 \rangle &= \tau \\ \langle \int_0^\tau W_s dW_s \rangle &= \frac{1}{2} W_\tau^2 \\ f(W_t) &= f(W_0) + \int_0^t f'(W_s)ds \end{aligned}$$

The last relation is known as the Ito's rule. The multidimensional system

$$dx = a(x)dt + b(x)dW_t \quad (2.29)$$

with $a(x), b(x) \in \mathbf{R}^{n \times n}$ $x \in \mathbf{R}^n$ and $W(t) \in \mathbf{R}^n$ being n independent Wiener processes is treated in complete analogy. Under a *stochastic differential equation* we will understand equations of type 2.29. Equations of general form are usually treated by reducing them to certain systems of (Ito or Stratanovich) stochastic equations [22] [28] [37].

One may pose various questions about solutions of the equations in question, such as first exit time from a domain etc. We are interested mainly in the evolution of the probability distribution supposing the initial distribution is given. Solutions of stochastic differential equations are Markov processes and thus must satisfy a Chapman-Kolmogorov equation 2.21. One calculates its coefficients by substituting 2.27 into 2.24 and exploiting the properties of stochastic integrals. For the Ito's integral one gets

$$\begin{aligned} K_1(x) &= \lim_{\tau \rightarrow 0} \frac{\langle x_\tau - x \rangle}{\tau} = \\ &= \lim_{\tau \rightarrow 0} \frac{1}{\tau} \left\langle \int_0^\tau a(x(s))ds + \int_0^\tau b(x(s))dW_s \right\rangle = a(x) \end{aligned}$$

$$K_2(x) = \lim_{\tau \rightarrow 0} \frac{\langle (x_\tau - x)^2 \rangle}{\tau} = \lim_{\tau \rightarrow 0} \frac{1}{\tau} \left\langle \left(\int_0^\tau a(x(s)) ds + \int_0^\tau b(x(s)) dW_s \right)^2 \right\rangle = b^2(x)$$

and the coefficients of order $n \geq 2$ vanish. With the definition of Stratanovich the coefficients are

$$K_1(x) = a(x) + b(x)b'(x) \quad (2.30)$$

$$K_2(x) = b^2(x) \quad (2.31)$$

and the higher order coefficients also vanish. Thus in both cases we arrive at the Fokker-Planck equation for the distribution function. Employing Ito's or Stratanovich's definition of the integral yields different Fokker-Planck equations. The convenience of Ito's variant is that the coefficients in the Fokker-Planck equation and in the stochastic equation coincide. But the Stratanovich's variant gives the right physical picture (a gradient in the diffusion coefficient will produce convection). Denoting

$$G(x) = K_1(x)f(x) - \frac{1}{2} \frac{\partial}{\partial x} [K_2(x)f(x)]$$

the Fokker-Planck equation takes the form

$$\dot{f}(x) + \frac{\partial G(x)}{\partial x} = 0 \quad (2.32)$$

which represents the conservation of probability. $G(x)$ is called the probability current or probability flux. For the Fokker-Planck equation to have a unique solution one normally needs to specify some additional conditions. They may include absorption or reflection conditions as well as sinks and sources of probability.

If a random process trajectory terminates (a particle is absorbed) at point a , then one requires that $f(a) = 0$. If at point a a reflection occurs, then no probability flux is present at this point and $G(a) = 0$. One could also specify an arbitrary law of behavior at the boundary. For instance, if at a boundary point a approached by a random process trajectory from the left a reflection occurs with probability α and absorption with probability $1 - \alpha$ then the boundary condition reads

$$\alpha G(a) = (1 - \alpha)f(a) \quad (2.33)$$

If one imposes complex additional conditions, then the existence and uniqueness of the solution of the Fokker-Planck equations are by no means guaranteed. However, if it describes a well-defined Markov process then its solution is expected at least to exist. Uniqueness, existence and stability of the solutions of the Fokker-Planck equations arising in this work are expected from their physical origin and are not studied.

Chapter 3

Discrete random perturbations and the Touschek effect

In this section we discuss random perturbations which have a jump character.¹ Such perturbations usually arise as a consequence of collision processes. These processes have kinetic nature and are described by certain kinetic equations. The latter normally have great complexity and do not allow an accurate analytical treatment. We discuss possible approximations and computational methods for these equations and propose to treat them with the method of "self-consistent chains" which is a slight modification of the usual notion of a Markov chain when the dependency of the transition probabilities on the distribution function is taken into account. It forms the basis of a quite simple computation procedure.

The methods developed are applied to the study of the Touschek effect and of the intra-beam scattering [49], [9], [18], [50]. Both processes are essentially of the same nature and represent the density change caused by Coulomb scattering of particles inside the bunch. We will call them both the Touschek effect. It has a considerable influence on the bunch dynamics for high intensity beams. An analytical treatment of such phenomena is complicated and is possible under a priori assumptions about the solution sought. Such assumption is the bunch distribution form which is assumed Gaussian. This approach gives reasonable estimates of emittance growth and instant loss rates, but does not necessarily give the right description of the density evolution and especially the distribution of the bunch tails. This is especially the case for nonlinear systems when the motion of tail particles strongly deviates from the average across the bunch. It seems misleading for the study of escape from the stable Rf bucket since such escape is most likely to happen for a tail particle. In interplay with noise the tail buildup due to the scattering processes can make a considerable effect on the coasting beam production which motivates the use of the method.

The discussed approach may be applied to other problems which are of the same nature: gas scattering, stochastic effects in beam-beam interactions and so on. At HERA they are not suspected to have a direct influence on the coasting beam accumulation.

3.1 The Touschek effect and the intra-beam scattering

Particles in a bunch are subject to Coulomb interactions. These interactions become weak at high energies. However, microscopic incoherent interactions, or collisions, still have a rather strong effect and cannot be neglected. Such collisions lead to random particle momentum change. A transition of momentum from the transverse to the longitudinal direction is enlarged by the relativistic factor γ and can be so large that both colliding particles leave the machine acceptance. This effect was recognized by B. Touschek on a

¹A random process with discontinuous paths is usually called a jump process

e^+e^- storage ring ADA [7] and is called the Touschek effect. The collisions resulting in small momentum changes do not lead to a particle loss but contribute to an increase in bunch dimensions. In combination with synchrotron radiation this may lead to a change in the stationary distribution, which can take place in electron storage rings. The theory of such processes was worked out basically by A.Piwinski [49] and is usually called the "intra-beam scattering" or the "multiple Touschek effect". We are also interested in collisions that neither contribute to bunch diffusion nor lead to a particle loss, but result in transitions of the particles to the bunch tail or to the coasting beam region. We will as well use the expression "single Touschek effect" for the particle loss, "intra-beam scattering" for effect of small collisions and "Touschek effect" for the general situation when all kinds of events are taken into account. Here we present basic theory following [49], [18].

In the center of mass system a collision is characterized by the impact parameter r . A collision of two particles with initial momenta p_1 and p_2 results in the rotation of their momenta by a polar angle ϕ and an azimuthal angle ψ . Under the assumption that the velocities are not relativistic in the center of mass system, in the laboratory system this results in

$$\delta p_{1,2} = \pm \frac{p}{2} \begin{pmatrix} \gamma\chi \cos\phi \sin\psi + \gamma\xi(\cos\psi - 1) \\ \frac{1}{\chi}(\zeta\rho \sin\phi - \theta\xi \cos\phi) \sin\psi + \theta(\cos\psi - 1) \\ \frac{1}{\xi}(-\theta\rho \sin\phi - \zeta\xi \cos\phi) \sin\psi + \zeta(\cos\psi - 1) \end{pmatrix} \quad (3.1)$$

$$\xi = \frac{p_1 - p_2}{\gamma p}, \quad \theta = \frac{p_{x,1} - p_{x,2}}{p}, \quad \zeta = \frac{p_{z,1} - p_{z,2}}{p}$$

$$\chi^2 = \theta^2 + \zeta^2, \quad \rho^2 = \xi^2 + \theta^2 + \zeta^2$$

The relativistic effects in the centre of bunch system have only a small effect for energy range of interest. For protons or ions the probability of scattering into a solid angle $d\Omega = \sin\psi d\phi d\psi$ is given by the Rutherford cross section

$$d\sigma = \left(\frac{r_0}{4\beta^2 \sin^2 \frac{\psi}{2}} \right)^2 \sin\psi d\Omega \quad (3.2)$$

with the minimum angle ψ_{min} determined by the maximum impact parameter r_{max}

$$\tan \frac{\psi_{min}}{2} = \frac{r_0}{2\beta r_{max}} \quad (3.3)$$

and $r_0 = \frac{e^2 Z^2}{4\pi\epsilon_0 m c^2}$, which is the classical proton radius for protons, β is the relative particle velocity. For electrons one should use the Møller cross section instead [51]. The collision does not lead directly to a change of the betatron coordinates x and z , but results in the change of the betatron angles and of the closed orbit as a consequence of the (longitudinal) momentum change

$$\delta r_{\beta 1,2} = \begin{pmatrix} 0 \\ \delta p_{x1,2}/p \\ 0 \\ \delta p_{z1,2}/p \end{pmatrix} - D \frac{\delta p}{p} \quad (3.4)$$

The synchrotron phase does not change noticeably after a collision as well. The effects of collisions on beam evolution can be different. For example, in electron storage rings with relatively low energy they can have a substantial influence on beam lifetime. To estimate the loss rate due to the single Touschek effect one needs to calculate the total cross section of events leading to particle loss. The loss occurs when the azimuthal angle exceeds a certain value ψ_m , so the total cross section of the Touschek loss takes the form

$$\sigma_{loss} = \left\langle \int_{\psi_m}^{\pi} d\sigma \right\rangle \quad (3.5)$$

The loss rate can be calculated assuming that the distribution function is known. One gets the dependency of the number of stored particles on time

$$N_B(t) = \frac{N_B(0)}{1 + \frac{t}{T_l}} \quad (3.6)$$

where T_l is the Touschek lifetime [11]. For high energy proton storage rings the direct losses are negligible. For example, for HERA a typical transverse momentum being completely transferred to the longitudinal direction leads to a momentum change $\Delta p \sim 10^{-5}$ and such particle won't leave the acceptance. Transitions to the coasting beam are possible but still quite rare. Here the Coulomb scattering mainly leads to small momentum changes. To estimate these changes one studies their averaged influence on the invariants of motion. These invariants are the transverse emittances $\varepsilon_{x,z}$ and the synchrotron invariant H . Analytical treatment of this problem is possible only under some restrictions. One assumes that the bunch shape is Gaussian in all directions

$$P(r_\beta, \delta p, s) = K e^{-(S_x + S_z + S_s)} \quad (3.7)$$

$$K = \int dr_\beta d\delta p d\phi e^{-(S_x + S_z + S_s)} \quad (3.8)$$

$$S_x = \frac{\varepsilon_x(x_\beta, x_\beta')}{2\varepsilon_x} = \frac{\beta_x}{2\varepsilon_x} x_\beta'^2 - \frac{\beta_x'}{2\varepsilon_x} x_\beta' x_\beta + \frac{1 + \beta_x'^2}{2\beta_x \varepsilon_x} x_\beta^2 \quad (3.9)$$

$$S_z = \frac{\varepsilon_z(z_\beta, z_\beta')}{2\varepsilon_z} = \frac{\beta_z}{2\varepsilon_z} z_\beta'^2 - \frac{\beta_z'}{2\varepsilon_z} z_\beta' z_\beta + \frac{1 + \beta_z'^2}{2\beta_z \varepsilon_z} z_\beta^2 \quad (3.10)$$

$$S_s = \frac{\Delta s^2}{2\sigma_s^2} + \frac{\delta p^2}{2\sigma_p^2} \quad (3.11)$$

The averaged emittances are

$$\varepsilon_{x,z} = \frac{\sigma_{x,z}^2}{\beta_{x,z}} \quad (3.12)$$

A momentum change Δp will produce the following changes in the invariants to the first order

$$\Delta\varepsilon_x = -\beta_x' \frac{\Delta p_x}{p} x_\beta + \frac{1 + \beta_x'^2}{\beta_x} \frac{p_x \Delta p_x}{p^2} \quad (3.13)$$

$$\Delta\varepsilon_z = -\beta_z' \frac{\Delta p_z}{p} z_\beta + \frac{1 + \beta_z'^2}{\beta_z} \frac{p_z \Delta p_z}{p^2} \quad (3.14)$$

$$\Delta H = 2\delta p \Delta p \quad (3.15)$$

Here only quadratic parts of the invariants are taken into account. If invariants of higher order are considered then the distribution is no more Gaussian and the calculations become more complicated. The number of scattering events per unit time is

$$M = 2\beta c P_0 \sigma / \gamma^2 \quad (3.16)$$

where β, γ are relativistic factors, P_0 spatial density in the laboratory system and σ the total cross section (the factor γ^2 comes from the transformations of cross-section and time to the laboratory frame). Taking in account the relations

$$x' = \frac{p_x}{p} \quad (3.17)$$

$$z' = \frac{p_z}{p} \quad (3.18)$$

using 3.1 and averaging over all angles and coordinates one can arrive at the averaged emittance change rates per unit time. One gets instantaneous rates [49]

$$\varepsilon_{x,z} = e^{\lambda_{x,z} \varepsilon_{x,z}^0 t} \quad (3.19)$$

$$\langle H \rangle = e^{\lambda_s \langle H \rangle^0 t} \quad (3.20)$$

where the rise times are defined as

$$\lambda_s = \left\langle A \frac{\sigma_h^2}{\sigma_p^2} f(a, b, q) \right\rangle \quad (3.21)$$

$$\lambda_x = \left\langle A \left[f\left(\frac{1}{a}, \frac{b}{a}, \frac{q}{a}\right) + \frac{D_x^2 \sigma_h^2}{\sigma_x^2} f(a, b, q) \right] \right\rangle \quad (3.22)$$

$$\lambda_z = \left\langle A \left[f\left(\frac{1}{b}, \frac{a}{b}, \frac{q}{b}\right) + \frac{D_z^2 \sigma_h^2}{\sigma_z^2} f(a, b, q) \right] \right\rangle \quad (3.23)$$

$$A = \frac{r_0^2 c N_p}{64 \pi^2 \beta^3 \gamma^4 \varepsilon_x \varepsilon_z \sigma_s \sigma_p} \quad (3.24)$$

$$\frac{1}{\sigma_h^2} = \frac{1}{\sigma_p^2} + \frac{D_x^2}{\sigma_x^2} + \frac{D_z^2}{\sigma_z^2} \quad (3.25)$$

$$a = \frac{\sigma_h \beta_x}{\gamma \sigma_x}, \quad b = \frac{\sigma_h \beta_z}{\gamma \sigma_z}, \quad q = \sigma_h \beta \sqrt{\frac{2d}{r_0}} \quad (3.26)$$

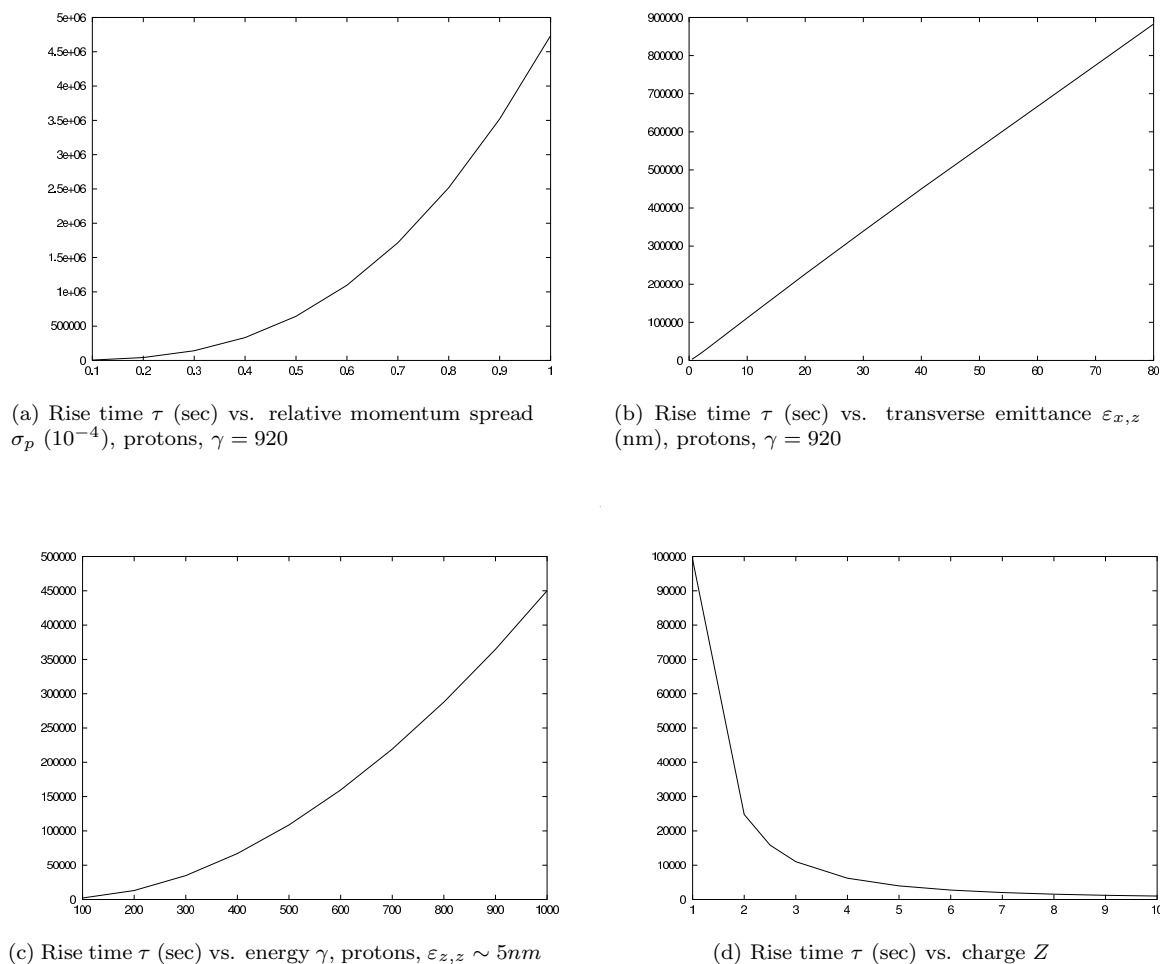
$$f(a, b, q) = 8\pi \int_0^1 2 \left(\ln \left(\frac{q}{2} \left(\frac{1}{P} + \frac{1}{Q} \right) \right) - 0.577... \right) \frac{1-3x^2}{PQ} dx \quad (3.27)$$

$$P = a^2 + (1-a^2)x^2, \quad Q = b^2 + (1-b^2)x^2 \quad (3.28)$$

Here d is the smaller of the beam radii. The effect becomes much stronger for ion beams. Say, for Au ions at RHIC the longitudinal rise time is within one hour, whereas for protons it is tens of hours. The transverse rise times are usually much smaller than the longitudinal and the intra-beam scattering can be often considered to be a one-dimensional process. Some example of growth rates calculated for HERA lattice are shown in figure 3.1. For HERA the transverse rise times are negligible and the longitudinal rise times are tens of hours, depending on initial bunch intensities and emittances.

For some problems the information about the rates of emittance growth is not sufficient. Such are, for example, the study of particle escape from the stable RF bucket and the longitudinal tail buildup due to intra-beam scattering. To treat them one has to follow another approach.

Figure 3.1: Bunch rise times due to intra-beam scattering for HERA parameters



3.2 Kinetic equations

The results from the previous section are applicable for Gaussian beams and harmonic synchrotron and betatron oscillations. The restriction that the shape is Gaussian is not essential, the calculations can in principle be performed for other bunch shapes. The major restriction of the theory is that the same averaged scattering amplitude is taken for all particles. This is a substantial limitation in the case of nonlinear motion. The synchrotron and betatron oscillations become nonlinear for large amplitudes. It can happen that then the behavior of particles with such large amplitudes deviates from the average and the distribution of tails will show a completely different behavior. Such situation is not excluded for the synchrotron motion. In the bunch tails the synchrotron frequency becomes smaller and the tail particles experience collisions rarely. Second, a particle may be lost longitudinally by experiencing a series of jumps of intermediate size. This situation does not correspond to the single Touschek effect or to the intra-beam scattering. Finally, the scattering amplitude must depend on the bunch distribution. To estimate

the escape rate one needs to take these facts into consideration. This is accomplished by employing the Boltzmann equation for the evolution of the distribution function [43]. Without interactions between particles the evolution of the bunch density $f(x)$ (here $x = \{r_\beta, \delta p, \phi\}$ for brevity) is governed by the Liouville equation

$$\frac{df}{ds} = \frac{\partial f}{\partial s} + \frac{\partial f}{\partial x} \frac{\partial x}{\partial s} = 0 \quad (3.29)$$

If collisions are taken into account then the density evolution can be described by the Boltzmann equation

$$\frac{df}{ds} = C(f, f) \quad (3.30)$$

with $C(f, f)$ being the collision integral which shows the change of the distribution function due to collisions per unit time. Let the total cross section of collisions leading to jumps $x_1, x_2 \rightarrow x'_1, x'_2$ be $\sigma(x_1, x_2; x'_1, x'_2)$, then the collision integral can be represented as

$$C(f, f) = \int [\sigma(x_1, x_2; x'_1, x'_2) f(x_1) f(x_2) - \sigma(x_1, x_2; x_1, x_2) f(x_1) f(x_2)] dx_1 dx_2 dx'_1 dx'_2 \quad (3.31)$$

This integral is a nonlinear complex functional of f . Together with the fact that the coefficients in the Liouville equation are fast oscillating this makes the Boltzmann equation impossible to solve straightforwardly. The fast oscillations are eliminated with an averaging procedure (see below). The nonlinear collision integral must also be simplified. One can approximate it with a linear one, say, a linear integral operator or a linear differential operator. Approximation with a linear integral operator would correspond to the physical assumptions that the collision process is a stationary Markov jump process, i.e. that the distribution function changes do not influence the free path distribution and other kinetic parameters significantly. It could also be justified if this assumption does not hold but we are interested in some stable regime only. Approximation with a partial differential equation of second order corresponds to the further assumption that the collisions result in small jumps and the process is a diffusion (Brownian motion). It may happen that the mentioned approximations are not applicable for the time scales of interest but give good results for relatively small time intervals. Then one can apply a calculation procedure which uses one of the approximations on a small time step.

3.3 Averaging of the kinetic equations

In the case of intra-beam scattering collisions happen rarely and thus their probabilities do not depend on the local bunch density, but on the average density along the particle trajectory over a large time interval. In other words by the value

$$\frac{1}{T} \int_0^T f(g_t x) dt = \hat{f}_T(x)$$

for large T or by its limit value

$$\hat{f}(x) = \lim_{T \rightarrow \infty} \hat{f}_T(x) \quad (3.32)$$

Here g_t is the transformation associated with the motion. Suppose now that our system is Hamiltonian, i.e. the motion takes place on surfaces of constant energy. Suppose 3.32 holds for all x lying on some energy surface and the motion on this surface is ergodic (i.e. this surface cannot be decomposed into pieces that are invariant under the motion). Then various statistical characteristics for a particle moving on this energy surface (like collision probability) can be derived from the distribution function $\hat{f}(x)$ defined on it.

Such distribution is called *microcanonical*. The whole system is then described by a distribution in energy only. These assumptions hold in the case of one-dimensional Hamiltonian system. For a multidimensional case the motion on an energy surface does not need to be ergodic. One can encounter following situations

1. The motion on the energy surface is ergodic. Then $\hat{f}(x)$ can be found.
2. The motion is not ergodic. Then the energy surface can be split into invariant components (manifolds). For example, in the case of an integrable system these components are determined by the remaining invariants of motion. These invariants can be used as variables to describe the kinetic process.

The case of an arbitrary multidimensional system can be complicated. The motion on the invariant components can turn to be not ergodic, but of some complicated chaotic nature. The invariant components can also have some complicated topology. But we encounter the situation where a small change in the motion does not influence the statistical properties, so we can always deal with a completely integrable system (which exists close to every Hamiltonian system thanks to the KAM theorem) which is a good approximation to the original system. Therefore, we assume that this system is a rather simple one and can be easily treated. In practice, it's only the fine structure in the synchrotron motion that we are interested in and we will be dealing with a one-dimensional case. In this situation the microcanonical distribution can be easily found. Suppose g_t is the motion of a Hamiltonian system

$$\begin{aligned}\dot{q} &= \frac{\partial H}{\partial p} \\ \dot{p} &= -\frac{\partial H}{\partial q}\end{aligned}$$

To find the limit

$$\lim \frac{1}{T} \int_0^T f(g_t(q, p)) dt = \hat{f}(q, p)$$

note that a Hamiltonian system can be brought to the action-angle form

$$\begin{aligned}\dot{I} &= 0 \\ \dot{\phi} &= \Omega(I)\end{aligned}$$

This can be done in any region that does not contain a separatrix. So the motion is equivalent to a rotation on a circle. Then

$$\lim_{T \rightarrow \infty} \frac{1}{T} \int_0^T f(g_t(q, p)) dt = \lim_{T \rightarrow \infty} \frac{1}{T} \int_0^T f(I, \phi) |J| d\phi = \hat{f}(I) \quad (3.33)$$

So, in action-angle variables the microcanonical distribution reduces to a function in action only. Then in (q, p) coordinates it will have the form $\hat{f}(q, p) = |J| \hat{f}(I)$ with $|J|$ being the Jacobian of the action-angle transformation. The procedure of finding the latter is outlined in appendix A. It is always assumed that when restricted to the level curve the microcanonical density is normalized to 1.

An average of a function $u(q, p)$ over the invariant curves with respect to the microcanonical density \hat{f} is

$$\langle u \rangle |_h = \int_{H(q, p)=h} u(q, p) \hat{f}(p, q) dq dp = \frac{1}{2\pi} \int_0^{2\pi} u(q(I, \phi), p(I, \phi)) |J| d\phi \quad (3.34)$$

For example, the averaged momentum for a linear oscillator is

$$\langle p \rangle = \frac{1}{2\pi} \int_0^{2\pi} p(I, \phi) |J| d\phi = \frac{1}{2\pi} \int_0^{2\pi} \sqrt{2I} \sin \phi |J| d\phi = 0$$

and the averaged squared momentum is

$$\langle p^2 \rangle = \frac{1}{2\pi} \int_0^{2\pi} p^2(I, \phi) |J| d\phi = \frac{1}{2\pi} \int_0^{2\pi} 2I \sin^2 \phi |J| d\phi = I$$

Now we can use the statistical distribution function of the form $\prod \hat{f}_i(I_i)$ where I_i are invariants of motion. One also has to assume that there are no correlations between these degrees of freedom over the particle ensemble, in other words the phases of all particles should be independent.

3.4 The diffusion (Fokker-Planck) approximation

Under certain conditions a kinetic equation may be substituted by a Fokker-Planck equation, which is the crudest approximation. This is possible when the particle motion is approximately a diffusion process. This process is assumed to be Markovian only locally so that the diffusion coefficient can depend on the distribution function and the Fokker-Planck equation can be nonlinear. Usually such an assumption is true when the collisions result in small deflections and the cross section does not change with time or depends on the distribution function only locally. For example, in plasma physics such representation is valid for motion of electrons among heavy ions. Another classical example is the Brownian motion. This approach may also be applied to the study of the intra-beam scattering. Assume that due to collisions the transverse beam distribution does not change considerably and the synchrotron invariant of each particle behaves like a diffusion process path. The equation for (longitudinal) density evolution becomes

$$\frac{\partial P_s(H)}{\partial t} = -\frac{\partial}{\partial H} (a(H)P_s(H)) + \frac{1}{2} \frac{\partial^2}{\partial H^2} (b^2(H)P_s(H)) \quad (3.35)$$

with drift and diffusion coefficients

$$a(H) = \lim_{\tau \rightarrow 0} \frac{1}{\tau} \langle H(\tau) - H(0) \rangle \quad (3.36)$$

$$b^2(H) = \lim_{\tau \rightarrow 0} \frac{1}{\tau} \langle (H(\tau) - H(0))^2 \rangle \quad (3.37)$$

A collision resulting in momentum change δp changes the synchrotron invariant by

$$\delta H = p\delta p + \frac{\delta p^2}{2} \quad (3.38)$$

denote the random scattering amplitudes from 3.1

$$A = (p_1 - p_2)(\cos \psi - 1) \quad (3.39)$$

then the synchrotron invariant changes as

$$\delta H = Ap + \frac{A^2}{2} \quad (3.40)$$

Let the probability of a collision per unit time be Q . Then

$$a(H) = \lim_{\tau \rightarrow 0} \frac{1}{\tau} \langle \delta H \rangle = \left\langle QA p + \frac{Q}{2} A^2 \right\rangle \quad (3.41)$$

$$b^2(H) = \lim_{\tau \rightarrow 0} \frac{1}{\tau} \langle (\delta H)^2 \rangle = \left\langle Q \left(A p + \frac{1}{2} A^2 \right)^2 \right\rangle \quad (3.42)$$

The averaging has to be performed over longitudinal momenta belonging to the constant energy surface and all other variables independently. Due to symmetry the contribution of odd power of p is zero. Therefore, the amplitudes $A_{1,2}$ are assumed to be symmetric so that $\langle A_{1,2} \rangle = 0$. The moments of order higher than three are also neglected. Averaging over the synchrotron phase we obtain the coefficients

$$a(H) = \frac{\langle QA^2 \rangle}{2} \quad (3.43)$$

$$b^2(H) = \langle QA^2 p^2 \rangle = \frac{1}{2\pi} \int_0^{2\pi} \langle 2QA^2 H \sin^2 \varphi \rangle d\varphi = \langle QA^2 H \rangle \quad (3.44)$$

Here the synchrotron oscillations are assumed harmonic for simplicity. Taking into account that A and Q are slowly varying functions of H and that

$$a(H) = \frac{\partial b^2(H)}{2\partial H} \quad (3.45)$$

we arrive at the Fokker-Planck equation

$$\frac{\partial P_s(H)}{\partial H} = \frac{\partial}{\partial H} \left(\frac{b^2(H)}{2} \frac{\partial P_s(H)}{\partial H} \right) \quad (3.46)$$

with the diffusion coefficient

$$\begin{aligned} b^2(H) = & H \frac{\beta}{2\gamma} c \langle P_0(H) \sigma \rangle \int_{-\infty}^{\infty} \int_{-\infty}^{\infty} \int_{-\infty}^{\infty} \int_{-\infty}^{\infty} \int_0^{2\pi} d\phi \int_{-\pi}^{\pi} d\psi \times \\ & \left[\frac{p_1 - p_2}{\gamma} (\cos \psi - 1) + \sqrt{(p_{x,1} - p_{x,2})^2 + (p_{y,1} - p_{y,2})^2} \sin \psi \cos \phi \right]^2 \times \\ & \frac{r_0^2}{4\beta^2} \frac{1}{\sin^4 \psi} \sin \psi P_x(p_{x,1}) P_x(p_{x,2}) P_y(p_{y,1}) P_y(p_{y,2}) dp_{x,1} dp_{x,2} dp_{y,1} dp_{y,2} \end{aligned} \quad (3.47)$$

One sees that the diffusion coefficient is itself a nonlocal function of density and we are dealing not with a Fokker-Planck equation in the strict sense. Using this method could be useful as soon as $\langle P(H) \rangle$ does not change fast. For example, the stationary solution of 3.35 will describe the stationary bunch density and it does not need to have any shape restrictions. This approach can be used, for example, for calculating equilibrium distribution of an electron beam when some scattering process together with synchrotron radiation are present. However, in the problem of proton escape the distribution is not stationary and such a diffusion method is not effective. One may hope to arrive at a solution assuming a specific bunch shape. If a Gaussian solution is assumed, it must coincide with the results of previous section and shouldn't give any new information. Altogether, the diffusion approximation is a loose one for scattering problems with nonlocal dependency of the scattering amplitude on the distribution function

3.5 Reduction to a linear integro-differential equation

The Fokker-Planck approximation described above is equivalent to the assumption that the scattering process is a white noise with slowly varying intensity given by the scattering amplitude. It employs only first two moments of the scattering amplitude and neglects the possible jump nature of the process. There are possible situations where neglecting this information may introduce a noticeable error. Say, for synchrotron motion the probability of a collision $Q(H)$ and thus the diffusion coefficient goes to zero as H approaches the separatrix value. The probability flux across the separatrix is thus zero. However, in reality this flux is not zero and is formed by particles performing jumps from inside of the bucket. The diffusion coefficient singularity could be eliminated in such a way that the probability flux is realistic. But the correct physical behavior is not guaranteed. The diffusion approximation mostly suits to describe the bunch core evolution, although perhaps with more accuracy than the emittance growths rate calculation. Therefore, in the intra-beam scattering problem the local nature of the Fokker-Planck equation is spoiled by the nonlocal character of the diffusion coefficient. A natural approach here would be to abandon the assumption of small jumps and pass to the integro-differential equation describing a Markov jump process

$$\frac{\partial P_s(H)}{\partial t} = \int_{-\infty}^{\infty} W(H', H) P_s(H') dH' \quad (3.48)$$

where $W(H, H')$ is the transition amplitude. If the differential cross-section for a scattering process as a function of the scattering angle θ $d\sigma/d\Omega$ is known, then the kernel can be represented in the form [43]

$$W(H, H') = k \left\langle \frac{d\sigma(\theta - \theta')}{d\theta} - \sigma_{total} \delta(\theta - \theta') \right\rangle \quad (3.49)$$

where k is some factor depending on the collision probability and the expression in the r.h.s. has to be averaged and expressed as a function of H and H' . Such a method was applied, for example, in [44] for a residual gas scattering problem. Here $W(H', H)$ can no more be easily calculated analytically and numerical methods must be employed. The algorithm described in the next section can be used as one of such methods.

3.6 Solution of the Boltzmann equation (method of self-consistent chains).

Here the method proposed in [2] is described which can be employed for the solution of the Boltzmann equation. Its features are studied and it is applied to the problem of particle escape due to intra-beam scattering. It takes jumps and the dependency of the kinetic parameters on the bunch distribution into account. The idea of the method is in short to reduce the evolution of the 3D bunch distribution to that of three one-dimensional distributions of slowly varying quantities, such that the bunch distribution could be reconstructed from them. Then for small time scales the evolution of these slowly varying quantities is assumed to be a Markov process and the appropriate techniques are used, the properties of the Markov process are recalculated after certain time steps. Since we are essentially interested in jump-like perturbations, the arising Markov process will be of jump type. Since the discretization is to be done at a certain point (in the numerical solution), we consider the process to be a Markov chain from the beginning on.

3.6.1 Self-consistent chains

Suppose the perturbation depends on the state of the system, but in such a way, that when we fix the system state it turns into a Markov process. This is the case for intra-beam scattering - under fixed bunch

density the scattering can be considered to be a Markov process and the density changes slowly. Then techniques practically identical with those of Markov processes can be applied. Suppose that we are given a Markov process of jump type. Then we can either consider it to have a continuous phase space, write down an appropriate (Chapman-Kolmogorov) integro-differential equation for the density evolution and then develop a discrete numerical scheme, or first consider the phase space to consist of discrete elements and then apply corresponding methods. We choose the latter option.

Let the transition probabilities $p_{ij}(h)$ have Taylor expansions near 0. Let the probability of leaving a state after a short time be small, this means that they can be represented in the form

$$\begin{aligned} p_{ii}(h) &= 1 - \varepsilon b_{ii}h + O(h^2) \\ p_{ij}(h) &= \varepsilon b_{ij}h + O(h^2), \quad i \neq j \end{aligned}$$

Then the infinitesimal generator a_{ij} of the Markov chain (see Chapter 2) will have elements

$$\begin{aligned} a_{ii} &= -\varepsilon b_{ii} \leq 0 \\ a_{ij} &= \varepsilon b_{ij} \geq 0 \end{aligned}$$

denote

$$\begin{aligned} x_1 &= p_{10}, \dots, x_{n+1} = p_{1n}, \\ x_{n+2} &= p_{20}, \dots, x_{2(n+1)} = p_{2n}, \\ &\dots \\ x_{(n-1)(n+1)} &= p_{n1}, \dots, x_{n(n+1)} = p_{nn} \end{aligned}$$

then the Kolmogorov equation 2.3 satisfied by the transition probabilities can be written as

$$\dot{x}(t) = \mathcal{A}x(t) \tag{3.50}$$

where

$$\mathcal{A} = \begin{pmatrix} \mathcal{A}_{11} & \dots & \mathcal{A}_{1n} \\ \dots & \dots & \dots \\ \mathcal{A}_{n1} & \dots & \mathcal{A}_{nn} \end{pmatrix} \tag{3.51}$$

and $\mathcal{A}_{ij} = \text{diag}\{a_{ij}\} \in \mathbb{R}^n$ is a diagonal matrix with diagonal elements all equal.

The Kolmogorov system is a linear system and thus there are numerous ways to solve it, for instance the solution can be written as

$$x = \exp\{\mathcal{A}t\}x(0)$$

The transition matrix $P(\tau) = \{p_{ij}(\tau)\}$ is thus found and the probability distribution at time t is $p(t) = p_0^T P(t)$ where p_0 is the initial distribution.

Applying this formalism in small steps and recalculating \mathcal{A} after each step, we have a tracking procedure for the distribution. To be able to apply this technique one needs to know how such kind of device behaves when the step size after which the kinetic parameters are recalculated becomes small and number of states of the chain large. Therefore, stable behavior of the result depending on the input parameters is to be assured. The estimates are summarized in Appendix C.

The size of the Kolmogorov system of differential equations growth as the square of the size of the transition matrix and thus as $n^2 \times n^2$ where n is the number of states in the chain. Therefore, it is not symmetric. An application of eigenvalue methods for the solution can thus yield a slow performance. But

thanks to its special block diagonal structure one may propose a faster method. The solution can be written (formally) as

$$x(t) = \exp\{\mathcal{A}t\}x_0 = (E + (\mathcal{A}t) + \frac{1}{2}(\mathcal{A}t)^2 + \frac{1}{3!}(\mathcal{A}t)^3 + \dots)x_0$$

If we have two matrices of the form 3.51, then $AB = C$ again has the same form and

$$c_{ij} = \sum_{k=1}^n a_{ik}b_{kj}$$

So $e^{\mathcal{A}t}$ may be calculated as

$$e^{\mathcal{A}t} = \sum_{i=0}^{\infty} C_i$$

$$C_i = C_{i-1} \frac{1}{i} (\mathcal{A}t)$$

$$C_0 = E$$

$O(n^3)$ operations are required for calculating C_i from C_{i-1} and if we keep $N(n)$ terms in the series the complexity will be $O(N(n)n^3)$. $N(n)$ is determined from precision requirements. Suppose $\|(At)\| \leq \delta$ and the norm is understood to be $\|C\| = \max_{i,j} |c_{ij}|$. Then $\|C_i\| \leq \|C_{i-1}\| \frac{\delta}{i}$. Suppose the series truncation is controlled by the condition $C_N < \varepsilon$. Then N is found from

$$\frac{\delta^N n^N}{(N+1)!} < \varepsilon$$

Using Stirling's formula to approximate the factorial

$$\frac{\delta^N n^N}{\sqrt{2\pi} N^{N+0.5} e^{-N}} < \varepsilon$$

For N not small

$$\frac{(\delta n)^N}{\sqrt{2\pi} N^N} < \varepsilon$$

$$\delta n < N \varepsilon^{1/N}$$

$$N > \delta n$$

One sees that the number $N(n)$ of terms in the series growth linearly with the number of states. This stays in good correspondence with practice. From the same approximation one can show that the number of terms grows as the logarithm of precision.

$$\delta n < N(\varepsilon) \varepsilon^{1/N} = N(\varepsilon) \left(1 + \frac{1}{N} \log \varepsilon + O\left(\frac{1}{N^2}\right)\right)$$

$$N(\varepsilon) > \delta n - \log \varepsilon$$

Thus the number of operations required to calculate $e^{\mathcal{A}t}$ with precision ε is $O(n^4)$. In practice the number of states of the chain for which the method can be employed is bounded by approximately 1000.

3.6.2 Computation procedure

The chain method can be applied for numerical simulations of arbitrary kinetic processes. To apply it to the Touschek effect one needs to define the states of the chain and the infinitesimal generator. We consider the motion in the three-dimensional space of invariants. The longitudinal invariant is given naturally by the Hamiltonian of the synchrotron motion. The other invariants are taken to be the Courant-Snyder invariants. If one wants to take into account the nonlinearity of the transverse motion, one can introduce invariants of higher order. However, this is not necessary in the case of a proton storage ring. All possible values of invariants are divided into states $\{\Omega_i^{x,z,s}\}_{i=1}^{N_x, N_z, N_s}$. For betatron motion $(q_{x,z}, p_{x,z}) \in \Omega_i^{x,z}$ if $h_i^{x,z} \leq I_{x,y}(q_{x,z}, p_{x,z}) \leq h_{i+1}^{x,z}$ for some partitions $h^{x,y}$. States $\Omega_{N_x, N_z}^{x,z}$ are absorbing and correspond to a transversely lost particle. In the longitudinal plane we take the nonlinearity into account and have to distinguish between various regions of the phase space which may have the same value of the invariant. So we first divide the phase space into domains not containing separatrices and then enumerate them as before.

The distributions are then given by three vectors $\{\rho_i^x\}_{i=1}^{N_x}$, $\{\rho_i^z\}_{i=1}^{N_z}$, $\{\rho_i^s\}_{i=1}^{N_s}$. When a collision occurs the collided particle either stays in the same state or jumps to another. Transition probabilities $p_{ij,t}^{x,y,z}(\tau)$ (depending on time) in each chain denote the probability that a particle starting in an arbitrary point lying in state i lands in state j after time τ . To apply the chain formalism one needs to know the infinitesimal generators

$$a_{ij,t}^{x,z,s} = \lim_{\tau \rightarrow 0} \frac{p_{ij,t}^{x,z,s}(\tau) - \delta_{ij}}{\tau} \quad (3.52)$$

It is obtained by inserting some finite time τ into 3.52 for which $p_{ij,t}^{x,y,z}(\tau) - \delta_{ij}$ is still small. This can be, for example, the time of one turn in the ring, one second or any other time for which the probability of two or more collisions is negligibly small compared to the probability of just one collision. In practice this time can be rather large. Then one calculates $p_{ij,t}^{x,z,s}(\tau)$. Let the transition probabilities between the states resulting in a single collision be given by the matrix $T = \{T_{ij}\}$, i.e. T_{ij} is the probability of an arbitrary particle in state i to be scattered into state j . It is a discrete analogue of the differential cross section for the collision. Let the probabilities of (one) collision averaged over the state i be given by $\bar{Q}_i(\tau) = Q_i\tau + O(\tau^2)$, then for sufficiently small τ

$$\{p_{ij}(\tau)\} = \begin{pmatrix} T_{11}Q_1\tau + (1 - Q_1\tau) & T_{12}Q_1\tau & \dots & T_{1n}Q_1 \\ T_{12}Q_2\tau & T_{22}Q_2\tau + 1 - Q_2\tau & \dots & T_{2n}Q_2 \\ \dots & \dots & \dots & \dots \\ T_{n1}Q_n\tau & T_{n2}Q_n\tau & \dots & T_{nn}Q_n + (1 - Q_n\tau) \end{pmatrix} + O(\tau^2) \quad (3.53)$$

and

$$\{a_{ij}\} = \lim_{\tau \rightarrow 0} \frac{p_{ij} - \delta_{ij}}{\tau} = \text{diag}\{Q_i\}(T - E) \quad (3.54)$$

In each dimension T and Q mean of course values averaged over other dimensions. From 3.1 one sees that the state to which the particle comes after collision $T_j^{x,z,s}(q, p, \phi, r)$ is completely defined by coordinates and momenta before the collision, polar angle and impact parameter, ϕ is assumed to be a random variable with uniform distribution on $[0, 2\pi]$, r - with uniform distribution on $[0, r_{max}]$. So T_{ij} becomes a well-defined random function of coordinates. To obtain T_{ij} one has to average $T_j(q, p, \phi, \psi, r)$ over ϕ and r with respect to uniform distribution and over q, p with respect to the microcanonical distribution for $q, p \in \Omega_i$. Q is given by

$$Q(t) = 2\beta c \langle P_0 \rangle \sigma / \gamma^2 \quad (3.55)$$

where P_0 is the spatial density and σ is the total collision cross section. The calculations of all averages are done numerically with the help of expressions from section 3.2. To obtain transition probabilities in single collision one needs to get a transition probability between two physical coordinates as a function of random values - the impact parameter, the polar angle and the momenta and average it over the invariant curve. Say, $V(I, I', x)$ is such transformation, where x is the vector of random parameters, I and I' are the initial and end invariant values. Suppose the distribution function of x is $d\mu(x)$, then the transition probability

$$T_{ij} = \int_{I \in \Omega_i, V(I, I', x) \in \Omega_j} d\mu(x) dI \quad (3.56)$$

Calculation of such an integral is complicated and is the most time-consuming operation. It is performed by a Monte-Carlo method.² $Q(t)$ is calculated easily as soon as the spatial density can be reconstructed from the distribution of the invariants.

Simulations with the chain method show that for proton and ion storage rings the Touschek effect indeed normally results in slow bunch diffusion. The growth rate decreases with time. A nonzero stationary distribution does not exist as long as transition probability between two neighbour states does not vanish and there exists a probability of loss (to the coasting beam), which is a known fact from the Markov chain theory [29]. But the relaxation to a distribution with only absorbing state filled can take a very long time. Usually the distribution changes fast when the initial bunch length is smaller than some critical value. On reaching this value the evolutions slows down and then slow relaxation to zero is observed. In general, the bunch dimension growth logarithmically.

An increase in bunch intensity will increase the collision frequency by the same amount and results in speeding up the time scales by the same number.

The dependency of the bunch dynamics on the bunch intensity is linear, i.e.

The accumulated distribution can have different forms (figure 3.2). The tails are practically Gaussian when the scattering is weak. When the scattering is strong, non-Gaussian tails appear (figure 3.2 (c)).

The dynamics of loss rates depends on the initial distribution. When starting with a Gaussian beam, the loss rate normally increases as soon as the tails are accumulated, then the loss rate decreases and finally relaxes to some asymptotic value. Typical beam length evolution and loss rate are shown in figures 3.3 and 3.4.³ Note that the chain dynamics would be quite different if one applies the method to electron storage rings. There stationary distributions can exist. Therefore, the calculation procedure should be altered to take the synchrotron radiation into account.

3.6.3 Results for HERA

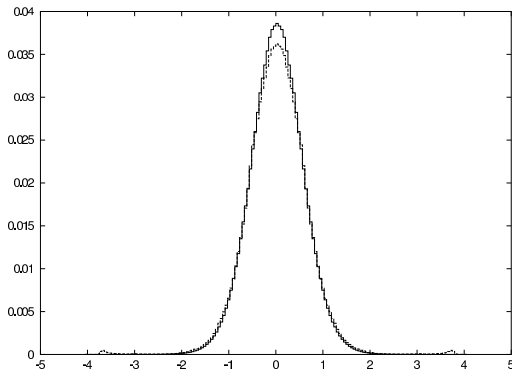
We applied the chain method to estimate the coasting beam production in HERA (for parameters see Appendix A). The simulated distribution evolution is a slow diffusion with rates consistent with the rise times given by the intra-beam scattering theory (see figure 3.5). The amount of lost particles is shown in figure 3.6. This value is below that required to accumulate the observed coasting beam. It gives the value of unavoidable DC current which lies around $0.1 - 0.2 mA$ when $100 mA$ are initially stored with typical emittances and bunch lengths. This quantity of course depends on the operating conditions such as the positions of the collimators. The second RF system has no influence on the dynamics of intra-beam scattering. The side buckets are extremely unlikely to be populated since collisions do not result in synchrotron phase shifts in the first approximation. The oscillations across three buckets do not introduce any layer where the particles can be accumulated.

For high energy protons the influence of intra-beam scattering is weak. But for ions this effect can be very strong. For example, for gold ions in RHIC the bunch growth due to intra-beam scattering is fast

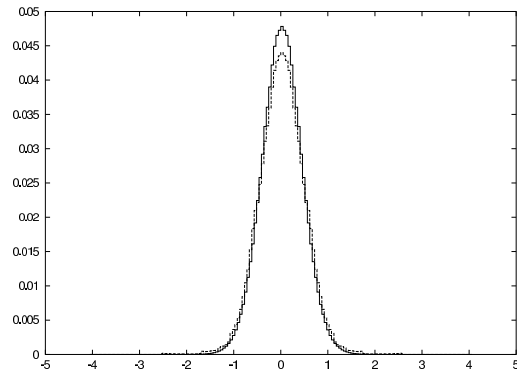
²This method is used to simplify the algorithm. Of course, more effective numerical methods can be used, but this would make the calculations somewhat less transparent.

³Here simulations with particle charge $Z = 10$ are shown to underline the effect

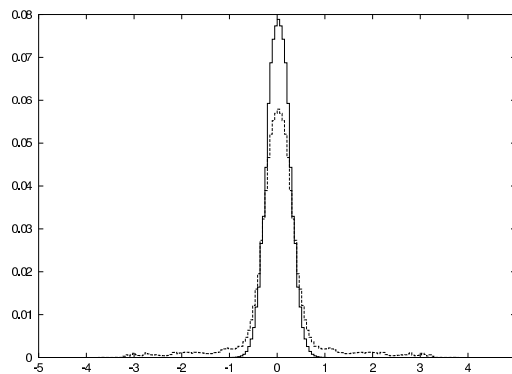
Figure 3.2: Distribution forms appearing as a consequence of intra-beam scattering. Simulations done for HERA lattice with different initial bunch intensities and emittances



(a) Intensity loss with preservation of bunch form and length, $N_p = 0.5 \cdot 10^{11}$, $\gamma = 920$, $\sigma_p = 0.5 \cdot 10^{-4}$



(b) Diffusion with growth of bunch length and intensity loss, $N_p = 10^{11}$, $\gamma = 920$, $\sigma_p = 0.5 \cdot 10^{-4}$



(c) Diffusion with buildup of Non-Gaussian tails, $N_p = 10^{11}$, $\gamma = 920$, $\sigma_p = 0.3 \cdot 10^{-4}$

and the amount of accumulated coasting beam is huge. Here the discussed effects can be clearly seen. A simulation of bunch distribution evolution for particles with $Z = 10$, $A = 10$ HERA lattice is shown in figure 3.7.

3.7 Summary

- Employing averaging and kinetic approximations one can study various scattering processes in non-linear media.
- The setup of the chain method can be viewed as a particular case of a more general idea. Namely, one can effectively use the notion of operator exponent for numerical studies of dissipative systems.

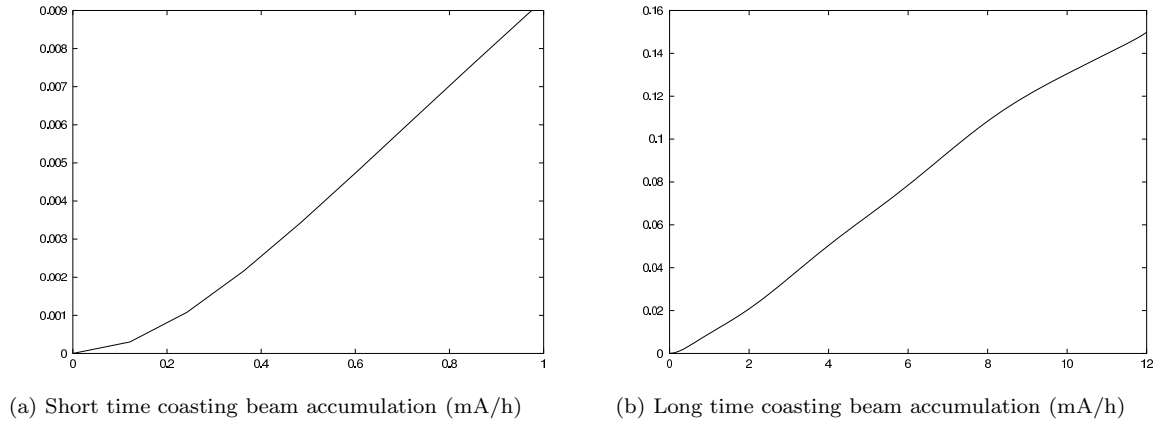
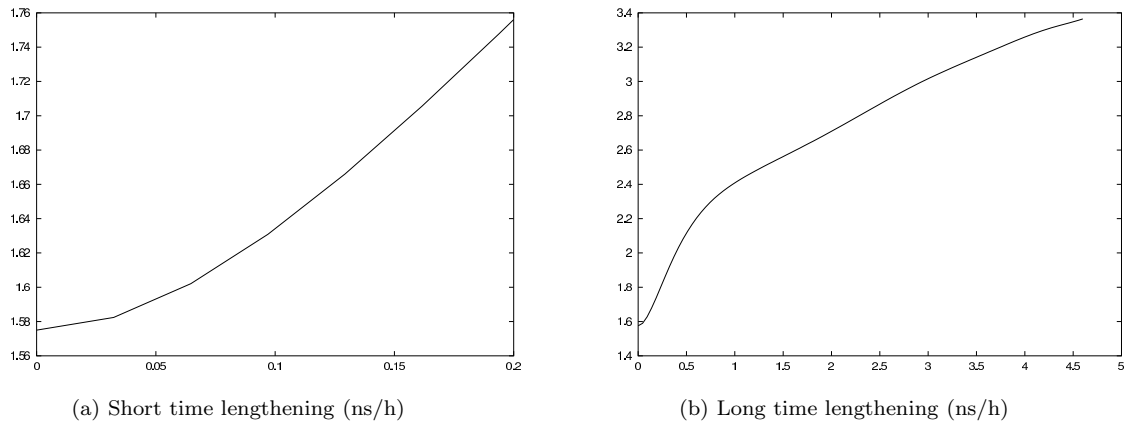
Figure 3.3: Particle loss dynamics. Calculations done for HERA lattice and ions with $Z=10$ 

Figure 3.4: Beam length dynamics



Here the operator is the infinitesimal generator of the chain. One can draw an analogy with the use of the Lie derivative operator and the associated exponent in numerical studies of Hamiltonian systems.

- Numerical estimations of escape rate from the RF bucket due to intra-beam scattering indicate that this effect plays a noticeable role only for high beam intensities. Such intensities are not reached at HERA (see also Chapter 5).

Figure 3.5: Bunch evolution in HERA under influence of intra-beam scattering

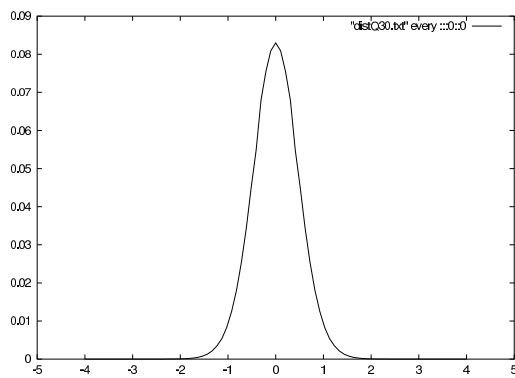
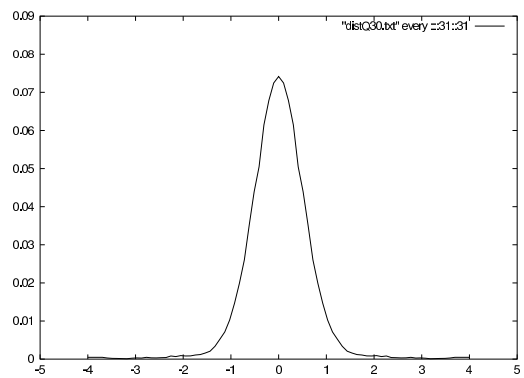
(a) Initial distribution $\varepsilon_{x,z} = 3nm$, $N = 10^{11}$ (b) Distribution after 10 h, $\varepsilon_{x,z} = 3nm$, $N = 10^{11}$

Figure 3.6: Proton losses in HERA

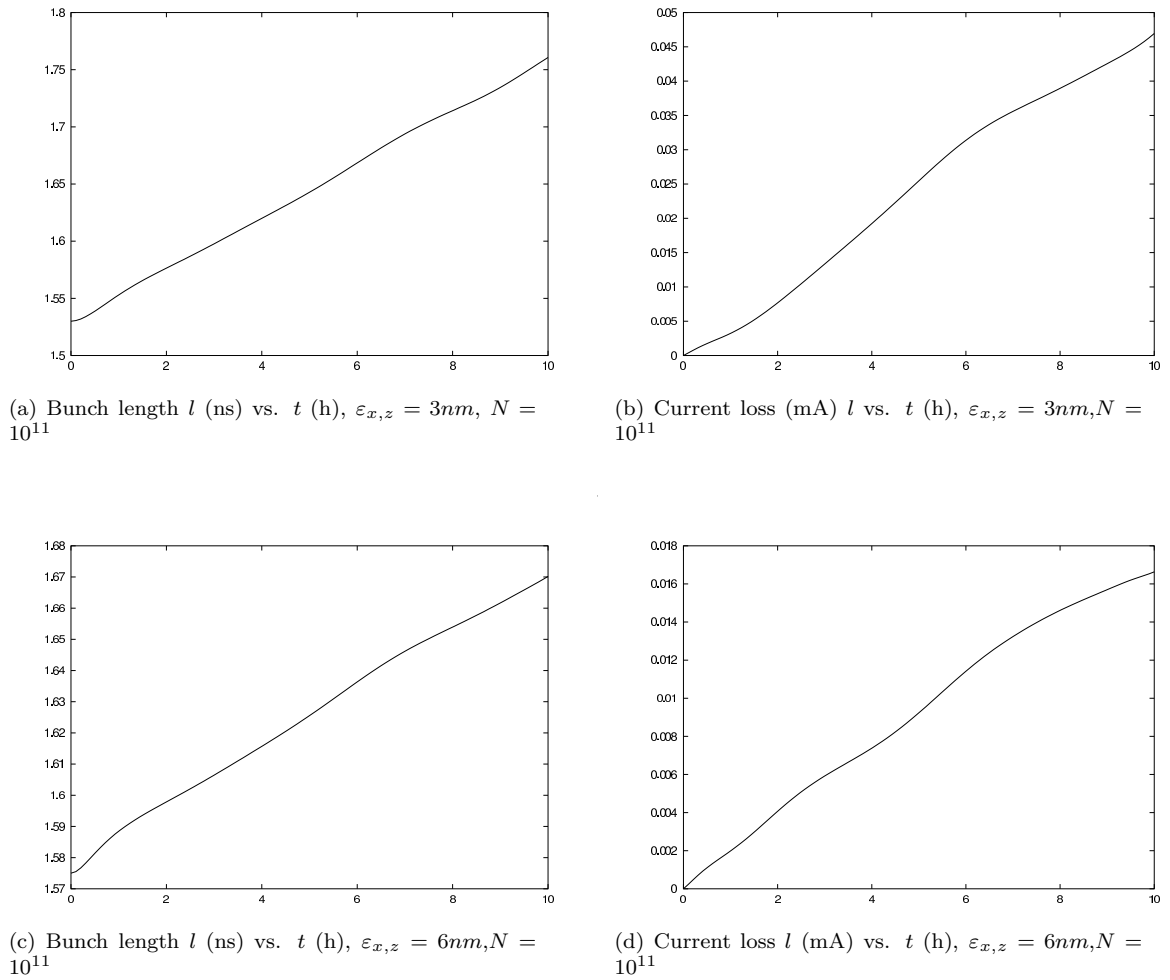
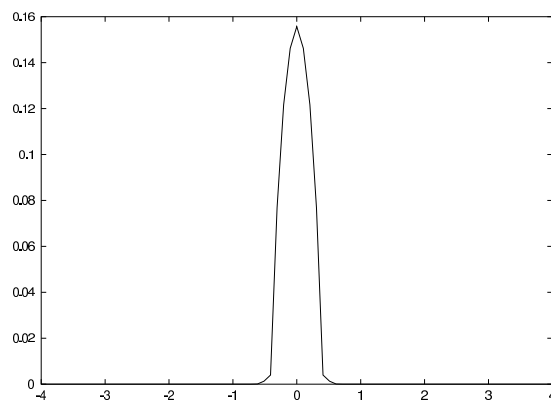
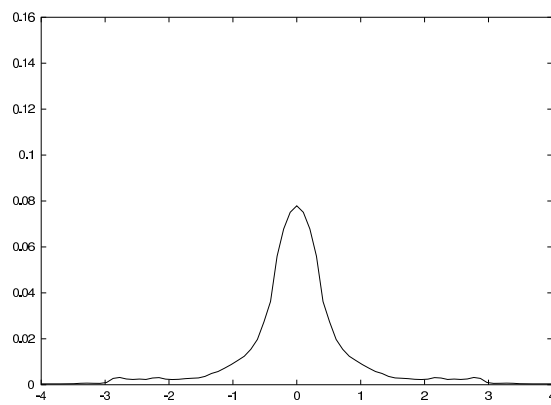


Figure 3.7: Bunch evolution for ions ($Z=10$) with the HERA lattice

(a) Initial distribution



(b) Distribution after 12 hours

Chapter 4

RF noise

In this section we examine some issues related to the behavior of synchrotron oscillations under smooth random external perturbations. Such perturbations arise from fluctuations in the guiding electromagnetic fields, namely in the strengths of the focusing and bending magnets and to a much larger extent from the noise in the field of the accelerating RF cavities. Here the case of cavity noise is treated, other cases can be dealt with in complete analogy. It can have its origin in imperfections of the RF feedback loops, power amplifiers, frequency generators and so on. As the noise model we choose colored Gaussian noise both in cavity voltage and phase. This model seems general and realistic enough and is common in engineering practise. Our goal is to simulate the bunch evolution over the longitudinal phase space and to understand the rate of coasting beam production when the beam is subject to such kind of noise. First, the equations of synchrotron oscillations in the presence of noise are derived. Since the noise is small compared to the RF voltage, it will exhibit noticeable influence on time scales much greater compared to a synchrotron oscillation period. So, one needs to pass to an equation in a slow variable. The solution of the averaged equation does not need to be a Markov process, but only for Markov processes one is able to easily analyse the evolution of the probability density. Applying standard averaging techniques [37], [28], [22] one arrives at a Markov diffusion process in action (or any other slow) variable only that approximates the solution of the original equation. The probability density evolution of the particle ensemble is governed by a certain Fokker-Planck equation, supplied with appropriate initial and boundary conditions. To analyse the solution with respect to the statistical properties of the fluctuations one would ideally want to have its explicit representation. This is generally not possible except for some simple cases. If one considers a double RF system and takes into account diffusion across separatrices and into the side buckets, then numerical calculations need to be employed. Methods of numerical solution of such a problem are discussed.

For the problem of coasting beam estimation in a double RF system the mechanism of separatrix crossing is important. This is because the separatrices introduce a kind of branching in the trajectories of the random particle motion: they can either populate the side buckets or contribute to the coasting beam. Depending on the ratio between the rates of such events quite different coasting beam currents are expected.

Finally, the estimates for HERA are presented.

4.1 Randomly perturbed synchrotron oscillations

Consider the synchrotron motion with a double frequency RF system, the voltages being

$$V_1(t) = U_1 \sin(2\pi\omega_{RF1}t + \phi_{10})$$

$$V_2(t) = U_2 \sin(2\pi\omega_{RF2}t + \phi_{20})$$

Assume now that in each RF system there are small amplitude and phase fluctuations, then the voltages become

$$V_1(t) = U_1 \left(1 + \varepsilon \hat{\xi}_1(t)\right) \sin(2\pi\omega_{RF1}t + \phi_{10} + \varepsilon \hat{\eta}_1(t)) \quad (4.1)$$

$$V_2(t) = U_2 \left(1 + \varepsilon \hat{\xi}_2(t)\right) \sin(2\pi\omega_{RF2}t + \phi_{20} + \varepsilon \hat{\eta}_2(t)) \quad (4.2)$$

$$(4.3)$$

where $\hat{\xi}_{1,2}$ and $\hat{\eta}_{1,2}$ are some random processes and the factor ε means that the magnitude of the fluctuations is small. Say, the stored particles pass the accelerating gap once per revolution. The energy shift per turn is

$$E(t_{n+1}) = E(t_n) + qV_1(t_n) + qV_2(t_n) - \Delta E_\gamma \quad (4.4)$$

where ΔE_γ is the synchrotron radiation energy loss. The same is true for the energy difference with respect to the reference particle

$$\Delta E(t_{n+1}) = \Delta E(t_n) + qV_1(t_n) + qV_2(t_n) - \Delta E_\gamma \quad (4.5)$$

The RF phases are

$$\begin{aligned} \phi_1(t_{n+1}) &= 2\pi\omega_{RF1}t_{n+1} + \phi_{10} + \varepsilon\hat{\eta}_1(t_{n+1}) = \\ &= \phi_1(t_n) + 2\pi\omega_{RF1}(t_{n+1} - t_n) + \varepsilon(\hat{\eta}_1(t_{n+1}) - \hat{\eta}_1(t_n)) \\ \phi_2(t_{n+1}) &= 2\pi\omega_{RF2}t_{n+1} + \phi_{20} + \varepsilon\hat{\eta}_2(t_{n+1}) = \\ &= \phi_2(t_n) + 2\pi\omega_{RF2}(t_{n+1} - t_n) + \varepsilon(\hat{\eta}_2(t_{n+1}) - \hat{\eta}_2(t_n)) = \\ &= \nu\phi_1(t_{n+1}) + \phi_{20} + \varepsilon\hat{\eta}_2(t_{n+1}) - \nu\phi_{10} - \varepsilon\nu\hat{\eta}_1(t_{n+1}) \end{aligned}$$

here t_n and t_{n+1} are times of consequent passages through the accelerating gap, ϕ_{10} and ϕ_{20} are the initial phases. Denoting as usual $\phi_n = \phi_1(t_n)$, $\Delta E_n = \Delta E(t_n)$ and substituting the formula for the revolution time dependence on energy

$$\frac{\Delta T}{T} = \left(\alpha - \frac{1}{\gamma^2}\right) \frac{\Delta E}{\beta^2 E} \quad (4.6)$$

with $\nu = \omega_2/\omega_1$ the one turn map of synchrotron coordinates becomes

$$\begin{aligned} \Delta E_{n+1} &= \Delta E_n + qU_1 \left(1 + \varepsilon \hat{\xi}_1(t_n)\right) \sin(\phi_n) + qU_2 \left(1 + \varepsilon \hat{\xi}_2(t_n)\right) \sin(\nu\phi_n + \varepsilon(\hat{\eta}_2(t_{n+1}) - \nu\hat{\eta}_1(t_{n+1}))) - \Delta E_\gamma \\ \phi_{n+1} &= \phi_n + 2\pi h \left(\alpha - \frac{1}{\gamma^2}\right) \frac{\Delta E_{n+1}}{\beta^2 E} + \varepsilon(\hat{\eta}_1(t_{n+1}) - \hat{\eta}_1(t_n)) \end{aligned} \quad (4.7)$$

using synchrotron coordinates $p = \frac{\Delta E}{E}$ and ϕ , dividing the equations by the reference revolution period T and passing from difference to differential equations we get

$$\begin{aligned} \dot{p} &= -K_1 (1 + \varepsilon \xi_1(t)) \sin(\phi) - K_2 (1 + \varepsilon \xi_2(t_n)) \sin(\nu\phi + \varepsilon \xi_4(t)) - \delta p_\gamma \\ \dot{\phi} &= K_3 p + \varepsilon \xi_3(t) \end{aligned} \quad (4.8)$$

Here the reference phases are assumed zero and

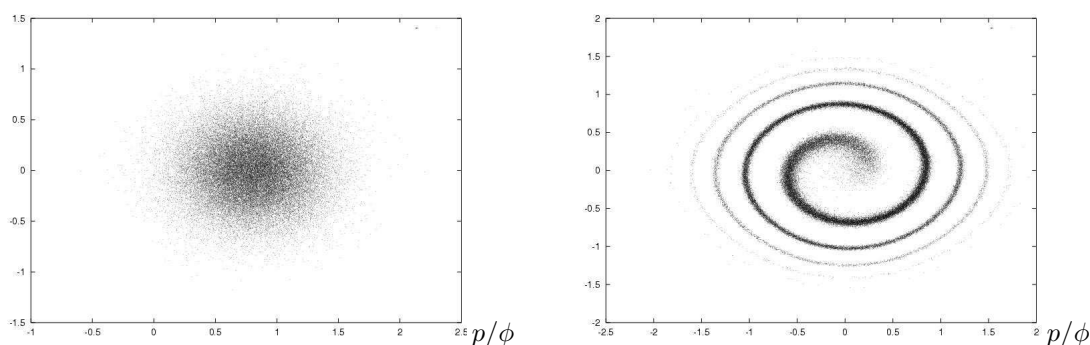
$$\begin{aligned} K_1 &= -\frac{qU_1}{TE} \\ K_2 &= -\frac{qU_2}{TE} \\ K_3 &= \frac{2\pi h}{\beta^2 T} \left(\alpha - \frac{1}{\gamma^2} \right) \end{aligned}$$

the radiation loss rate δp_γ (approximately 10 eV/turn for HERA) can be neglected in the stable RF buckets and the random processes entering the equations stand in the following relations to voltage fluctuations.

$$\begin{aligned} \xi_1(t) &= \hat{\xi}_1(t) \\ \xi_2(t) &= \hat{\xi}_2(t) \\ \xi_3(t) &= \frac{\hat{\eta}_1(t+T) - \hat{\eta}_1(t)}{T} \\ \xi_4(t) &= \hat{\eta}_2(t) - \nu \hat{\eta}_1(t) \end{aligned}$$

The random voltage fluctuations are assumed to be well modeled by second order random processes. Since the cavity voltage fluctuations are sampled with the frequency of particle revolution along the ring, fluctuations with correlation times less than the revolution period do not play any role (more precisely, they have the same influence as white noise). Therefore, the mean values of all random processes are assumed to be zero. Indeed, a nonzero mean of amplitude fluctuations is just a small voltage correction and has no noticeable effect on the bunch diffusion. A nonzero mean phase error has an effect of a shift in the RF bucket position.

Figure 4.1: An exaggerated example of the decoherence effect in the longitudinal phase space



(a) First the bunch is coherently displaced

(b) After some time the excitation decoheres

A fundamental question is if the evolution of the beam density in a random potential is the same as the evolution of the probability density of the corresponding random process. The latter is the statistical distribution of all end points of the process paths under different noise realisations assuming the starting point is also statistically distributed. This means that for trajectories starting at different points different

noise realisations are taken into account. But in reality all particles from the bunch are subject to the same realization of the perturbation.

First consider the phase noise which acts like a random phase shift. If the bunch moved as a rigid body, then the observed bunch density would not change (with respect to bunch centre), but the probability density obtained from the random process would exhibit diffusive behavior. Its meaning would be the mean coordinate of a particle in a region of the phase space when the motion is observed a large number of times. The problem of a coherently perturbed motion of a particle ensemble may sometimes be reduced to treating it as an evolution of a distribution function for a random process for systems exhibiting nonlinear behavior. For oscillating systems an example of such behavior is presented by the decoherence effect. The synchrotron frequency depends on the amplitude and, after some time, two particles having even small amplitude difference will have an arbitrary phase difference. Coherent excitations will be diluted (see figure 4.1). This is true if the excitation is not "faster" than the decoherence time, so this effect will take place if roughly

$$\frac{1}{\tau_{dec}} \gtrsim f_{pert} \quad (4.9)$$

where f_{pert} is the perturbation frequency and τ_{dec} the decoherence time. Consider oscillations with frequency depending on the amplitude $\omega(H)$ on some interval $[H_0, H_1]$ and suppose that in the region of interest this dependency is almost linear, i.e. $\omega''(H) \ll 1$. Then the phase shift between particles with amplitudes H_0 and H_1 after a time t is $(\omega(H_1) - \omega(H_0))t$. The decoherence time is the time for which this phase shift becomes large

$$(\omega(H_1) - \omega(H_0))\tau_{dec} \gg 2\pi \quad (4.10)$$

(to be correct, one should speak of the order of the decoherence time). Under specified conditions this leads to

$$\frac{\partial\omega(H)}{\partial H}\Delta H \gg \nu \quad (4.11)$$

So, perturbation of frequency higher than $\frac{\partial\omega(H)}{\partial H}\Delta H$ are expected to introduce coherent bunch excitations which will result in small fluctuations of the bunch dipole moment. However, the situation cannot be so simply described in the case of small random perturbations. First, they are irregular and don't have any specific frequency. Second, they are small and their influence is seen on long time scales which are usually larger than the decoherence time. It is not obvious whether the coherent motion is destroyed or it builds up over this time scale.

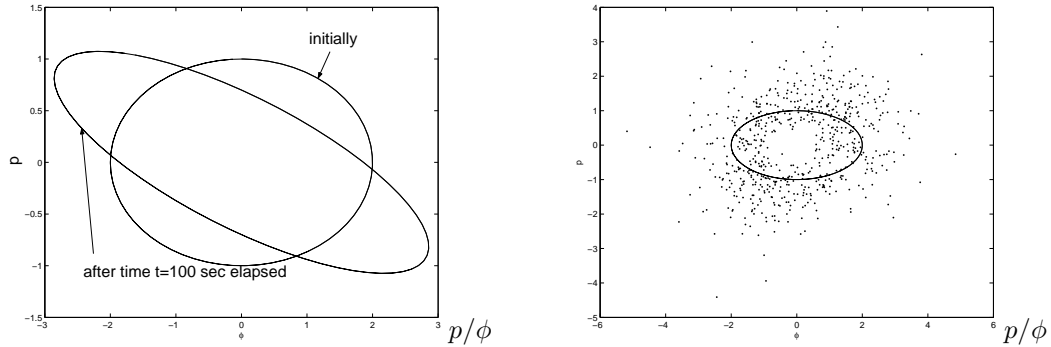
For the amplitude noise decoherence effect also justifies the probabilistic treatment, but here effects can be seen even if 4.9 does not hold. This happens because for the amplitude noise the value of the perturbation also depends on the phase. Even in the absence of decoherence the volume of the phase space occupied by particles may explode. But the motion within this phase space is coherent. An example is given in figure 4.2. It shows the density evolution of a linear oscillator

$$\begin{aligned} \dot{p} &= (1 + \xi(t))q \\ \dot{q} &= p \end{aligned}$$

when all particles experience the same realisation of a certain (delta-correlated in the simulation) process $\xi(t)$ starting from a circle distribution. The effect of the noise is that the density is randomly stretched along the p axis. The resulting distribution is a random ellipse centered at zero, but no diffusion occurs.

Our argumentation shows that the frequency spread determines to which extent the effect of a random coherent perturbation will be diffusive. If this spread vanishes then no diffusion can occur. But even if

Figure 4.2: Effect of coherent noise

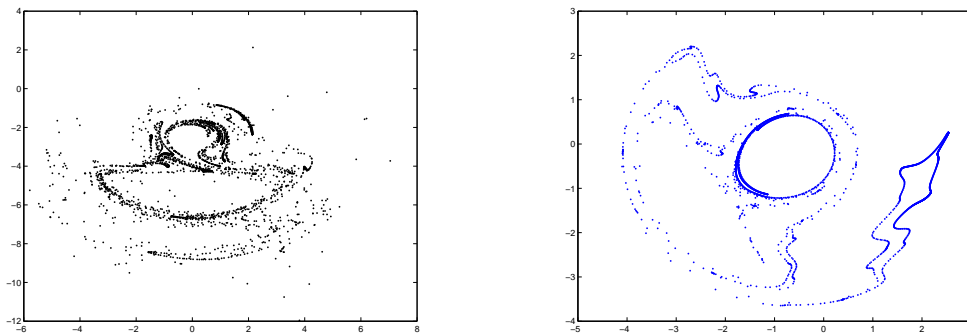


(a) Effect of amplitude noise for the linear model (without frequency spread)

(b) Effect of amplitude noise for the linear model (without frequency spread) when the perturbation is incoherent for the same conditions

the condition 4.9 holds it does not mean that the system possesses sufficient mixing. Obvious examples can be constructed. Computer simulations show that such systems can exhibit complicated behavior (see examples in figure 4.3) and it is not excluded that some correlations are introduced.

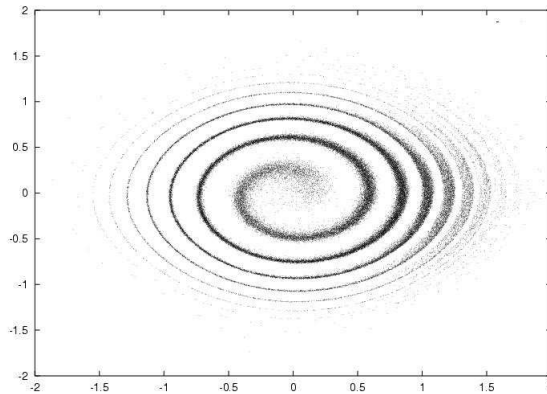
Figure 4.3: With a nonlinear frequency/amplitude dependency the effect of the perturbation can be complicated. The shown patterns are formed by perturbed rotation of a circle with frequency dependency of the form $1 + \sin(H)$ for different parameters



An evidence that the process of decoherence does not need to result in the loss of correlation is presented by echo effects. Such effects were observed in plasma physics (plasma echo after Landau damping), solid state physics (spin echo) as well as in high energy beams [56], [1]. The longitudinal beam echoes in a proton machine are produced by introducing an excitation of the bunch dipole moment by shifting the RF phase. After this excitation decoheres one is able to recover it by introducing an amplitude perturbation (see figure 4.4). Such experiments demonstrate that even the presence of decoherence is not sufficient to guarantee that the random perturbations of synchrotron motion will result in bunch diffusion but not

in collective oscillating modes. The fundamental reason behind the possibility of observation of beam echo is that the synchrotron motion does not possess any mixing properties and is not even ergodic [14]. Physically this means that the system is not dissipative.

Figure 4.4: Bunched beam echo



For weak noise the situation becomes much easier. Here the large time scales over which the diffusion proceeds guarantee that even weak nonlinearity introduces a loss of correlation. In this case the effect of coherence becomes weak and can be estimated. The presentation of such estimates follows conceptually the derivation of the Fokker-Planck equation and is given in section 4.3 ¹.

4.2 The averaged Fokker-Planck equation

The equations derived in the previous section cannot be studied directly due to fast oscillations in the r.h.s. compared to the time scales at which the fluctuations are expected to influence the dynamics. Therefore, such equations do not correspond to a diffusion process unless the entering random processes are white noise. Thus there is normally no Fokker-Planck equation associated with the stochastic differential equation. It is natural to study the behavior of some invariant of motion of the unperturbed system first bringing the equation to a standard action-angle form. Then if the random perturbations satisfy the law of large numbers due to their fast oscillations, this stochastic equation is approximated by a certain diffusion which we now can associate with a Fokker-Planck equation. In [17] such averaging was applied to harmonic cavity voltages, i.e. with $V(t) = U \sin(\omega t)$. In such case the transformation to action-angle variables can be explicitly written in terms of elliptic integrals. This is however not possible in a general situation where the cavity voltage is an arbitrary periodic function. Such situation is encountered, for instance, in HERA with the double RF system. It can be amended by using perturbation techniques. Here an alternative approach is shown in which the action-angle variables are not used. The diffusion equation is derived for the unperturbed synchrotron invariant as the slow variable provided the Fourier spectrum of the solution depending on this variable can be found. First, it allows to obtain the diffusion coefficient when the system is not Hamiltonian. Second, it is also convenient in situations when the system is Hamiltonian, but the potential is of complicated form and the transformation to action-angle variables takes a large amount of computations. Then the numerical calculation of the spectrum and thus of the diffusion coefficient appears to be simpler. The averaging procedure in action-angle variables is also

¹The results are apparently at the physical level of rigor (under the physical level of rigor the level of rigor usual for a physics textbook is understood). We were not able to give any presentation from the point of view of the mathematical theory of dynamical systems.

outlined. These variables are convenient when treating the effect of noise coherence and the interaction of noise with nonlinear resonance. Therefore, a slightly more rigorous justification of the averaging procedure is presented from which it follows, for example, that the stochastic averaging may fail for some random processes even in the presence of fast oscillations if the noise magnitude is not sufficiently small. Then the calculations according to the Fokker-Planck equation may introduce a noticeable error.

Now we turn to equation 4.8 from section 4.1. To the second order in ε it reads

$$\begin{aligned}\dot{p} &= -K_1(1 + \varepsilon\xi_1(t))\sin(\phi) - K_2(1 + \varepsilon\xi_2(t))\sin(\nu\phi) - \\ &\quad \varepsilon K_2\xi_4(t)\cos(\nu\phi) + \frac{1}{2}\varepsilon^2 K_2\xi_4^2(t)\sin(\nu\phi) - \varepsilon^2 K_2\xi_2(t)\xi_4(t)\cos(\nu\phi) \\ \dot{\phi} &= K_3p + \varepsilon\xi_3(t)\end{aligned}\tag{4.12}$$

One can choose, for example, the Hamiltonian of the unperturbed system as the slow variable.

$$H = K_3\frac{p^2}{2} + K_1(1 - \cos(\phi)) + \frac{K_2}{\nu}(1 - \cos(\nu\phi))\tag{4.13}$$

Then its time derivative is

$$\frac{\partial H}{\partial t} = \frac{\partial H}{\partial p}\frac{\partial p}{\partial t} + \frac{\partial H}{\partial \phi}\frac{\partial \phi}{\partial t}\tag{4.14}$$

which after substituting 4.8 gives

$$\begin{aligned}\frac{\partial H}{\partial t} &= \varepsilon K_3p[-K_1\xi_1(t)\sin(\phi) - K_2\xi_2(t)\sin(\nu\phi) - K_2\xi_4(t)\cos(\nu\phi)] + \\ &\quad \varepsilon\xi_3(t)[K_1\sin(\phi) + K_2\sin(\nu\phi)] + \varepsilon^2 K_2 K_3p\left[\frac{1}{2}\xi_4^2(t)\sin(\nu\phi) - \xi_2(t)\xi_4(t)\cos(\nu\phi)\right]\end{aligned}\tag{4.15}$$

We want to average out the fast oscillations in the r.h.s. of 4.15 by eliminating fast variables p, ϕ and obtain a stochastic equation for H only. Since the diffusion rate is generally proportional to the square of fluctuation (see 2.24) we should expect a noticeable influence of the random perturbations on time scales of ε^2 [38]. Substitute $\tau = \varepsilon^2 t$ and rewrite this equation in integral form

$$H(\tau) = H(0) + \frac{1}{\varepsilon}\int_0^\tau g_\varepsilon(p(\varepsilon^{-2}s), \phi(\varepsilon^{-2}s), \varepsilon^{-2}s)ds + \int_0^\tau f_\varepsilon(p(\varepsilon^{-2}s), \phi(\varepsilon^{-2}s), \varepsilon^{-2}s)ds\tag{4.16}$$

where we denoted for convenience

$$\begin{aligned}g_\varepsilon(p, \phi, t) &= K_3p[-K_1\xi_1(t)\sin(\phi) - K_2\xi_2(t)\sin(\nu\phi) - K_2\xi_4(t)\cos(\nu\phi)] + \\ &\quad \xi_3(t)[K_1\sin(\phi) + K_2\sin(\nu\phi)] \\ f_\varepsilon(p, \phi, t) &= K_2 K_3p\left[\frac{1}{2}\xi_4^2(t)\sin(\nu\phi) - \xi_2(t)\xi_4(t)\cos(\nu\phi)\right]\end{aligned}\tag{4.17}$$

Proposition 1 *On a bounded interval $[0, T]$ equation 4.16 can be approximated by an Ito stochastic differential equation*

$$dH(t) = a(H)dt + b(H)dW_t\tag{4.18}$$

where

$$a(H) = \lim_{T \rightarrow \infty} \frac{1}{T} \int_0^T \langle f_\varepsilon(p, \phi, s) \rangle ds + \lim_{T \rightarrow \infty} \frac{1}{T} \int_0^T ds \int_{-T}^s \left\langle \frac{\partial g_\varepsilon}{\partial H}(p, \phi, s) g_\varepsilon(p, \phi, t) \right\rangle dt \quad (4.19)$$

$$b^2(H) = \lim_{T \rightarrow \infty} \frac{1}{T} \int_0^T \int_0^T \langle g_\varepsilon(p, \phi, s) g_\varepsilon(p, \phi, t) \rangle ds dt \quad (4.20)$$

and the integrals taken along the surface $H(p, \phi) = H = \text{const.}$

From this proposition it follows that on a time scale of ε^{-2} a random perturbation of order ε^2 has a deterministic effect given by its average value. Fluctuations are introduced by perturbations of order ε . For sketch of the proof see Appendix B. The coefficients on the original time scale is obtained by multiplying 4.19 and 4.20 by ε^2 . Now let us look how this coefficients can be obtained in practice.

The functions g_ε and f_ε are given as linear combinations of some random processes (see section 4.1). So, they can be represented as Fourier series

$$g_\varepsilon(t) = \sum_j \zeta_j(t) \sum_{k=-\infty}^{\infty} g_{jk} e^{i\omega_k t} \quad (4.21)$$

$$f_\varepsilon(t) = \sum_j \chi_j(t) \sum_{k=-\infty}^{\infty} f_{jk} e^{i\nu_k t} \quad (4.22)$$

where the expansion coefficients depend on H and $\chi_j(t)$ and $\zeta_j(t)$ are some random processes. Then the contribution to the drift from the ε^2 order terms f_ε becomes

$$\lim_{T \rightarrow \infty} \frac{1}{T} \int_0^T \langle f_\varepsilon(p, \phi, s) \rangle ds = \lim_{T \rightarrow \infty} \frac{1}{T} \int_0^T \sum_j \langle \chi_j(s) \rangle \sum_k f_{jk} e^{i\nu_k s} ds \quad (4.23)$$

The last expression equals

$$\sum_j f_{j0} \langle \chi_j(s) \rangle \quad (4.24)$$

with f_{j0} the coefficients of the zero frequency $\nu_0 = 0$. The contribution to the diffusion of g_ε is

$$\begin{aligned} & \lim_{T \rightarrow \infty} \frac{1}{T} \int_0^T \int_0^T \langle g_\varepsilon(p, \phi, s) g_\varepsilon(p, \phi, t) \rangle ds dt = \\ & \lim_{T \rightarrow \infty} \frac{1}{T} \int_0^T \sum_{j,l,k,m} \int_0^T \langle \zeta_j(s) \zeta_l(t) \rangle g_{jk} g_{lm} e^{i\omega_k s} e^{i\omega_m t} ds dt = \\ & \lim_{T \rightarrow \infty} \frac{1}{T} \int_0^T \sum_{j,l,k,m} e^{i\omega_k s} ds \int_{-s}^{T-s} \langle \zeta_j(s) \zeta_l(s+\tau) \rangle g_{jk} g_{lm} e^{i\omega_m(s+\tau)} d\tau = \\ & \lim_{T \rightarrow \infty} \frac{1}{T} \int_0^T \sum_{j,l,k,m} e^{i(\omega_k + \omega_m)s} ds \int_{-\infty}^{\infty} \langle \zeta_j(s) \zeta_l(s+\tau) \rangle g_{jk} g_{lm} e^{i\omega_m \tau} d\tau = \\ & \lim_{T \rightarrow \infty} \frac{1}{2T} \int_0^T \sum_{j,k,l,m} e^{i(\omega_k + \omega_m)s} g_{jk} g_{lm} S_{jl}(\omega_m) ds \end{aligned} \quad (4.25)$$

$$(4.26)$$

here only the "resonant terms" (with $\omega_k + \omega_m \neq 0$) make contribution and finally

$$b^2(H) = \frac{1}{2} \sum_{j,l} \sum_{\omega_k + \omega_m = 0} g_{jk} g_{lm} S_{jl}(\omega_k) \quad (4.27)$$

where $S_{ij}(\omega)$ is the cross-spectral density of the processes $\zeta_i(t)$ and $\zeta_j(t)$ (see chapter 2). Next we show that the contribution to the drift coefficient arising from the gradient in g_ε is related to the diffusion coefficient as

$$\begin{aligned} & \lim_{T \rightarrow \infty} \frac{1}{T} \int_0^T ds \int_{-T}^s \left\langle \frac{\partial g_\varepsilon}{\partial H}(p, \phi, s) g_\varepsilon(p, \phi, t) \right\rangle dt = \\ & \frac{1}{2} \frac{\partial}{\partial H} \lim_{T \rightarrow \infty} \frac{1}{T} \int_0^T \int_0^T \langle g_\varepsilon(p, \phi, s) g_\varepsilon(p, \phi, t) \rangle ds dt \end{aligned} \quad (4.28)$$

This can be shown, for example, in the following way. Let the function $g_\varepsilon(H, t)$ be represented as a Fourier integral

$$g_\varepsilon(H, t) = \int_{-\infty}^{\infty} G(H, \omega) e^{i\omega t} d\omega \quad (4.29)$$

Then

$$\begin{aligned} & \lim_{T \rightarrow \infty} \frac{1}{T} \int_0^T \int_{-T}^s \left\langle \frac{\partial g_\varepsilon}{\partial H}(p, \phi, s) g_\varepsilon(p, \phi, t) \right\rangle ds dt = \\ & \lim_{T \rightarrow \infty} \frac{1}{T} \int_0^T \int_{-T}^s \int_{-\infty}^{\infty} \int_{-\infty}^{\infty} d\omega_1 d\omega_2 \left\langle \frac{\partial G(H, \omega_1)}{\partial H} G(H, \omega_2) \right\rangle e^{i\omega_1 s} e^{i\omega_2 t} ds dt = \\ & \frac{1}{2} \frac{\partial}{\partial H} \lim_{T \rightarrow \infty} \frac{1}{T} \int_{-\infty}^{\infty} \int_{-\infty}^{\infty} d\omega_1 d\omega_2 \int_0^T \int_0^{T+s} \langle G(H, \omega_1) G(H, \omega_2) \rangle e^{i\omega_1 s} e^{i\omega_2 t} ds dt = \\ & \frac{1}{2} \frac{\partial}{\partial H} \lim_{T \rightarrow \infty} \frac{1}{T} \int_0^T \int_{-T}^s \langle g_\varepsilon(H, s) g_\varepsilon(H, t) \rangle ds dt = \\ & \frac{1}{4} \frac{\partial}{\partial H} \lim_{T \rightarrow \infty} \frac{1}{T} \int_0^T \int_{-\infty}^{\infty} \langle g_\varepsilon(H, s) g_\varepsilon(H, t) \rangle ds dt = \\ & \frac{1}{2} \frac{\partial}{\partial H} \lim_{T \rightarrow \infty} \frac{1}{T} \int_0^T \int_0^T \langle g_\varepsilon(H, s) g_\varepsilon(H, t) \rangle ds dt = \frac{1}{2} \frac{\partial}{\partial H} b^2(H) \end{aligned} \quad (4.30)$$

Here we used the fact that $\langle g_\varepsilon(H, s) g_\varepsilon(H, t) \rangle \rightarrow 0$ as $|s - t| \rightarrow \infty$ and is symmetric with respect to $s - t$.

Now we need to obtain the Fourier representations of g_ε and f_ε . Expanding g_ε and f_ε in Taylor series one gets

$$\begin{aligned} g_\varepsilon(p, \phi, t) &= -\xi_1(t) K_1 K_3 p \left(\phi - \frac{1}{3!} \phi^3 + \frac{1}{5!} \phi^5 - \dots \right) \\ &\quad - \xi_2(t) K_2 K_3 p \left(\nu \phi - \frac{1}{3!} \nu^3 \phi^3 + \frac{1}{5!} \nu^5 \phi^5 - \dots \right) + \\ &\quad \xi_3(t) \left([K_1 + K_2 \nu] \phi - \frac{1}{3!} [K_1 + K_2 \nu^3] \phi^3 + \frac{1}{5!} [K_1 + K_2 \nu^5] \phi^5 - \dots \right) \end{aligned}$$

$$\begin{aligned}
& -\xi_4(t)K_2K_3p \left(1 - \frac{1}{2!}\nu^2\phi^2 + \frac{1}{4!}\nu^4\phi^4 - \dots \right) \\
f_\varepsilon(p, \phi, t) = & \frac{1}{2}\xi_4^2(t)K_2K_3p \left(\nu\phi - \frac{1}{3!}\nu^3\phi^3 + \frac{1}{5!}\nu^5\phi^5 - \dots \right) \\
& -\xi_2(t)\xi_4(t)K_2K_3p \left(1 - \frac{1}{2!}\nu^2\phi^2 + \frac{1}{4!}\nu^4\phi^4 - \dots \right)
\end{aligned}$$

Obtaining Fourier series for ϕ and p and inserting it into the last expression solves the problem. Suppose

$$\begin{aligned}
\phi(t) &= \sum_k \phi_k e^{i\omega_k t} \\
p(t) &= \sum_k p_k e^{i\omega_k t}
\end{aligned} \tag{4.31}$$

Then

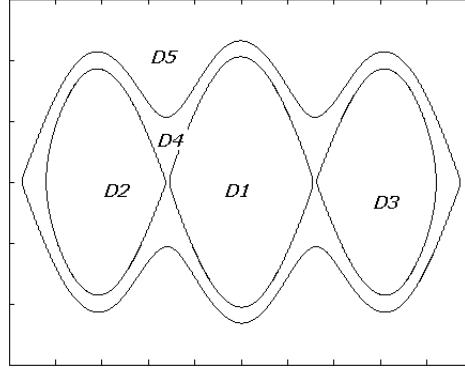
$$\begin{aligned}
g_\varepsilon(p, \phi, t) = & \xi_1(t)K_1K_3 \sum_{n=1}^{\infty} \frac{(-1)^{2n-1}}{(2n-1)!} \sum_{|k|=2n-1} \sum_m \phi_{k_1} \dots \phi_{k_{2n-1}} p_m e^{i(k_1\omega_{k_1} + \dots + k_{2n-1}\omega_{k_{2n-1}} + \omega_m)t} + \\
& \xi_2(t)K_2K_3 \sum_{n=1}^{\infty} \frac{(-1\nu)^{2n-1}}{(2n-1)!} \sum_{|k|=2n-1} \sum_m \phi_{k_1} \dots \phi_{k_{2n-1}} p_m e^{i(k_1\omega_{k_1} + \dots + k_{2n-1}\omega_{k_{2n-1}} + \omega_m)t} + \\
& \xi_3(t) \sum_{n=1}^{\infty} \frac{(-1\nu)^{2n}}{(2n-1)!} \sum_{|k|=2n-1} \phi_{k_{i_1}} [K_1 + K_2\nu^{k_1}] \dots \phi_{k_{2n-1}} [K_1 + K_2\nu^{k_{2n-1}}] e^{i(k_1\omega + \dots + k_{2n-1})t} + \\
& \xi_4(t)K_2K_3 \sum_{n=1}^{\infty} \frac{(-1\nu)^{2n-1}}{(2n)!} \sum_{|k|=2n} \sum_m \phi_{k_1} \dots \phi_{k_{2n}} p_m e^{i(k_1\omega_{k_1} + \dots + k_{2n}\omega_{k_{2n}} + \omega_m)t}
\end{aligned}$$

and

$$\begin{aligned}
f_\varepsilon(p, \phi, t) = & \xi_4^2(t) \frac{1}{2} K_2K_3 \sum_{n=1}^{\infty} \frac{(-1\nu)^{2n}}{(2n-1)!} \sum_{|k|=2n-1} \sum_m \phi_{k_1} \dots \phi_{k_{2n-1}} p_m e^{i(k_1\omega_1 + \dots + k_{2n-1}\omega_{2n-1} + \omega_m)t} + \\
& \xi_4(t)\xi_2(t)K_2K_3 \sum_{n=1}^{\infty} \frac{(-1\nu)^{2n-1}}{(2n)!} \sum_{|k|=2n} \sum_m \phi_{k_1} \dots \phi_{k_{2n}} p_m e^{i(k_1\omega_1 + \dots + k_{2n}\omega_{2n} + \omega_m)t} -
\end{aligned}$$

One sees that for any periodic solution infinitely many "resonance" conditions are met. In a general situation the resonances will form a dense set and the entire spectrum will influence the diffusion coefficient. We would have arrived at the same situation using action-angle variables. The impact of a resonance however goes to zero with increasing order. Taking this into account and noticing also that the physically

Figure 4.5: Domain decomposition



realizable part of spectrum is always bounded, one ends up with only finite number of terms. Combining 4.27 and 4.31 one can obtain the diffusion coefficient for arbitrary potentials and arbitrary noise spectra.

Now we need to obtain the Fourier representation of the solution 4.31. This can be generally done by means of a perturbation technique in each of the domains D_i that do not contain separatrices (see figure 4.5). We now demonstrate the Lindstedt's method [27] of frequency adjustment to do this ². In domains D_1 , D_2 and D_3 the solution is sought as a perturbations to a harmonic oscillator.

Write the unperturbed equation of synchrotron motion as a second order equation and expand the r.h.s in power series around the stable phase $\phi = 0$

$$\ddot{\phi} = -\lambda_1\phi + \lambda_3\phi^3 - \lambda_5\phi^5 + \dots \quad (4.32)$$

where

$$\lambda_1 = K_1 + K_1\nu, \quad \lambda_3 = K_1\frac{1}{3!} + K_2\frac{\nu^3}{3!}, \quad (4.33)$$

and so on (i.e. the equation 4.8 with all ξ_i set to 0). Introduce $\phi = \sqrt{\eta}x$. Then 4.32 becomes

$$\ddot{x} = -\lambda_1x + \eta\lambda_3x^3 - \eta^2\lambda_5x^5 - \dots \quad (4.34)$$

Consider η to be a small parameter. For $\eta = 0$ the solution is

$$x(t) = A \sin(\sqrt{\lambda_1}t + \alpha) \quad (4.35)$$

One seeks for the solution as a series in η

$$x(t) = x_0(t) + \eta y_1(t) + \eta^2 y_2(t) + \dots \quad (4.36)$$

As $x_0(t)$ one takes

$$x_0(t) = A \sin(\omega t) \quad (4.37)$$

²This method is somewhat two hundred years old. Perturbation methods exploiting the Hamiltonian structure of the system are of course more usual now. An example is shown in Appendix A. The advantage there is the rate of convergence which solves the problem of "small denominators". This small denominators appear in the Lindstedt's method. However, for our system they are of no great advantage and result in an equivalently cumbersome solution as far as only low order approximations are concerned.

where ω itself is sought as a perturbation series to the zeroth order frequency $\sqrt{\lambda_1}$. The initial phase is dropped because it does not play a role when averaging is performed.

$$\omega^2 = \lambda_1 + \eta\omega_1 + \eta^2\omega_2 + \dots \quad (4.38)$$

Then

$$\ddot{x} + \omega^2 x = x(\eta\omega_1 + \eta^2\omega_2 + \dots) + \eta\lambda_3 x^3 - \eta^2\lambda_5 x^5 - \dots \quad (4.39)$$

Equating the coefficients before powers of η

$$\begin{aligned} \ddot{y}_1 + \omega^2 y_1 &= \omega_1 x_0 + \lambda_3 x_0^3 \\ \ddot{y}_2 + \omega^2 y_2 &= \omega_1 y_1 + \omega_2 x_0 + 3\lambda_3 x_0^2 y_1 - \lambda_5 x_0^5 \\ &\dots \end{aligned}$$

The first order in η :

$$\ddot{y}_1 + \omega^2 y_1 = \omega_1 A \sin(\omega t) + \lambda_3 A^3 \frac{1}{4} (3 \sin(\omega t) - \sin(3\omega t)) \quad (4.40)$$

This equation admits periodic solution if we eliminate resonant terms by choosing $\omega_1 = -\frac{3}{4}\lambda_3 A^2$

$$\ddot{y}_1 + \omega^2 y_1 = -\frac{1}{4}\lambda_3 A^3 \sin(3\omega t) \quad (4.41)$$

and the solution is

$$y_1(t) = B \sin(\omega t + \beta) + \frac{\lambda_3 A^3}{32\omega^2} \sin(3\omega t) \quad (4.42)$$

where B and β are found from the condition

$$y_1(0) = \dot{y}_1(0) = 0 \quad (4.43)$$

which gives

$$\beta = 0, \quad B = -\frac{3\lambda_3 A^3}{32\omega^2} \quad (4.44)$$

and one gets the asymptotic expansion to the first order in η

$$\begin{aligned} x &= A \sin(\omega t) + \eta \left(-\frac{3\lambda_3 A^3}{32\omega^2} \sin(\omega t) + \frac{\lambda_3 A^3}{32\omega^2} \sin(3\omega t) \right) \\ \dot{x} &= \omega A \cos(\omega t) + \eta \left(-\frac{3\lambda_3 A^3}{32\omega} \cos(\omega t) + \frac{3\lambda_3 A^3}{32\omega} \cos(3\omega t) \right) \end{aligned}$$

where

$$\omega^2 = \lambda_1 - \frac{3}{4}\eta\lambda_3 A^2$$

With the same method one arrives at the expansion for y_2 .

$$\begin{aligned}
\ddot{y}_2 + \omega^2 y_2 &= \sin(3\omega t) \frac{A^5}{16} \left[5\lambda_5 + \frac{\lambda_3^2}{\lambda_1 - \eta \frac{3}{4} \lambda_3 A^2} \right] + \\
&\quad \sin(5\omega t) \frac{-A^5}{16} \left[\lambda_5 + \frac{3}{8} \frac{\lambda_3^2}{\lambda_1 - \eta \frac{3}{4} \lambda_3 A^2} \right] \\
y_2 &= \left(\frac{A^5}{8 \cdot 16 \omega^2} \frac{5}{3} \left[\lambda_5 + \frac{3}{8} \frac{\lambda_3^2}{\lambda_1 - \eta \frac{3}{4} \lambda_3 A^2} \right] - 3 \left[5\lambda_5 + \frac{\lambda_3^2}{\lambda_1 - \eta \frac{3}{4} \lambda_3 A^2} \right] \right) \sin(\omega t) \\
&\quad \left(\frac{A^5}{8 \cdot 16} \left[5\lambda_5 + \frac{\lambda_3^2}{\lambda_1 - \eta \frac{3}{4} \lambda_3 A^2} \right] \right) \sin(3\omega t) \\
&\quad \left(\frac{-A^5}{24 \cdot 16} \left[\lambda_5 + \frac{3}{8} \frac{\lambda_3^2}{\lambda_1 - \eta \frac{3}{4} \lambda_3 A^2} \right] \right) \sin(5\omega t) \tag{4.45}
\end{aligned}$$

$$\omega_2 = -\frac{27\lambda_3^2 A^4}{128(\lambda_1 + \eta\omega_1)} + \frac{5}{8} \lambda_5 A^4 \tag{4.46}$$

Now one can put $\eta = 1$, express A from the initial condition and obtain the desired asymptotic.

In domain D_4 the motion becomes more complicated, there higher order harmonics in the expansion must be included. An example is shown in figure 4.8. It turns out that to approximate the double RF potential in this region quite many terms in the power series are required and even with a "fast" perturbation technique one would end up with a lengthy procedure. One could obtain the spectrum by numerical integration instead. It appears that this spectrum is rather regular and contains three considerable harmonics - first, third and fifth harmonics of the base frequency.

In domain D_5 the motion is not oscillatory. It is not difficult to perform the same procedure for that case using asymptotic expansion in $\phi(t) = \alpha t + \beta \hat{\phi}(\omega t)$. However, the motion in that region is not related to the escape problem. Putting the aforesaid together, one represents the motion as

$$\phi(t) = \phi_1 \sin(\omega t) + \phi_3 \sin(3\omega t) + \phi_5 \sin(5\omega t) + \dots \tag{4.47}$$

$$p(t) = p_1 \cos(\omega t) + p_3 \cos(3\omega t) + p_5 \cos(5\omega t) + \dots \tag{4.48}$$

where the coefficients and the frequency are obtained either by the asymptotic expansion or by numerical integration.

Finally, we write down the Fokker-Planck equation. Since the drift and diffusion coefficients satisfy

$$a(H) = \frac{1}{2} \frac{\partial [b^2(H)]}{\partial H} \tag{4.49}$$

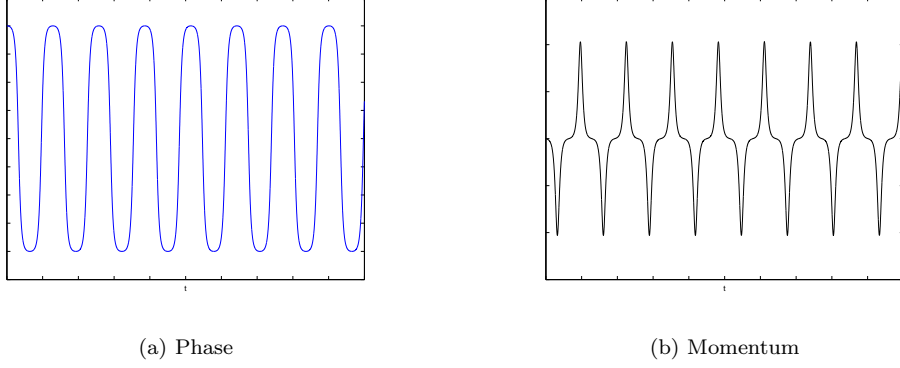
the Fokker-Planck equation for the density evolution takes the form

$$\frac{\partial f(H)}{\partial t} = \frac{\partial}{\partial H} \left(\frac{b^2(H)}{2} \frac{\partial f(H)}{\partial H} \right) \tag{4.50}$$

Some cases are shown below

1. Amplitude noise, $\xi_1(t) \neq 0$, $\xi_{2,3,4} = 0$.

Figure 4.6: Motion close to the separatrix



$$\begin{aligned}
g_\varepsilon = & -K_1 K_3 \xi_1(t) \times \\
& \left\{ \frac{i}{4} [e^{i2\omega t} - e^{-i2\omega t}] [-\phi_1 p_1 + \phi_1 p_3 - \phi_3 p_1 + \phi_3 p_5 - \phi_5 p_3 + \dots] + \right. \\
& \frac{i}{4} [e^{i4\omega t} - e^{-i4\omega t}] [-\phi_1 p_3 + \phi_1 p_5 - \phi_3 p_1 - \phi_5 p_1 + \dots] + \\
& \frac{i}{4} [e^{i6\omega t} - e^{-i6\omega t}] [-\phi_1 p_5 - \phi_3 p_3 + \phi_5 p_1 + \dots] + \\
& \frac{i}{4} [e^{i8\omega t} - e^{-i8\omega t}] [-\phi_3 p_5 - \phi_5 p_3 + \dots] + \\
& \left. \frac{i}{4} [e^{i10\omega t} - e^{-i10\omega t}] [-\phi_5 p_5 + \dots] + \dots \right\}
\end{aligned} \tag{4.51}$$

the diffusion coefficient becomes

$$b^2(H) = \frac{1}{32} K_1^2 K_3^2 \sum_n G_{2n}^2 S_{11}(2n\omega(H)) \tag{4.52}$$

where G_{2n} is the coefficient appearing before $e^{\pm i2n\omega t}$ in 4.51. If one employs the asymptotic expansion then p_j and q_j are polynomials of degree $\frac{j}{2}$ in H and one gets

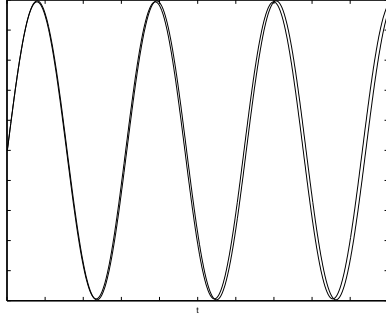
$$b^2(H) = b_2 H^2 + b_3 H^3 + b_4 H^4 + \dots \tag{4.53}$$

$$b_2 H^2 = \frac{1}{32} K_1^2 K_3^2 [\phi_1^2 p_1^2] S_{11}(2\omega(H)) + \dots \tag{4.54}$$

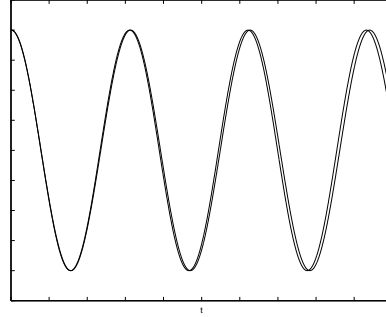
$$b_3 H^3 = \frac{1}{32} K_1^2 K_3^2 [-\phi_1 p_1 \phi_1 p_3 + \phi_1 p_1 \phi_3 p_1] S_{11}(2\omega(H)) + \dots \tag{4.55}$$

$$b_4 H^4 = \frac{1}{32} K_1^2 K_3^2 [(\phi_1^2 p_3^2 + \phi_3^2 p_1^2) S_{11}(2\omega(H)) + (\phi_1^2 p_3^2 + \phi_3^2 p_1^2) S_{11}(4\omega(H))] + \dots \tag{4.56}$$

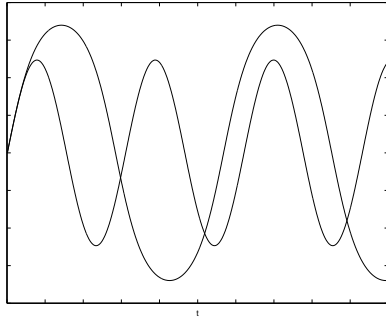
Figure 4.7: Comparison of first order solutions obtained with method of frequency adjustment to numerical integration



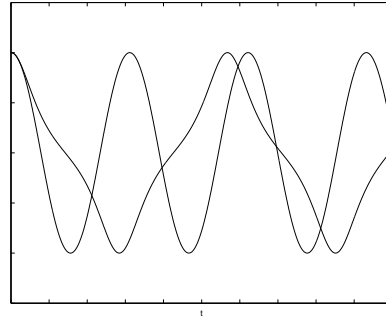
(a) Phase, small amplitude



(b) Momentum, small amplitude



(c) Phase, large amplitude



(d) Momentum, large amplitude

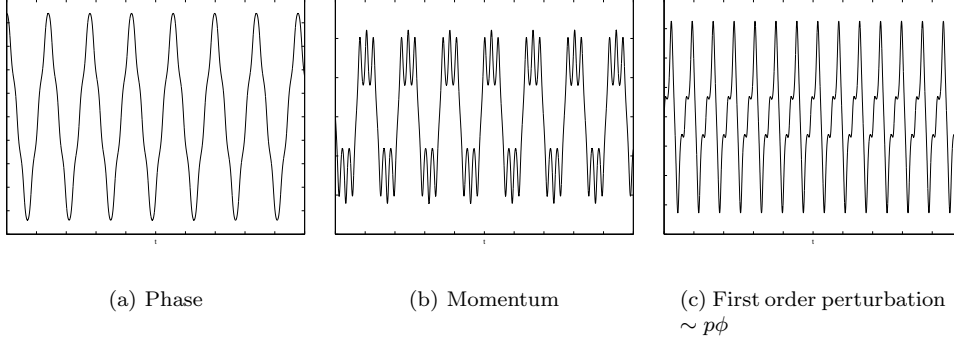
and the omitted terms are small. The stronger the nonlinearity the more terms should be taken in account. The $2n$ -th harmonic of the synchrotron frequency in the spectral density has a contribution of order H^{2n} because the spectrum of the asymptotic expansion decays as $H^{(2n-1)/2}$.

2. Phase noise, $\xi_3(t) \neq 0$, $\xi_{1,2,4} = 0$. To the second order

$$\begin{aligned}
 g_\varepsilon = & -K_1 \xi_3(t) \times \left\{ \frac{i}{2} [e^{i\omega t} - e^{-i\omega t}] \left[\phi_1 - \frac{1}{3!} (\phi_1^3 + \phi_3^2) + \right] + \right. \\
 & \frac{i}{2} [e^{i3\omega t} - e^{-i3\omega t}] [\phi_3 -] + \\
 & \left. \frac{i}{2} [e^{i5\omega t} - e^{-i5\omega t}] [\phi_5 -] + \dots \right\}
 \end{aligned} \tag{4.57}$$

$$b^2(H) = \frac{1}{8} K_1^2 \sum_n G_n^2 S_{33}(n\omega(H)) \tag{4.58}$$

Figure 4.8: Motion in the gap created by two RF systems



$$b^2(H) = b_1H + b_2H^2 + b_3H^3 + \dots \quad (4.59)$$

$$b_1H = \frac{1}{8}K_1^2(\phi_1^2)S_{33}(\omega(H)) = \quad (4.60)$$

The expressions were derived in the absence of the second RF system voltage $K_2 = 0$. It is easy to see that it does not introduce any qualitative (and quantitative) difference as far as first few terms in the expansion are concerned and just contributes additively some portion to the diffusion coefficient. To this end it can be neglected.

The asymptotic solutions can fail on approaching the separatrix. Moreover there the averaging procedure is also not applicable. So the meaning of the diffusion coefficient in the separatrix vicinity is somewhat undefined. We propose that the motion near the separatrix be rather related to the boundary conditions imposed on the Fokker-Planck equation by determining the distribution of exit domains. This issue is discussed in more detail in section 4.4.3.

A similar procedure can be applied to arrive at the Fokker-Planck equation in action-angle variables. Suppose the Hamiltonian is expressed as

$$H(J, \varphi) = H_0(J) + V(J, \varphi)\xi(t) \quad (4.61)$$

Then the averaging with respect to the random perturbation $\xi(t)$ will also lead to the Fokker-Planck equation with the drift and diffusion coefficients expressed through the spectral density. Here we write down the equation for the case of white noise $\xi(t) = dW_t$ (J and φ subscripts indicate differentiation and the superscript indices mean indices, $\omega(J) = \frac{\partial H_0}{\partial J}$)

$$f_t = -(A^J f)_J - (A^\varphi f)_\varphi + \frac{1}{2} (D^{JJ} f)_{JJ} + \frac{1}{2} (D^{\varphi\varphi} f)_{\varphi\varphi} + (D^{J\varphi} f)_{J\varphi} \quad (4.62)$$

The coefficients are derived according to the usual rule

$$\begin{aligned} A^J(J_0) &= \lim_{t \rightarrow 0} \frac{\langle J(t) - J_0 \rangle}{t} = \lim_{t \rightarrow 0} \frac{1}{t} \left\langle \int_0^t -V_\varphi(J(s), \varphi(s)) dW_s \right\rangle = \\ &= \lim_{t \rightarrow 0} \frac{1}{t} \int_0^t \left\langle dW_s \int_0^s - \left[V_\varphi(J_0, \varphi_0) - V_{J\varphi}(J_0, \varphi_0) \int_0^s V_\varphi(J, \varphi) dW_\tau + V_{\varphi\varphi}(J_0, \varphi_0) \int_0^s V_J(J, \varphi) dW_\tau \right] \right\rangle = \end{aligned}$$

$$\lim_{t \rightarrow 0} \frac{1}{t} \int_0^t \langle -[V_\varphi(J_0, \varphi_0)dW_s - V_{J\varphi}(J_0, \varphi_0)V_\varphi(J_0, \varphi_0)W_s + V_{\varphi\varphi}(J_0, \varphi_0)V_J(J_0, \varphi_0)W_s] \rangle = -\frac{1}{2}(V_{\varphi\varphi}V_J - V_{J\varphi}V_\varphi)$$

$$D^{JJ}(J_0) = \lim_{t \rightarrow 0} \frac{\langle (J - J_0)^2 \rangle}{t} = \lim_{t \rightarrow 0} \frac{1}{t} \int_0^t \langle [V_\varphi(J_0, \varphi_0)dW_s - V_{J\varphi}(J_0, \varphi_0)V_\varphi(J_0, \varphi_0)W_s + V_{\varphi\varphi}(J_0, \varphi_0)V_J(J_0, \varphi_0)W_s]^2 \rangle = V_{\varphi\varphi}^2$$

Here properties of the stochastic integral were used (see Chapter 2). The other coefficients are obtained in the same fashion. So

$$\begin{aligned} A^J &= -\frac{1}{2}(V_{\varphi\varphi}V_J - V_{J\varphi}V_\varphi) \\ A^\varphi &= \frac{1}{2}(V_{J\varphi}V_J - V_{JJ}V_\varphi) + \omega(J) \\ D^{JJ} &= V_\varphi^2 \\ D^{\varphi\varphi} &= V_J^2 \\ D^{J\varphi} &= -V_JV_\varphi \end{aligned}$$

one can average out the angle variable in case of fast oscillations. With the Hamiltonian

$$H(J, \varphi) = H_0(J) + \sum_n V_n(J)e^{i\omega_n\varphi}\xi(t) \quad (4.63)$$

the Fokker-Planck equation reduces to

$$f_t = (D(J)f_J)_J \quad (4.64)$$

with

$$D(J) = \frac{1}{2} \sum_n V_n^2(J)\omega_n^2 \quad (4.65)$$

In action-angle variables the diffusion coefficient has a simpler dependency on the perturbation V , but the latter is obtained by a series of canonical transformations of the original perturbation and normally has complex dependency on the angle variable.

4.3 Effect of coherence

Now we are in a position to come back to the problem of the coherent nature of noise. With techniques similar to those used in the sketch of the proof of the limit theorem in Appendix B it can be shown that in the limit of weak noise this effect is expected to disappear as soon as the system possesses a finite frequency spread.

To arrive at more useful estimates one considers the distribution function itself to be a random quantity. Consider a Hamiltonian system with random potential of the form

$$H(q, p) = \frac{p^2}{2} + U(q) + V(q, p)\xi(t) \quad (4.66)$$

The distribution function satisfies the Liouville equation with random coefficients

$$\frac{\partial f}{\partial t} + \left(p + \frac{\partial V}{\partial p}\xi(t) \right) \frac{\partial f}{\partial q} - \left(\frac{\partial U}{\partial q} + \frac{\partial V}{\partial q}\xi(t) \right) \frac{\partial f}{\partial p} = 0 \quad (4.67)$$

To fully describe the statistical properties of the density one would need to define the probability measure in the appropriate functional space, or the density functional. It is equivalent to assigning probabilities to all possible configurations in the particle phase space. One can argue that this complete statistical information can be roughly reduced to the knowledge of some averaged quantities. To the second order these are the mean and the space correlation of the distribution function

$$\bar{f}(q, p, t) = \langle f(q, p, t) \rangle_\xi \quad (4.68)$$

$$K(q, p, q', p', t) = \langle [f(q, p, t) - \bar{f}(q, p, t)] [f(q', p', t) - \bar{f}(q', p', t)] \rangle_\xi \quad (4.69)$$

The averages are taken over all possible realisations of the random process. The correlation describes the fluctuations of the average density. Higher order space and time correlations can be defined as well and give statistical information of less significance.

Here we sketch how to calculate the evolution of the correlator for an oscillating system with frequency spread subject to white noise. For colored noise the equations can be obtained with averaging techniques similar to those applied in section 4.2 and no principal difficulty is introduced at least in the weak noise limit. Unlike for the case of the averaged Fokker-Planck equation, in this problem the fast oscillations in the phase space cannot be directly averaged. The average is taken with respect to the random perturbation only. It is convenient to consider the problem in action-angle variables. Let the Hamiltonian be

$$H(J, \varphi) = H_0(J) + V(J, \varphi)\xi(t) \quad (4.70)$$

It can be argued that the mean density is given by the same Fokker-Planck equation as the probability density of individual trajectories in the incoherent case. This is possible as soon as the time scale of interest is much greater than any correlation time of the random perturbation. The increment of the distribution function on time interval Δt is

$$\Delta f(J, \varphi) = f_J \Delta J + f_\varphi \Delta \varphi + \frac{1}{2} f_{JJ} (\Delta J)^2 + \frac{1}{2} f_{\varphi\varphi} (\Delta \varphi)^2 + f_{J\varphi} (\Delta J) (\Delta \varphi) \quad (4.71)$$

where the increments of the averages determine the usual drift and diffusion coefficient in the Fokker-Planck equation, i.e.

$$\langle \Delta J \rangle = A^J, \quad \langle \Delta \varphi \rangle = A^\varphi, \quad \langle (\Delta J)^2 \rangle = D^{JJ}, \quad \langle (\Delta \varphi)^2 \rangle = D^{\varphi\varphi}, \quad \langle (\Delta J \Delta \varphi) \rangle = D^{J\varphi}, \quad (4.72)$$

One can obtain the partial differential equation for the correlator by considering its increment, expanding it to the second order and then tending the time increment to zero. With the prime denoting the function argument to be primed coordinates and the subscripts denoting partial differentiation, this equation reads

$$\begin{aligned} K_t = & \frac{1}{2} [V_{J\varphi} V_J - V_{JJ} V_\varphi + \omega(J)] K_\varphi + \frac{1}{2} [V_{J'\varphi} V_{J'} - V_{J'J'} V_{\varphi'} + \omega(J')] K_{\varphi'} - \\ & \frac{1}{2} [V_{\varphi\varphi} V_J - V_{J\varphi} V_\varphi] K_J - \frac{1}{2} [V_{\varphi'\varphi'} V_{J'} - V_{J'\varphi'} V_{\varphi'}] K_{J'} + \frac{1}{2} V_J^2 K_{\phi\phi} + \frac{1}{2} V_{J'}^2 K_{\phi'\phi'} + \end{aligned}$$

$$\begin{aligned} & \frac{1}{2}V_\varphi^2 K_{JJ} + \frac{1}{2}V_{\varphi'}^2 K_{J'J'} - V_\varphi V_J K_{J\varphi} - V_{\varphi'} V_{J'} K_{J'\varphi'} + \\ & V_\varphi V_{\varphi'} K_{JJ'} - V_\varphi V_{J'} K_{J\varphi'} - V_{\varphi'} V_J K_{J'\varphi} + V_J V_{J'} K_{\varphi\varphi'} + \\ & V_\varphi V_{\varphi'} \hat{f}_{JJ} - V_\varphi V_{J'} \bar{f}_{JJ} - V_J V_{\varphi'} \hat{f}_{\varphi J'} + V_J V_{J'} \bar{f}_{\varphi J'} \end{aligned}$$

Taking in account the smallness of noise compared to the oscillation period one arrives at the averaged equation in which only the difference between the angle variables φ and φ' enters

$$K_t = [\omega(J) - \omega(J')] K_\varphi + [D(J)K_J]_J + [D(J')K_{J'}]_{J'} + G_1(J, J', \varphi) K_{\varphi\varphi} + G_2(J, J', \varphi) [\bar{f}_{JJ} + K_{JJ'}] \quad (4.73)$$

with

$$G_1(J, J', \varphi) = \frac{1}{2} \sum_n [V_{n,J}^2 + V_{n,J'}^2] + \sum_n V_{n,J} V_{-n,J'} e^{i\omega_n \varphi} \quad (4.74)$$

$$G_2(J, J', \varphi) = \frac{1}{2} \sum_n n^2 V_n(J) V_{-n}(J') \quad (4.75)$$

An asymptotic solution for the correlation function was found in [26]. One can estimate the value of the correlation at the same point $J = J'$ which shows the intensity of density fluctuations. It turns to be of order

$$K(J, J') \sim \left(D / \frac{\partial \omega}{\partial J} \right)^{2/3}. \quad (4.76)$$

This can be qualitatively explained by the fact that the first term in 4.73 is oscillating and the correlation itself "decoheres". The diffusive term in the equation destroys the fine structure produced by this oscillations and the correlation is finally dissipated.

So for sufficiently weak noise the spatial correlations will be small and the density evolution can be calculated according to the Fokker-Planck equation. This results were obtained in [26]. For the case of RF noise the part of the beam where the correlations can persist over the time scale of interest are negligibly small for the usual parasitic noise levels. An exceptional situation may arise, for example, if the random perturbation is not stationary. If the system is subject to noise which acts in short "pulses" but is of moderate intensity so that its total intensity is still small, then such correlations can appear. This can happen, for example, when employing noise for various stabilisation purposes (see Chapter 5). There the beam response may turn to be a collective oscillation rather than a diffusion. In systems which can exhibit self-excitation (like beam-cavity systems) enhancements of this effect may be observed.

4.4 Solving the Fokker-Planck equation

A diffusion equation may be solved by a variety of methods. An analytical solution is of course more desirable than a numerical one since it can be easier analysed with respect to parameters. A usual analytical method is reducing the equation to the eigenvalue problem for the Fokker-Planck operator by separation of variables. The simplest possible boundary value condition for the probability density is the absence of flux at $H = 0$ and loss of particles at some value of H , say, $H = 1$. Even in this situation many difficulties arise. The coefficients entering the Fokker-Planck operator are polynomials of H of the form

$$b_1 H + b_2 H^2 + b_3 H^3 + \dots \quad (4.77)$$

The first difficulty is that analytical solutions to the eigenvalue problem cannot be generally found for polynomials of high order. This difficulty is not essential, since the coefficients of higher powers

appear to be small and perturbation techniques may be employed to evaluate the spectrum. However such calculations may be extremely cumbersome and lengthy. A more fundamental difficulty is that the coefficients are "singular" at $H = 0$ and the Fokker-Planck operator is not "strictly elliptic" there. This means that the spectrum needn't be discrete. But for a continuous spectrum the eigenvalue analysis is not convenient.

Later it is shown that more complicated boundary conditions can arise for which the spectral analysis is even more difficult. In a general situation only a numerical solution is possible.

4.4.1 A two-point boundary value problem

Assume that the particles are lost when they reach some value $H = H_0$ (say, the separatrix). Therefore, there is a unique diffusion process describing the evolution of the particle ensemble on $[0, H_0]$ and since no particles disappear in the centre of the bunch ($H = 0$), one requires that there is zero probability flux at $H = 0$. Using the variable x instead of H for convenience, the boundary value problem for the diffusion process becomes

$$\begin{aligned}\frac{\partial u(x, t)}{\partial t} &= L_{FPO}u(x, t) \\ u(x, t)|_{x=1} &= 0 \\ (b^2(x)u'(x, t)|_{x=0}) &= 0 \\ u(x, 0) &= f(x)\end{aligned}$$

with the Fokker-Planck operator

$$L_{FPO}u(x, t) = \left(\frac{1}{2}b^2(x)u'(x, t) \right)' \quad (4.78)$$

Consider the eigenvalue problem, i.e. the problem of finding g and λ such that

$$L_{FPO}g = -\lambda g \quad (4.79)$$

and g satisfies the boundary conditions. If the set of eigenfunctions $\{g_i\}$ is a complete countable set then we may search the solution as

$$u(x) = - \sum g_i(x)T_i(t) \quad (4.80)$$

where $T_i(t)$ are arbitrary functions of time. Substituting this representation into 4.78 we get

$$\begin{aligned}\dot{T}_i(t) &= -\lambda_i T_i(t) \\ \sum g_k(x)T_k(0) &= f(x)\end{aligned} \quad (4.81)$$

If $\{g_i\}$ is also orthonormal set of functions, then multiplying the second of equations 4.81 scholarly by $g_i(x)$ we arrive at

$$\begin{aligned}\dot{T}_i(t) &= -\lambda_i T_i(t) \\ T_i(0) &= (f(x), g_i(x)) = c_i\end{aligned} \quad (4.82)$$

and

$$u(x) = \sum c_i g_i(x) e^{-\lambda_i t} \quad (4.83)$$

The spectrum may also be continuous and then

$$u(x) = \int c(\lambda) g_\lambda(x) e^{-\lambda t} d\lambda \quad (4.84)$$

The eigenvalue problem can be solved explicitly only in rare cases. Sometimes we may calculate the spectrum approximately with the help of perturbation techniques [36] or with the help of a numerical method.

Some important special cases can be treated analytically [34]

1.

$$(aux')' = -\lambda u \quad (4.85)$$

The solution is

$$u = C_1 J_0 \left(2\sqrt{\frac{\lambda x}{a}} \right) + C_2 Y_0 \left(2\sqrt{\frac{\lambda x}{a}} \right) \quad (4.86)$$

Where J_0 and Y_0 are Bessel functions of first and second type. $C_{1,2}$ and λ_n are determined from the boundary condition. Say, if $xu(x) \rightarrow 0$ at $x \rightarrow 0$ and $u(1) = 0$ then the eigenvectors are

$$u_i = C_1 J_0 \left(2\sqrt{\frac{\lambda_i x}{a}} \right) \quad (4.87)$$

where λ_i is the root of

$$J_0 \left(2\sqrt{\frac{\lambda}{a}} \right) = 0 \quad (4.88)$$

2.

$$([bx^2 + Ax]u')' = -\lambda u \quad (4.89)$$

The solution with $[bx^2 + ax]u' = 0$ at $x \rightarrow 0$ is given by

$$u(x) = CP_\nu \left(1 + \frac{2bx}{a} \right), \quad \nu = \frac{-\sqrt{b} + \sqrt{b-4\lambda}}{2\sqrt{b}} \quad (4.90)$$

where $P_\nu(x)$ is the Legendre polynomial and ν is the root of

$$P_\nu \left(1 + \frac{2b}{a} \right) = 0 \quad (4.91)$$

3. If one lets $a = 0$ in the previous case then

$$(bx^2u')' = -\lambda u \quad (4.92)$$

The solution of this equation is

$$u(x) = C_1 x^{\frac{-\sqrt{b}-\sqrt{b-4\lambda}}{2\sqrt{b}}} + C_2 x^{\frac{-\sqrt{b}+\sqrt{b-4\lambda}}{2\sqrt{b}}} \quad (4.93)$$

The condition $u(1) = 0$ leads to $C_1 = C_2 = C$ and $x^2 u(x) \rightarrow 0$ at $x \rightarrow 0$ leads to

$$0 < 1 - 4\frac{\lambda}{b} < 9 \quad (4.94)$$

One sees that in the first case the spectrum is discrete whereas in the second and third it is continuous. Case 1 arises in the averaged Fokker-Planck operator for systems with phase noise, case 2 and 3 when the amplitude noise is present (see section 4.5).

Numerical methods of solving a two-point boundary value problem (Neumann or Dirichlet) for the Fokker-Planck equation are well known [13] and do not deserve a discussion.

4.4.2 The system of equations with coupled boundary values arising from averaging of stochastic systems with complicated phase space where branching can occur

The averaging procedure is applicable to regions of the phase space which do not contain separatrices. In the vicinity of a separatrix the oscillation period grows infinitely and the averaging does not work. Therefore, the Hamiltonian cannot be used as the slow variable for domains of phase space containing separatrices and unstable fixed points since then there will be multiple trajectories corresponding to the same value of H . (This is the case with center and side RF buckets). One also has to keep in mind that the synchrotron coordinate map might be no more well approximated by the differential equation in the vicinity of an unstable fixed point for some parameters. To overcome these difficulties we treat the vicinity of a separatrix as some layer. After a particle enters this layer it escapes it after a short time in case the layer is sufficiently thin compared to the magnitude of the random perturbation. The point of escape belongs to one of the domains D_i where the slow variable obeys a certain Fokker-Planck equation. We can characterize the "transition layer" by probabilities with which it transports a particle from domain D_i to domains D_j . Then a sort of balancing condition arises that the fluxes at the boundaries of the domains must satisfy. Taking into consideration the fact that in each domain we have an averaged diffusion process in only one variable H , this situation may be represented by the following model. Consider a set of N unit intervals and N diffusion processes on these intervals. Suppose that on each interval a particle reaching one of the boundary points can disappear, be reflected from this point or jump to some other boundary point of any of the intervals from the set.

Say, a diffusion process on the i -th interval is governed by the Fokker-Planck equation

$$\frac{\partial u_i(x, t)}{\partial t} = \frac{\partial}{\partial x} (G_i(x)) \quad (4.95)$$

with

$$G_i(x) = \frac{b_i^2(x)}{2} u_i'(x) \quad (4.96)$$

Suppose the thickness of the "layers" is sufficiently small compared to the absolute value of the drift and diffusion coefficients. Then one can assume that a particle reaching the 'layer' will necessarily cross it and no reflection occurs (this assumption is reasonable since the variation of the paths of a Brownian motion is infinite). Therefore, assume that absorption can occur only at the points which are not 'branching' ³.

Suppose that a particle leaving the left (right) boundary of a certain interval i appears at the left boundary of interval j with probability T_{ij}^{LR} (T_{ij}^{RR} , T_{ij}^{RL} , T_{ij}^{LL}). Consider a simple case with $N = 3$ and $T_{12}^{RL} = \alpha$, $T_{13}^{RL} = 1 - \alpha$

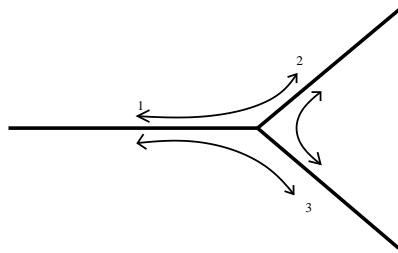
³with reflections and absorptions allowed at arbitrary points the conditions become more complicated, but this is not required in our case

This is a simple model of branching behavior at the unstable fixed point nearest to the bunch center, where a particle can either go to the side bucket or start to drift in the coasting beam. Then one requires

$$\begin{aligned} G_2(0+) &= \alpha G_1(1-) \\ G_3(0+) &= (1 - \alpha)G_1(1-) \end{aligned}$$

More general cases are treated by imposing the balancing conditions in the same manner.

Figure 4.9: When the phase space is complicated the problem of density evolution can be reduced to a diffusion on a graph.

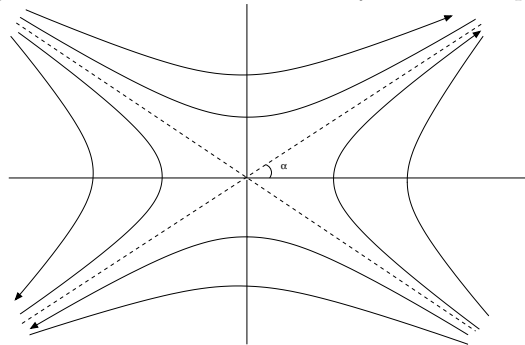


We do not touch uniqueness and existence for such kind of boundary value problems. But since the random process under consideration is a well-defined Markov process with jumps, they are expected.

4.4.3 On the mechanism of separatrix crossing

Now we want to study the "transport properties" of the "separatrix layers". One can introduce a new coordinate system moving with the particle which travels on one side of the separatrix sufficiently close to it. Then the problem can be reduced to the problem of exit of a certain random process from a certain domain. However, the resulting domain and the random process will have complex properties and such setup seems to be not useful in practice and one would generally need to perform some brute force simulations.

Figure 4.10: Motion in the vicinity of a saddle point



The situation can be simplified in the limit of weak noise $\varepsilon \rightarrow 0$. Approaching the separatrix, the trajectory will spend more and more time in the neighbourhood of the fixed point. Then for sufficiently small perturbations the probability that the trajectory deviates from the unperturbed one outside of such

neighborhood is small and the whole effect of the perturbation will take place around the fixed point (see fig. 4.10). There the linear part of the equation dominates and one has a linear stochastic equation describing the motion sufficiently well. Then from the distribution of exit points from this neighborhood one will know the transition probabilities between the domains after crossing the separatrix. The diffusion coefficient of the random process will have some singularity due to divergence of trajectories going on different sides of the separatrix. This makes the analytical treatment difficult⁴. But the numerical study of the linear system is trivial. Unlike for the nonlinear case, one can with a linear transformation arrive at a system with no small parameters and easily simulate the distribution of exit points.

Consider the linear system

$$\begin{aligned}\dot{\phi} &= p + \varepsilon\xi_1(t) \\ \dot{p} &= \lambda\phi(1 + \varepsilon\xi_2(t))\end{aligned}$$

which after transformation $\hat{p} = \frac{p}{\sqrt{\lambda}}$, $\hat{\phi} = \phi$ becomes

$$\begin{aligned}\dot{\hat{\phi}} &= \sqrt{\lambda}\hat{p} + \varepsilon\xi_1(t) \\ \dot{\hat{p}} &= \sqrt{\lambda}\hat{\phi}(1 + \varepsilon\xi_2(t))\end{aligned}$$

The sample paths of the system are shown in figure 4.11. One can immediately see the qualitative influence of the separatrix slope $\sqrt{\lambda}$ on the dynamics of the random motion. The influence of the phase noise ξ_1 increases as $\lambda \rightarrow 0$ and drops as $\lambda \rightarrow \infty$. The amplitude noise ξ_2 acts in the same manner, but the time it has for its action grows as $\frac{1}{\sqrt{\lambda}}$. The most probable displacement of a random process is along the drift and against the gradient of the diffusion. The drift is given by the trajectories in figure 4.10, the diffusion gradient is zero for phase noise and upwards for amplitude. So, by stretching the trajectories of the unperturbed motion "vertically" or "horizontally" one gets the enhancement of the amplitude and phase noise correspondingly. This is the geometrical meaning of the slope $\sqrt{\lambda}$. These considerations lead to the conclusion that the increase of the slope leads to larger escape rate to the domains D_1 and D_3 under influence of both noise species. Such behavior is a consequence of the fact that it is easier to get out of the steep potential well.

In practice the particular escape rates can be estimated numerically. An example of the histogram of exit domain distribution is shown in figure 4.12. This distribution depends weakly on the changes of the slope. A slight change can be observed when the main voltage is changed considerably, but small changes like that introduced by the second RF system have no influence.

It has to be understood that the linearized system even when solved precisely would introduce some small error in the escape rate. But it can give

4.4.4 On numerical solution of the coupled system

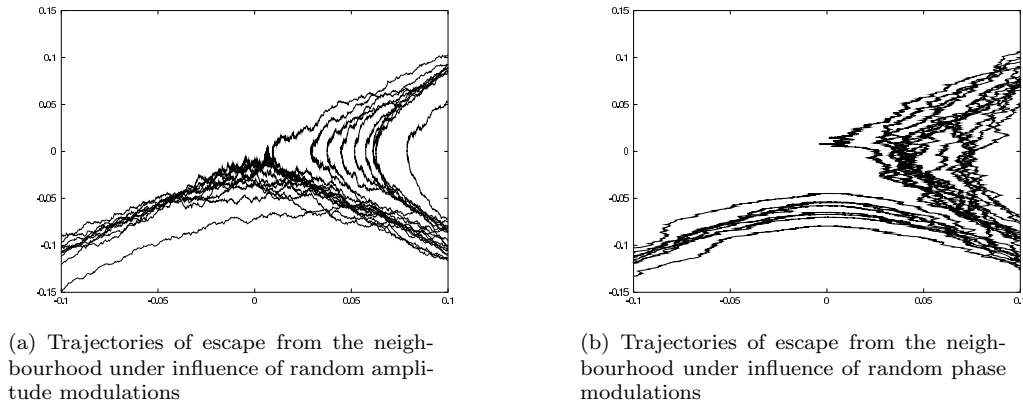
As we have seen, analytical methods of solution fail even in the case of a two-point boundary value problem when the coefficients are sufficiently "bad". In case of the system of equations with coupled boundary values the situation can become only worse. To obtain a solution numerical methods must be employed. We have tried several methods:

1. Algorithms based on Laplace transform [6]. Let $u(t)$ be a real-valued function, then its Laplace transform is given by

$$v(s) = L[u; s] = \int_0^{\infty} e^{-st}u(t)dt \quad (4.97)$$

⁴An asymptotic expansion was attempted by the author, but did not give satisfactory results. Further study is required.

Figure 4.11: Perturbed Motion in the vicinity of a saddle point



Applying the Laplace transform to a Fokker Planck equation and noticing that

$$L\left[\frac{\partial u(t)}{\partial t}\right] = -u(0) + L[u]$$

one gets with $v(s, x) = L[u(x, t); s]$

$$-f(x) + sv(s, x) = \left(\frac{b^2(x)}{2}v'(s, x)\right)' \quad (4.98)$$

Therefore, $v(s, x)$ satisfies the same boundary conditions as $u(x, t)$ in case they don't depend on t . This equation is one-dimensional and sometimes easier to solve than the original one. If we are able to find the solution of 4.98 $v(s, x)$ for all s then $u(x, t)$ is found by inversion. The use of Laplace transform is motivated by the fact that the coupling conditions are easier to treat in the one-dimensional case. However, the inversion of the Laplace transform is not stable and requires special algorithms involving a priori estimates of the solution. Thus this method could work very well for special situations, but it is not robust enough.

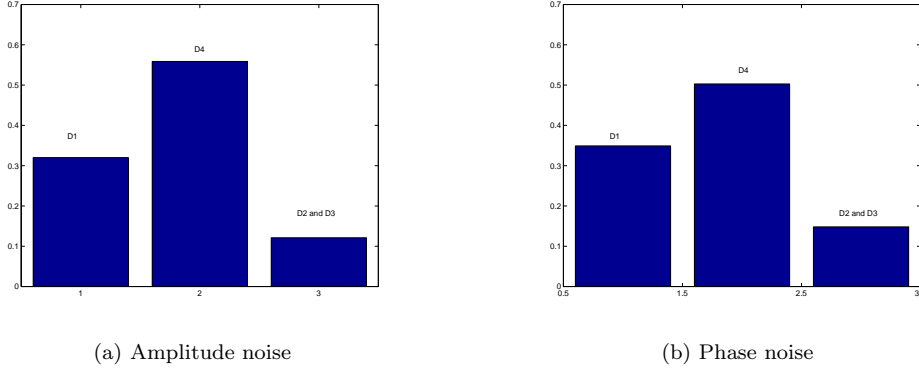
2. Grid methods [13]. We use a standard finite difference scheme for solution of two-point boundary-value problems. For the coupled system the boundary values will introduce difficulties and grid methods are avoided.
3. Monte-Carlo methods. One generates sample paths of the averaged diffusion process and computes the averaged distribution at times of interest. A Fokker-Planck equation

$$\frac{\partial u}{\partial t} = \frac{\partial}{\partial x} \left(\frac{b^2(x)}{2} \frac{\partial u}{\partial x} \right) \quad (4.99)$$

governs the density evolution of the process

$$x(t) = x(0) + \int_0^t b'(x(s))b(x(s))ds + \int_0^t b(x(s))dW_s \quad (4.100)$$

Figure 4.12: A sample histogram of distribution of exit domains from the vicinity of a unstable fixed point



For small h the increment $x(t+h) - x(t)$ is approximately normally distributed with mean $b(x(t))b'(x(t))h$ and variance $b(x(t))h$. A straightforward application of this fact together with treating absorptions and reflections leads to a Monte-Carlo algorithm. Two issues are important for implementation. First, to obtain a correct treatment of reflections, absorptions and to accurately represent the paths, one should have

$$h \sim \frac{|b^2(x)|}{|b'^2(x)| \sqrt{N}} \quad (4.101)$$

Another difficulty is connected with the singularity (vanishing) of the coefficients. The flux through such singular point is zero, no path can reach it, but this condition does not need to hold for approximation with 4.100. Such situation is shown in figure 4.13. Here the flux $0.5b^2(x)u'(x)$ at point 0 (bunch center) is zero, this condition is always satisfied for a bounded density due to vanishing coefficient $b^2(0) = 0$. The Monte-Carlo algorithm however "does not know" about the singularity since the trials are made for some neighbouring points with $x \neq 0$, and finds a solution with vanishing derivative. This solution will have larger escape rate from the vicinity of a singular point than in reality. The error vanishes as the number of trials is increased, but due to this fact the convergence of the method for singular coefficients is substantially slower.

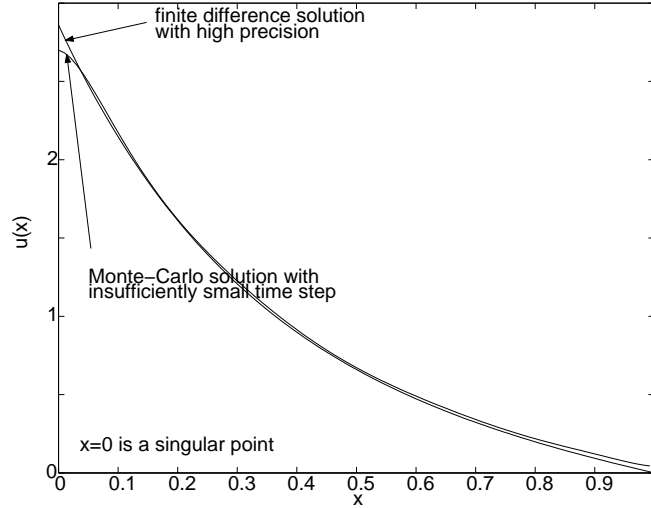
One should also take care of the random number generator. Normally one uses simple formulae like

$$x = \sqrt{-2 \log(u)} \sin(2\pi v) \quad (4.102)$$

with u and v uniformly distributed random numbers. Since uniform random variables are generated with fast recurrent arithmetical methods, this will work rather fast. But the numbers thus generated have a cutoff. This introduces a small error and makes analysis of extreme paths difficult.

Monte-Carlo methods have poor convergence, but are robust and simple to implement. They are good for rough estimate of complex system behavior, but are rarely useful when high precision is required. The estimation of the coasting beam population does not require such precision and with modern computers the performance is acceptable.

Figure 4.13: Derivative error at a singular point



4.5 Impact on synchrotron motion

4.5.1 Bunch diffusion - rough estimates

To estimate the diffusion of particles in the bunch core it is sufficient to take only few terms in the diffusion coefficient representation. Under assumption that phase and amplitude noise are uncorrelated

$$b^2(H) = b_{phase}^2(H) + b_{ampl}^2(H) \quad . \quad (4.103)$$

The first order expansion of the synchrotron oscillations in H gives

$$\begin{aligned} \phi(t) &= \sqrt{H} \sqrt{\frac{2}{K_1}} \sin(\omega t) \\ p(t) &= \sqrt{H} \sqrt{\frac{2\omega^2}{K_1 K_3^2}} \cos(\omega t) \end{aligned}$$

$$\begin{aligned} K_1 &= \frac{qU}{ET} \\ K_3 &= \frac{2\pi h\alpha}{T} \\ \omega &= K_1 K_3 - \frac{1}{4} K_3 H \end{aligned} \quad (4.104)$$

If we are not interested in the effects produced by the form of the spectral density, we can drop the synchrotron frequency shift and assume that the perturbation is white noise with intensity ε . Then

$$b_{phase}^2(H) = \frac{1}{4} \varepsilon^2 H \quad (4.105)$$

$$b_{ampl}^2(H) = \frac{1}{8}\varepsilon^2 H^2 \omega^2 \quad . \quad (4.106)$$

The amplitude noise has much more influence on the tails of the bunch than on the core. Some numerical examples with exponential initial distribution and zero boundary value at some H_{max} are shown in figure 4.14. In practice such a considerable change in the distribution over the time scale of beam storage can be only possible when the noise is very strong. Usually a much weaker effect is observed.

The first order approximation can be used to describe the bunch core diffusion whereas for tail evolution and the escape rate problem higher order terms should be employed as well as the proper boundary conditions imposed.

4.5.2 Escape from the stable bucket

To assess the escape rate and to determine the ratio between loss and halo population more accurate representation of the diffusion coefficient as well as the calculation of the distribution of escape domains is required. An example of calculations with exaggerated noise level is shown in figure 4.15 and 4.16.

4.5.3 On effects of noise spectral density

Under the assumption that the noises are second order random processes one arrives at a substantial dependency of the results on the form of the spectral density. For systems with amplitude dependent frequencies this may lead to a rather arbitrary behavior, i.e. one can adjust the spectrum so that the diffusion coefficient of the averaged system will have arbitrary form at least to some extent. The synchrotron oscillations usually lie within a rather narrow bandwidth (f.e. 0-30 Hz for HERA) and the spectrum of oscillations is rather broad-band, so in reality this possibility is restricted. It can be easily shown that the derivative of the diffusion coefficient is bounded by the quantity of order $\frac{\partial \omega}{\partial H} \frac{\partial S}{\partial \omega}$ where ω is the synchrotron frequency and S is the spectral density of the random perturbation. But the measured spectral densities still have a noticeable gradient. A qualitative example of two quite similar spectral densities and diffusion coefficients derived from them is shown in figure 4.17. If the spectral density is allowed to be more irregular then even larger divergence can occur. It should illustrate the fact that estimating the diffusion in the beam tail is a subtle issue unless the spectral density is known quite precisely.

Adding the second RF system does not qualitatively change the behavior inside the buckets. There it results only in a slight shift of the synchrotron frequency. But for the gap between the inner and outer buckets (domain D_4 in figure 4.5) the motion becomes more irregular (see figure 4.18). The oscillation spectrum includes more higher order harmonics. This means that the noise spectral density at these higher harmonics and their multiples will contribute to the diffusion coefficient.

The synchrotron oscillations spectrum in the beam tail D_4 coming from the second RF system differs from the spectrum in the beam tail without the second system, this can influence the tail diffusion and decide between the formation of bunch tail or the coasting beam. The estimation of this effect is again restricted by the precision of knowledge of the noise spectral density.

4.5.4 Estimates for HERA

A measurement of the cavity voltage fluctuations is not trivial. An attempt to perform such measurements for phase noise at HERA was made [33]. It indicates that there is a possibility that the spectral density is such that the diffusion coefficient at lower synchrotron frequencies is somewhat larger than at the high (figure 4.19). For such a spectrum shape the peaks turn out to be harmonics of the synchrotron frequency of some tail particles, but not of the core. However, the relation of the measured noise to the actual voltage fluctuation during a run is not obvious. The phase noise is usually more likely to appear due to

the complexity of the phase control system. The amplitude is normally generated with a better precision and its fluctuations are usually neglected.

We were not aiming at precise estimates of the bunch diffusion. We suspect that the error in the measurements of the noise spectrum might be considerable enough and definite conclusions cannot be drawn. Even if it is not so, this problem requires a separate investigation and falls out of the scope of this work.⁵ The main goal is to show which impact the double RF system can have on the escape from the bucket and halo formation. The simulations were performed for noise spectra consistent with the measurements [33] for the phase noise.

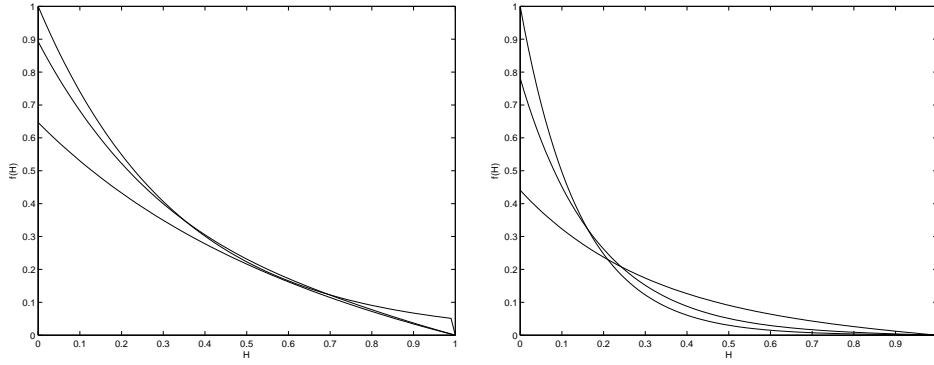
Due to the mentioned difficulties the simulations have a somewhat qualitative nature. They indicate that under certain circumstances the accumulation of noticeable bunch tails in the side buckets is possible. It appears that particles can drift into their centers and accumulate there. The coasting beam itself is also produced with a higher rate, but is then naturally cleaned by the synchrotron radiation mechanism. The halo corresponding to the "gap" (domain D_4) does not usually build up. For details see figures 4.20 and 4.21.

⁵More careful measurements and analysis are planned at the moment.

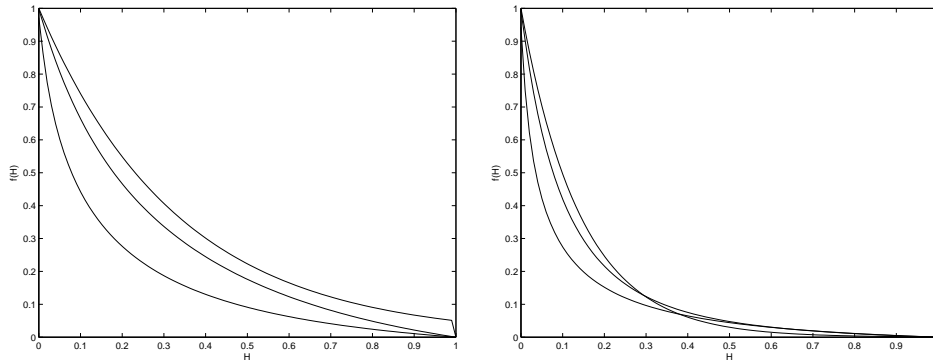
4.6 Summary

- The synchrotron tune spread is responsible for turning random coherent perturbations into random incoherent ones. Without synchrotron tune spread it could be possible to reduce the effect of the RF noise by feedback. But it could hardly have any practical use.
- Both the bunch dilution and the escape rate from the RF bucket can be estimated provided the spectral density of the noise is known. Its incomplete knowledge introduces a substantial uncertainty in the expected escape rate as well as in the entire bunch density evolution.
- Noticeable influence on the core may be produced by the phase noise. Amplitude noise has much more impact on the tails than on the bunch core.
- The second RF voltage introduces a region where a broader region of the noise spectral density influences the motion, this can lead to diffusion enhancement in the bunch tails or halo formation.
- The RF noise can be well responsible for the coasting beam production by sweeping away the bunch tails.

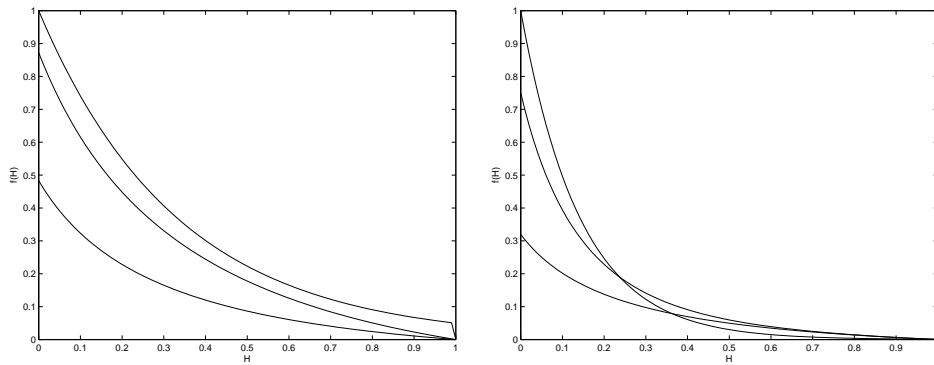
Figure 4.14: Examples of density evolution of the synchrotron invariant under influence of phase and amplitude noise for some model parameters. Distributions are shown for $t = 0h$, $t = 1h$ and $t = 2h$



(c) Phase noise, probability distribution $u(H)$



(f) Amplitude noise, probability distribution $u(H)$



(i) Phase and amplitude noise, probability distribution $u(H)$

Figure 4.15: An exaggerated example of bunch density and halo evolution 1

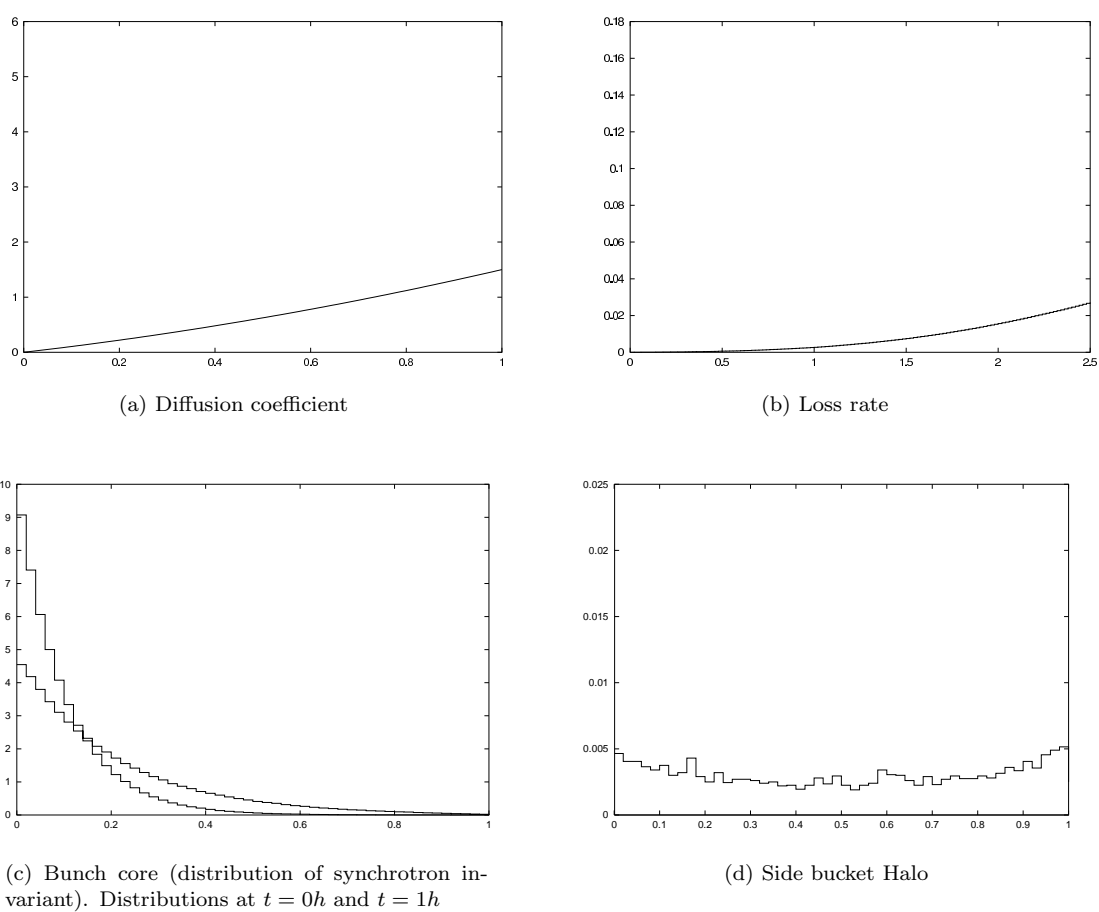
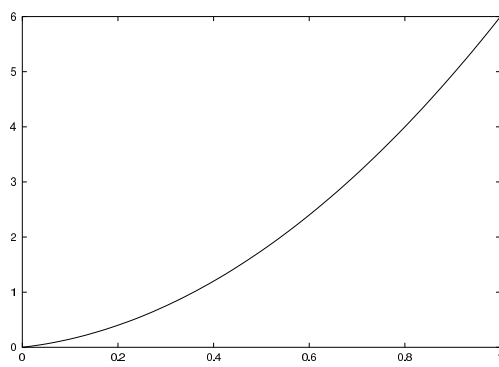
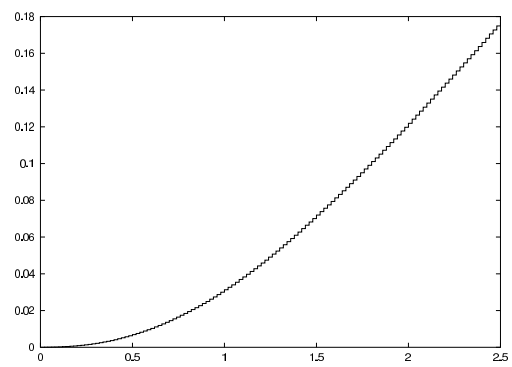


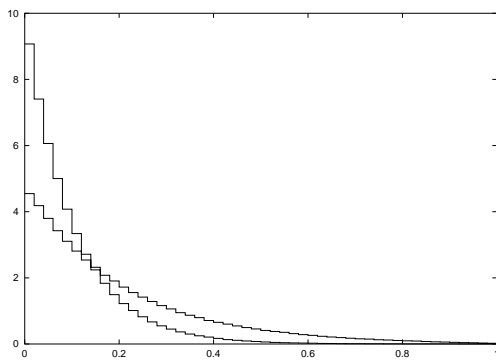
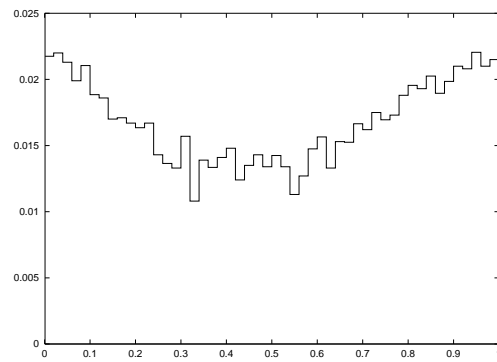
Figure 4.16: An exaggerated example of bunch density and halo evolution 2



(a) Diffusion coefficient



(b) Loss rate

(c) Bunch core (distribution of synchrotron invariant). Distributions at $t = 0h$ and $t = 1h$ 

(d) Side bucket Halo

Figure 4.17: Two spectral densities and diffusion coefficients obtained from them

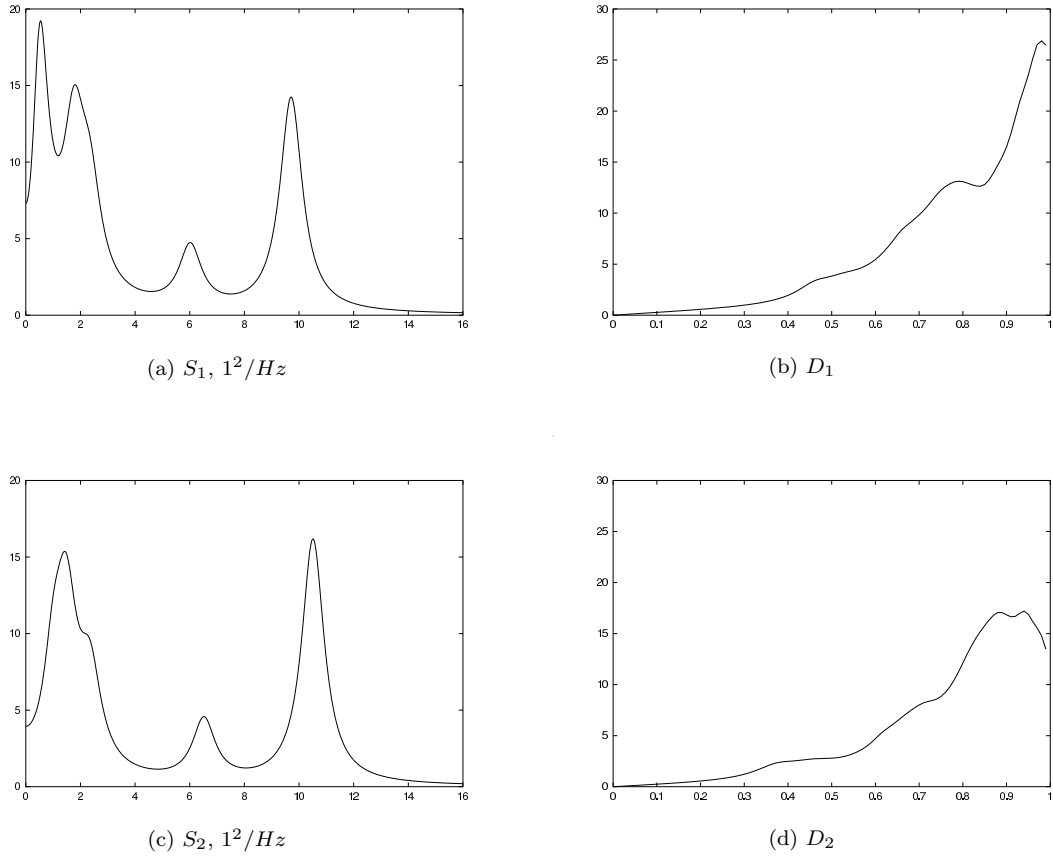


Figure 4.18: Spectrum of the synchrotron oscillations in the gap between inner and outer buckets

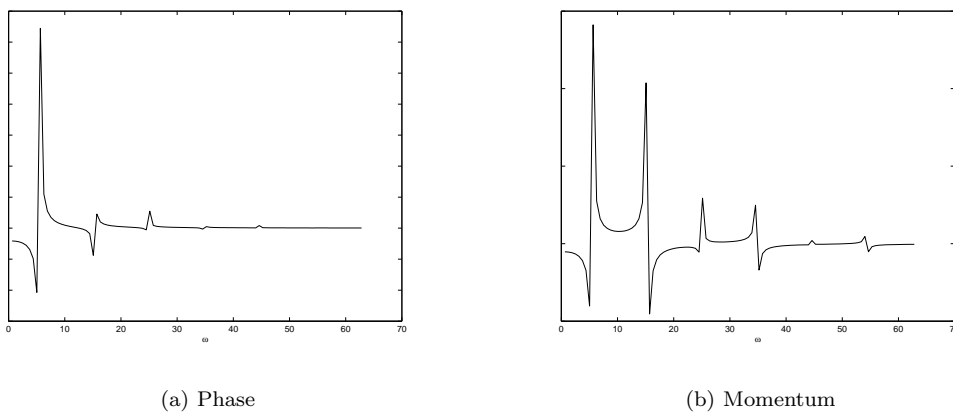
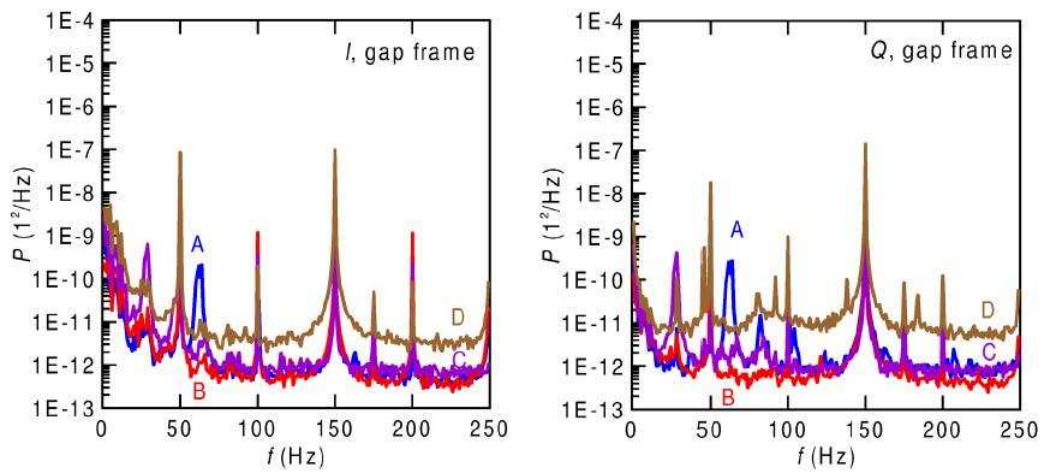


Figure 4.19: A sample spectral power density of RF noise measured at HERA (courtesy S. Ivanov.



(a) 208 MHz system

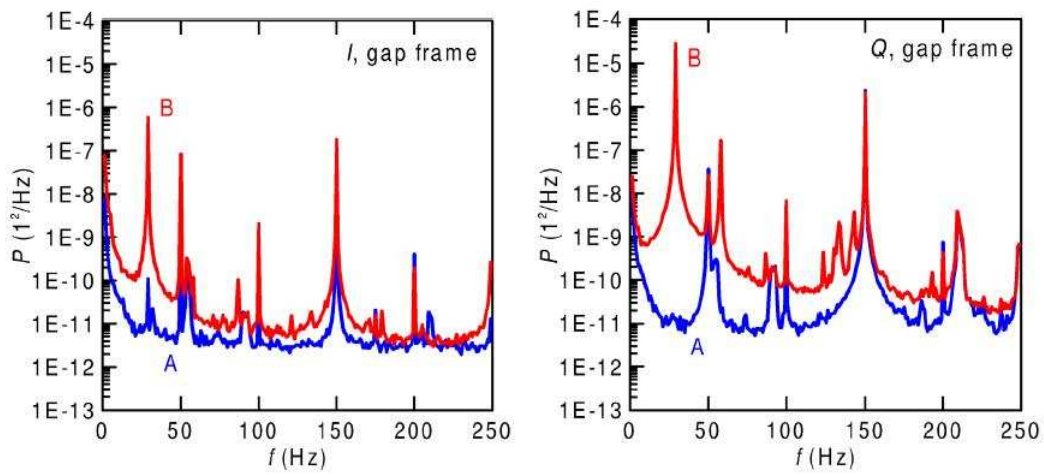
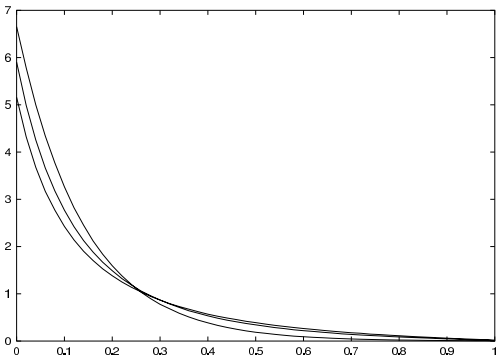
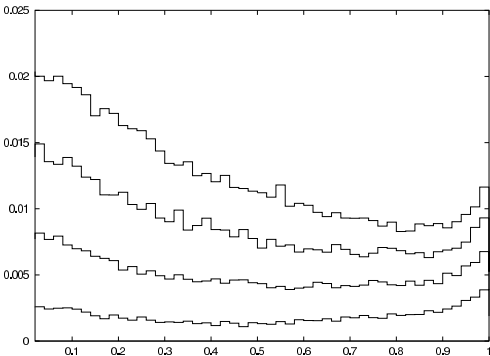


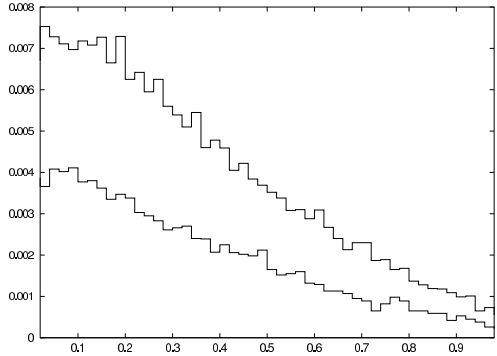
Figure 4.20: Example of dynamics for HERA double RF system



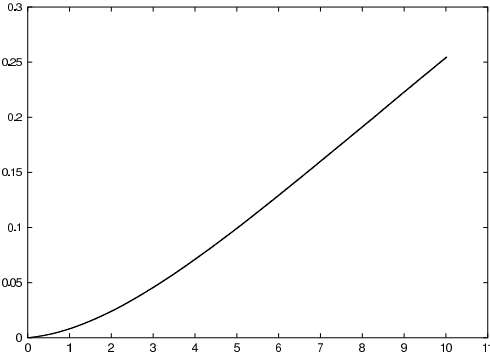
(a) Density



(b) Side bucket halo

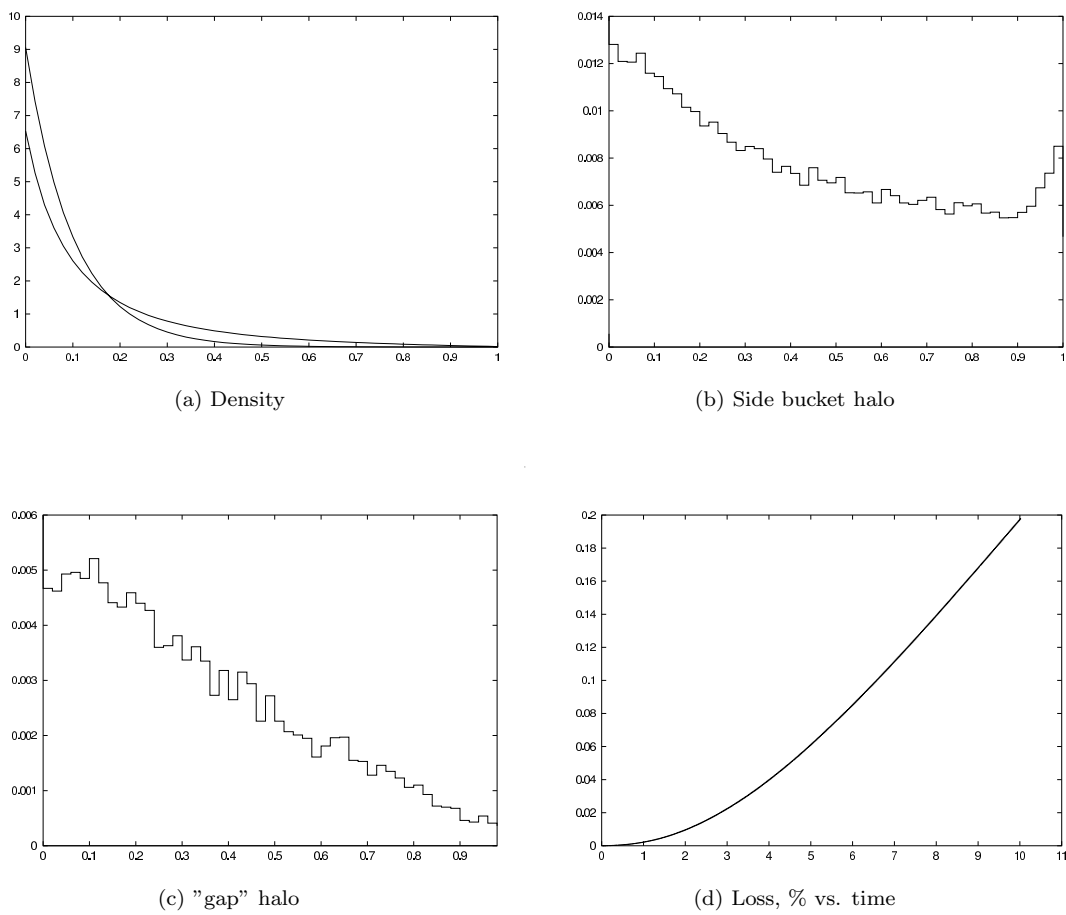


(c) "gap" halo



(d) Loss, % vs. time

Figure 4.21: Another example with initially somewhat shorter bunches



Chapter 5

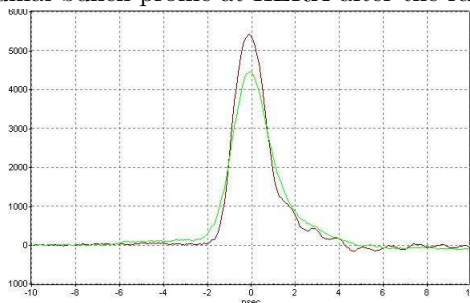
Some experimental observations

In this section we present the observed longitudinal bunch evolution in HERA and its connection to background rates. Perturbations can not only lead to parasitic losses but can also be employed for various useful purposes. We shortly discuss how RF voltage modulations can be employed to depopulate bunch tails and to achieve stabilization of multibunch oscillations.

5.1 Backgrounds and longitudinal bunch evolution

In HERA the longitudinal bunch profile is measured by analysing the current picked up from a resistive gap monitor. There are two systems. The first one is designed to measure the bunch distribution with relatively high accuracy. It has a dead-time of around one second and cannot detect fast bunch oscillations. The second [65] has short dead-time and can measure bunch signal each turn, but the resolution is low and it is used for analysis of fast bunch dipole oscillation modes and lengthening. A typical bunch profile evolution is shown in figure 5.1. The current in bunch tails is low and the measurement of its distribution is not possible due to limited resolution of the monitor. However, the amount of coasting beam can be assessed by measuring the difference between the bunched and unbunched (DC) current. The amount of coasting beam was also estimated by measuring the scattering rate at HERA-B target wires that were moved across the beam [19].

Figure 5.1: Typical longitudinal bunch profile at HERA after the ramp and after a 10 hours run



The proton background is measured with counters installed in the detectors. The background rates are also correlated with the loss rates measured at the collimators and with values taken from the beam loss monitors.

Figure 5.2: ZEUS C5 Counter with high background rates

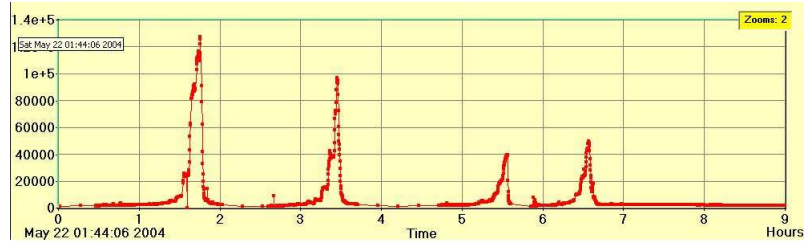
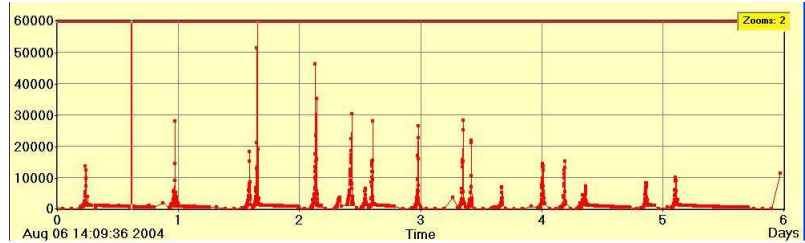


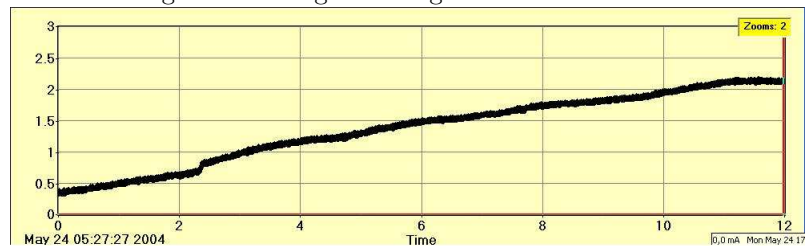
Figure 5.3: ZEUS C5 Counter with moderate background rates



The background increases during the run which is explained by the proton halo accumulation. By removing a bad cable connection it was possible to improve the noise level in the RF system which resulted in a considerable background reduction. In figures 5.2 and 5.3 the rates before and after the improvement are shown.

The increase of the coasting beam with time under poor noise conditions is shown in figure 5.4, with better conditions - in figure 5.5.

Figure 5.4: Large coasting beam accumulation



The comparison of the observed coasting beam currents under improved noise conditions with simulations is shown in figure 5.6. For the intra-beam scattering a slight overestimates is given. For the noise the rates are show for various possible tail diffusion coefficients. To gain consistence of the bunch diffusion with escape rate a significant increase of the coefficient towards the tail is to be assumed, which was suggested in [32].

Figure 5.5: Moderate coasting beam accumulation

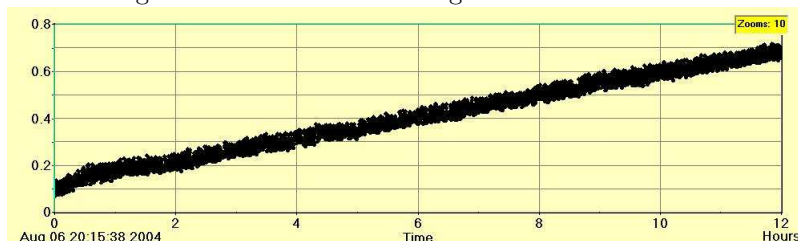
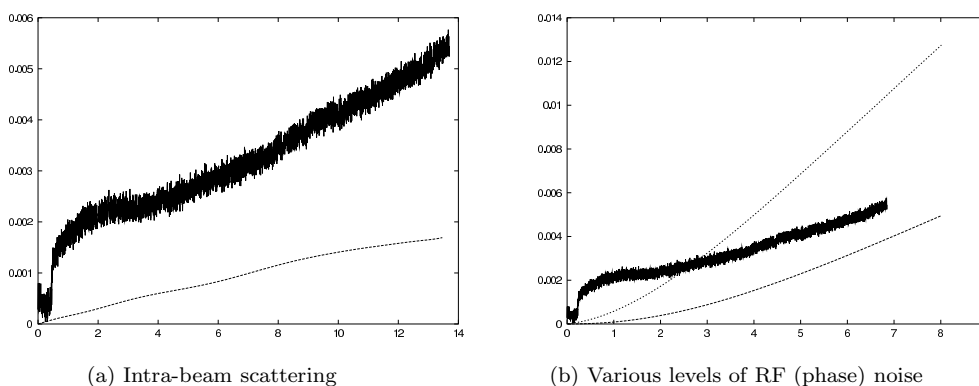


Figure 5.6: Comparison of observed and simulated coasting beam currents



5.2 Bunch manipulations with amplitude and phase modulations

By manipulating cavity voltage amplitudes and phases one can control to some extent the longitudinal beam parameters. Such techniques are widely used to damp the longitudinal instabilities which can occur during the ramp. By applying specific modulations one can influence particular parts of the beam, for example depopulate the beam tail. With such technique one can in principle reduce the amount of the coasting beam.

As was shown in Chapter 4, the diffusion coefficient arising from RF noise depends on its spectral density. That means that by applying noise with spectral density concentrated in the synchrotron frequency band of the bunch tail one can destroy the tail without influencing the longitudinal emittance considerably. The particles swept from the tail will mostly go into the coasting beam and will produce a background increase within some time. But since after such modulation the loss rate from the bucket should decrease whichever loss mechanism is present, there would be a decrease in the background afterwards. An alternative technique is based on the fact that amplitude noise results in the diffusion coefficient that grows towards the bunch tails. The amplitude modulation can now be made with a rather broad frequency band, which will have approximately the same effect. Say, a white noise can be used.

We attempted an experimental confirmation of this facts. Synchrotron frequencies of tail particles in HERA are around 1 Hz and voltage modulation of this frequencies turned to be technically difficult. We applied white noise instead. The noise signal with amplitude of 1 kV was applied to the cavity for 10 minutes. The collimator rates were observed. The applied noise resulted in a slight collimator rate

increase and had no influence on the bunch core. After 1 hour the collimator rates increased significantly. The time interval corresponds to the time required for the particles pulled out from the tail to drift to the aperture limitation under influence of synchrotron radiation. After that the backgrounds decreased and were lower than those which should have been without the perturbation. A usual background evolution is shown in figure 5.8. The backgrounds observed after the amplitude modulation is shown in figure 5.7. A decrease in the coasting beam production was also observed (figure 5.9).¹

Figure 5.7: Collimator rates after the amplitude modulation. The modulation was applied at $\Delta t \approx 0.7h$

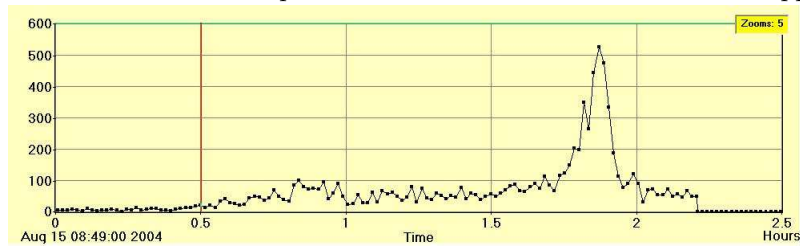
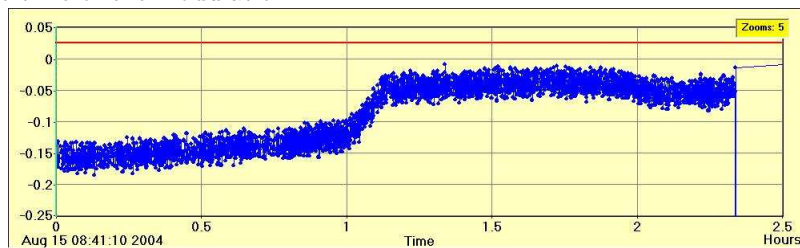


Figure 5.8: Usual picture of the collimator rates on the same time scale

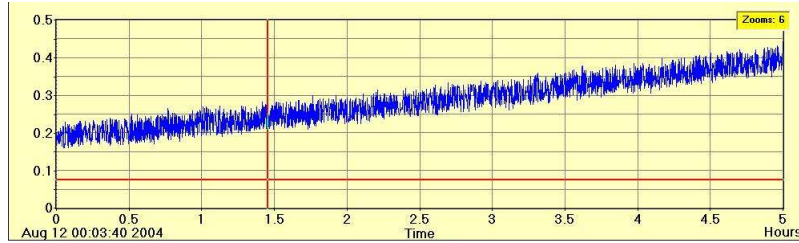


Figure 5.9: Coasting beam current after the amplitude modulation. The increase in the accumulation rate corresponds to the time of the modulation.



¹the coasting beam currents have different orders because of the different number of stored bunches. Low beam current was used for safety reasons.

Figure 5.10: Usual coasting beam accumulation observed on the same time scale goes linearly.



5.3 Summary

- There is some portion of coasting beam coming from the intra-beam scattering. For a proton ring like HERA it shouldn't have a serious background impact.
- Most of the halo seems to be accumulated due to the RF phase noise.
- It is hard to practically reduce further the noise level at HERA.
- Random perturbations can be used for beam control.

Chapter 6

Epilogue

6.1 Noise in nonlinear systems

The distinction between random and deterministic processes is rather subtle from the modern point of view. It is long known [14] that complex dynamical systems possess statistical properties. A random process can be viewed as an output of a chaotic dynamical system. One can consider a perturbation to be deterministic if it has a regular Fourier spectrum.

Such deterministic perturbations of the synchrotron motion arise as a consequence of wake fields produced by the bunch train travelling in the ring, higher order harmonics of the RF cavities and so on. A periodic driving of a linear system can result in resonant behavior and an instability can occur. For a nonlinear Hamiltonian system where frequency depends on the amplitude another behavior, the so called nonlinear resonance, is general [12]. A perturbation results in a set of points (or hypersurfaces) in the phase space where the resonant conditions are met. The perturbation has a strong effect in the vicinity of these points leaving the motion in all other regions practically unchanged. The region where the impact is strong is called the resonant band. Since such points generally form a dense set in the phase space, the effect of intersection of different resonant bands can be rather complicated. For a certain class of systems - steep Hamiltonian systems - a sufficiently small perturbation does not lead to instability. In one-dimensional case these systems are just Hamiltonian systems with positively definite Hamiltonian. Such is, for example, the pendulum representing the synchrotron oscillations. For such Hamiltonians motion along every resonant line introduces a frequency shift and the perturbation is thus stabilized. These issues are of great importance for the transverse beam dynamics where all kinds of resonances can appear due to multidimensionality [62], [59].

A general description of dynamics when nonlinear resonances are present is extremely complicated [12]. The situation becomes more difficult when a random force is added. Many interesting physical phenomena arise, especially in systems with multiple stable points or lattice systems - pattern formation, stochastic resonance, etc. (see for example [67], [23]). For Hamiltonian systems a rich variety of results can be drawn from simple models, for example from interaction of an isolated resonances with white noise [25], [57]. Here the phase space topology created by the nonlinearity introduces "channels" which host circulations of currents driven by noise. This behavior can strongly influence stationary distributions and various escape rates.

For one dimensional systems the behavior is much simpler. A resonant surface reduces to a point in the action space with trajectories oscillating around this point, an isolated resonance. An instability can occur when the isolated resonances intersect each other and this intersection is broad enough to provide an escape path to the trajectory. This effect is normally small for reasonably weak perturbations arising in the synchrotron motion which can be suspected to contribute to escape rate from the RF bucket. However,

it is not completely excluded. Another instability mechanism could come from the possibility of quick transport of a particle across a resonant band which in interaction with the noise can lead to a diffusion enhancement.

The discussed effects play much weaker role in the one dimensional case than in multidimensional. Therefore, it is as usual hard to estimate the perturbations experimentally due to their small magnitudes. However, these mechanisms are to be kept in mind. Note that the interaction with a resonance is to some extent already included in the Fokker-Planck equation obtained from the given spectral power density. Any perturbation acting in a physical device in reality has some bandwidth. A peak measured in the output of some device can be viewed as the spectral power density at this point. Then the diffusion coefficient 4.20 in the region with corresponding frequency spread will grow as well. The numerical correspondence of the diffusion rate to the reality is of course not that obvious. The description becomes somewhat loose as the bandwidth goes to zero and the peak becomes sharper. Then the influence of this peak from the random process point of view shrinks to a diffusion in a small region whereas in reality there should exist a certain resonant band with some “quasiregular” motion in it. So, sharp narrow peaks of high intensity in the noise should be rather considered as deterministic components.

6.2 Conclusion

The loss rates for HERA were estimated when intra-beam scattering and RF noise are present. The influence of intra-beam scattering turned out to be weak. The RF noise appears to be responsible for the major portion of the coasting beam. These values were estimated to a precision which is determined by the error in the measurement of the noise spectral density. The estimates of noise in this work have mainly of qualitative nature.

The discussed methods can be potentially applied to some other problems concerning random particle motion and backgrounds which can appear in connection with the coming operation of the LHC and, possibly, other accelerators.

Substantial complications arise in extending the methods to general multidimensional nonlinear systems where chaotic behavior can take place. The averaging becomes not trivial, the numerical integration and Monte-Carlo trials require much more computations.

Another difficulty in the study of random phenomena is the selection of a correct noise model. Conventional models are presented by the second order processes or by white noise. However, there is a variety of situations when they cannot be used [24].

The problem of escape from the potential well under influence of random perturbations has no general elegant solution. It has been widely studied in particle accelerator theory and in connection to other problems. For particular applications one can normally achieve a satisfactory solution by combining analytical and numerical methods and exploiting the specific properties of the system. The demonstration of such methods for the problem of escape from the RF potential bucket in a storage ring was attempted in this work. We hope that at least some ideas have a shade of originality at least for the accelerator community.

Appendix A

Particle motion in a storage ring

A.1 Equations of motion

The horizontal and vertical coordinates of a particle are measured in a Cartesian coordinate system moving along the design orbit

$$r(s) = \begin{pmatrix} x(s) \\ x'(s) \\ z(s) \\ z'(s) \end{pmatrix}$$

They are sums of the coordinates of the closed orbit for a given momentum deviation Δp and the coordinates of betatron oscillations around the closed orbit

$$r_\beta(s) = \begin{pmatrix} x_\beta(s) \\ x'_\beta(s) \\ z_\beta(s) \\ z'_\beta(s) \end{pmatrix}$$

$$r(s) = r_\beta(s) + D(s) \frac{\Delta p}{p} \quad (\text{A.1})$$

The betatron motion can be represented by a certain coordinate map

$$r_\beta(s+L) = M(s+L, s) r_\beta(s) \quad (\text{A.2})$$

When all nonlinear elements are taken into account, M becomes a complex nonlinear map. However, for applications like intra-beam scattering linear optics approximation is sufficient. Neglecting the coupling between the transverse planes and nonlinear effects, M becomes a matrix expressed in terms of the optical functions (linear optics)

$$M(s+L, s) = \begin{pmatrix} M_x(s+L, s) & 0 \\ 0 & M_y(s+L, s) \end{pmatrix}$$

$$M_{x,y}(s+L, s) = \begin{pmatrix} \sqrt{\frac{\beta_{x,y}(s+L)}{\beta_{x,y}(s)}} (\cos(\Psi_{x,y}) + \alpha(s) \sin(\Psi_{x,y})) & \sqrt{\beta_{x,y}(s+L)\beta_{x,y}(s)} \sin(\Psi_{x,y}) \\ \frac{(\alpha_{x,y}(s) - \alpha_{x,y}(s+L)) \cos(\Psi_{x,y}) - (1 + \alpha_{x,y}(s)\alpha_{x,y}(s+L)) \sin(\Psi_{x,y})}{\sqrt{\beta_{x,y}(s)\beta_{x,y}(s+L)}} & \sqrt{\frac{\beta_{x,y}(s)}{\beta_{x,y}(s+L)}} (\cos(\Psi_{x,y}) - \alpha_{x,y}(s) \sin(\Psi_{x,y})) \end{pmatrix}$$

or explicitly

$$\begin{aligned}
r_{\beta,x,y} &= \sqrt{\varepsilon} \sqrt{\beta} (\cos \Psi \cos \phi - \sin \Psi \sin \phi) \\
r_{\beta,x',y'} &= -\sqrt{\frac{\varepsilon}{\beta}} (\alpha \cos \Psi \cos \phi - \alpha \sin \Psi \sin \phi + \sin \Psi \cos \phi + \cos \Psi \sin \phi) \\
\cos \phi &= \frac{r_{\beta,0}}{\varepsilon \beta_0} \\
\sin \phi &= -\frac{1}{\sqrt{\varepsilon}} \left(r_{\beta,0} \sqrt{\beta_0} + \frac{\alpha_0 r_{\beta,0}}{\sqrt{\beta_0}} \right)
\end{aligned} \tag{A.3}$$

Here $\beta_{x,z}$ is the betatron envelope function, $\alpha_{x,z} = -\frac{\beta'_{x,z}}{2}$, $\Psi_{x,z}$ is the betatron phase. The matrix M is symplectic and the transformation preserves area in the phase space. Normalized invariant phase space areas of this transformation are the emittances

$$\varepsilon_x = \frac{1 + \alpha_x^2(s)}{\beta_x(s)} x^2(s) + 2\alpha_x(s)x(s)x'(s) + \beta_x(s)x'^2(s) \tag{A.4}$$

$$\varepsilon_z = \frac{1 + \alpha_z^2(s)}{\beta_z(s)} z^2(s) + 2\alpha_z(s)z(s)z'(s) + \beta_z(s)z'^2(s) \tag{A.5}$$

Due to phase focusing particles perform slow synchrotron oscillations. Let the reference energy be E , the energy offset ΔE , the synchrotron phase ϕ , then the synchrotron one turn map is given by

$$\begin{aligned}
\Delta E_{n+1} &= \Delta E_n + eZV(\phi) - \Delta E_\gamma \\
\phi_{n+1} &= \phi_n + \frac{2\pi h}{\beta^2 E} \left(\alpha - \frac{1}{\gamma^2} \right) \Delta E
\end{aligned}$$

This map is approximated with a system of differential equations

$$\begin{aligned}
\Delta \dot{E} &= \frac{eZ}{T} V(\phi) - \frac{\Delta E_\gamma}{T} \\
\dot{\phi} &= \frac{2\pi h}{\beta^2 ET} \left(\alpha - \frac{1}{\gamma^2} \right) \Delta E
\end{aligned}$$

where

$$\begin{aligned}
\alpha = \frac{\Delta L}{L} \frac{p}{\Delta p} & \quad - \text{the momentum compaction factor,} \\
V(\phi) & \quad - \text{RF voltage,} \\
\beta, \gamma & \quad - \text{relativistic factors,} \\
h = \frac{\omega_{RF}}{\omega_{REV}} & \quad - \text{harmonic number,} \\
E & \quad - \text{reference energy,} \\
q = eZ & \quad - \text{particle charge,} \\
\Delta E_\gamma & \quad - \text{energy change from synchrotron radiation,} \\
T & \quad - \text{revolution period}
\end{aligned}$$

Since

$$\frac{E^2}{c^2} = p^2 + m^2 c^2 \tag{A.6}$$

and for ultrarelativistic particles

$$\delta p = \frac{\Delta p}{p} = \frac{\Delta E}{E} \quad (\text{A.7})$$

the equations of motion can be rewritten

$$\begin{aligned} \delta \dot{p} &= \frac{eZ}{TE} V(\phi) - \frac{\Delta E_\gamma}{ET} \\ \dot{\phi} &= \frac{2\pi h}{\beta^2 T} \left(\alpha - \frac{1}{\gamma^2} \right) \delta p \end{aligned}$$

The spacial longitudinal coordinate with respect to bunch centre is more convenient in kinetic equations and is related to the phase as

$$\Delta s = \frac{c\phi}{2\pi\omega_{RF}} \quad (\text{A.8})$$

The synchrotron radiation is emitted with mean power

$$P_\gamma = \frac{e^2 c}{6\pi\epsilon_0} \frac{\gamma^4}{R^2} \quad (\text{A.9})$$

where $\epsilon_0 = 8.8 \times 10^{-12} \text{farad} \times \text{m}^{-1}$ is the permittivity in vacuum. The fluctuations of the power due to quantum nature of the radiation are negligible for proton storage rings. The energy losses per turn are

$$\Delta E = c\Delta p = \int_0^T P_\gamma dt \approx \frac{Te^2 c}{6\pi\epsilon_0} \frac{\gamma^4}{R^2} \quad (\text{A.10})$$

In the case of stable synchrotron oscillations the radiation losses are compensated by the Rf system and the change of δp is given by the difference in the radiation losses with respect to the reference particle

$$\Delta E_\gamma = T \frac{\partial P_\gamma}{\partial E} \Delta E = \frac{4}{\gamma m_0 c} P_\gamma \Delta E \quad (\text{A.11})$$

When the motion is not oscillatory the energy losses are not compensated and

$$\Delta E_\gamma = TP_\gamma \quad (\text{A.12})$$

For example, for protons in HERA the synchrotron oscillation damping rate is of order $1\text{KeV}/\text{sec}$ and the damping time is tens of days. The drift is about $280\text{KeV}/\text{sec}$, the time required to drift from the bucket to the acceptance limit is about 40min . So, for the time scales involved, one can neglect the radiation damping for oscillating particles, but the drift in the coasting beam region is substantial and contributes to particle losses.

The radiation effects and all other perturbations are rather week and can be considered as small perturbations to the Hamiltonian system with

$$H(\phi, \delta p) = \frac{q}{T} U(\phi) + \frac{2\pi h}{\beta^2 T} \left(\alpha - \frac{1}{\gamma^2} \right) \frac{\delta p^2}{2} \quad (\text{A.13})$$

where $-U'(\phi) = V(\phi)$. For the case of sinusoidal RF voltage $V(\phi) = \sin(\phi)$ the Hamiltonian is

$$H_1(\phi, \delta p) = \frac{q}{ET} (1 - \cos(\phi)) + \frac{2\pi h}{\beta^2 T} \left(\alpha - \frac{1}{\gamma^2} \right) \frac{\delta p^2}{2} \quad (\text{A.14})$$

For the double RF system one takes the phase with respect to one of the systems (the dominant) as ϕ and supposing $\omega_{RF2} = \eta \cdot \omega_{RF1}$

$$H_2(\phi, \delta p) = \frac{q}{ET}(2 - V_1 \cos(\phi) - V_2 \cos(\eta\phi)) + \frac{2\pi h}{\beta^2 T} \left(\alpha - \frac{1}{\gamma^2} \right) \frac{\delta p^2}{2} \quad (\text{A.15})$$

The part of the Hamiltonian depending on ϕ is called the RF potential. In figures A.2 and A.3 the RF potentials and phase portraits of systems A.14 and A.15 are shown. System A.14 has fixed points

$$\phi = 0, \quad \pm \frac{\pi}{2}, \quad \pm \pi$$

The fixed points of system A.15 can be found to a good accuracy as corrections to single RF fixed points. To the first order the correction is zero and can be neglected when cavities voltages differ much. Some parameters for HERA are summarized in table A.1.

Table A.1: Some HERA parameters

First RF system frequency ω_{RF1}	208MHz
Second RF system frequency ω_{RF2}	52MHz
RF voltage	$U \sim 500KV$
Synchrotron frequency	$\omega \sim 30Hz$
Momentum compaction	$\alpha = 0.00128$
Averaged optical functions	$\langle \beta_x \rangle = 100m, \langle \beta_z \rangle = 80m$ $\langle \alpha_x \rangle = 7.4 \times 10^{-6}, \langle \alpha_z \rangle = 1.7 \times 10^{-4}$ $\langle D_x \rangle = 1.06m, \langle D_y \rangle = 0.002m$

The momentum acceptance is the maximum momentum offset that a particle can have without being lost transversely. For HERA the $\delta p/p$ acceptance is about 10^{-3} (at 920 GeV, with $U_{208} = 360KV$ and $U_{52} = 14KV$).

A.2 Action-angle variables

To analyze the long term stability of motion one normally looks at the behavior of some slowly varying quantities or invariants of motion. It is convenient to study weakly perturbed Hamiltonian systems in terms of action-angle variables of the unperturbed systems. A Hamiltonian can be brought by a canonical transformation of variables $(q, p) \rightarrow (J, \phi)$ to the form $H(J)$. If the system is integrable (which is always true for 1d Hamiltonian systems) then such action-angle transformation can always be made. In action-angle variables the equation of motion takes the form

$$\begin{aligned} \dot{J} &= 0 \\ \dot{\phi} &= \omega(J) = -\frac{\partial H}{\partial J} \end{aligned} \quad (\text{A.16})$$

This transformation to action-angle variables sometimes can be found explicitly. For example, for the pendulum

$$H(q, p) = \frac{p^2}{2} + \Omega(1 - \cos q) \quad (\text{A.17})$$

such transformation is given by the Jacobi elliptic functions [5]. However, analytical representations are exceptional and in practice one has to rely on an asymptotic expansion. A common perturbation

method to bring a Hamiltonian into action-angle form is the superconvergent method. Here it is shown for a simple one-dimensional case. For the pendulum (with $\Omega = 1$) the Hamiltonian can be represented as series

$$H = \frac{p^2}{2} + \frac{q^2}{2} - \frac{q^4}{4!} + \frac{q^6}{6!} - \frac{q^8}{8!} + \dots \quad (\text{A.18})$$

First $J = \frac{q^2}{2} + \frac{p^2}{2}$, $q = \sqrt{2J} \cos \phi$

$$H(J, \phi) = J - \frac{4J^2}{4!} \cos^4 \phi + \frac{8J^3}{6!} \cos^6 \phi - \frac{16J^4}{8!} \cos^8 \phi + \dots \quad (\text{A.19})$$

Dividing the Hamiltonian into the mean and oscillating parts

$$H(J, \phi) = J - \frac{4J^2}{4!} \langle \cos^4 \phi \rangle + \frac{8J^3}{6!} \langle \cos^6 \phi \rangle - \frac{16J^4}{8!} \langle \cos^8 \phi \rangle + \frac{4J^2}{4!} (\cos^4 \phi - \langle \cos^4 \phi \rangle) + \frac{8J^3}{6!} (\cos^6 \phi - \langle \cos^6 \phi \rangle) - \frac{16J^4}{8!} (\cos^8 \phi - \langle \cos^8 \phi \rangle) + \dots$$

one chooses the next transformation to eliminate the oscillating terms of order J^2 . One chooses the generating function

$$F(J_1, \phi) = J_1 \phi + S(J_1, \phi)$$

so that

$$J = J_1 + S_\phi \\ \phi_1 = \phi + S_{J_1}$$

the desired transformation is obtained with

$$S_\phi = \frac{1}{6} J_1^2 (\cos^4(\phi) - \frac{3}{8})$$

Then one needs to change $\phi \rightarrow \phi_1$ according to

$$\phi_1 = \phi + S_{J_1} = \phi + \int S_{\phi, J_1} d\phi = \phi - 8a_4 J_1 \int f_4(\phi) d\phi + c(\phi)$$

By the next transformation one can eliminate terms of order J^3 and J^4 . Up to fourth order this gives the Hamiltonian

$$H(\hat{J}_1) = J_1 - \frac{J_1^2}{16} - \frac{J_1^3}{256} - \frac{5J_1^4}{213} \quad (\text{A.20})$$

Note that the expression obtained by averaging the Hamiltonian $H(J)$ with respect to phase will differ from $\hat{H}(J_1)$

$$\langle H(J) \rangle = J_1 - \frac{J_1^2}{16} - \frac{J_1^3}{288} - \frac{5J_1^4}{9216} \quad (\text{A.21})$$

which differs noticeably in terms starting from fourth order. In many problems such averaging is sufficient and one can use such first order action. Action-angle variables are standard in treating small perturbations. Suppose that the original system was subject to a perturbation which is a smooth function in q and p . Then in action-angle variables it is some smooth function of J and periodic in ϕ . The perturbed Hamiltonian can be written in the standard form

$$H(J, \phi) = H_0(J) + \varepsilon \sum_{m,n} V_{m,n} e^{i w_m \phi + i \nu_n t} \quad (\text{A.22})$$

With such a representation averaging and resonance analysis can be now more easily performed.

Figure A.1: Optical functions at HERA

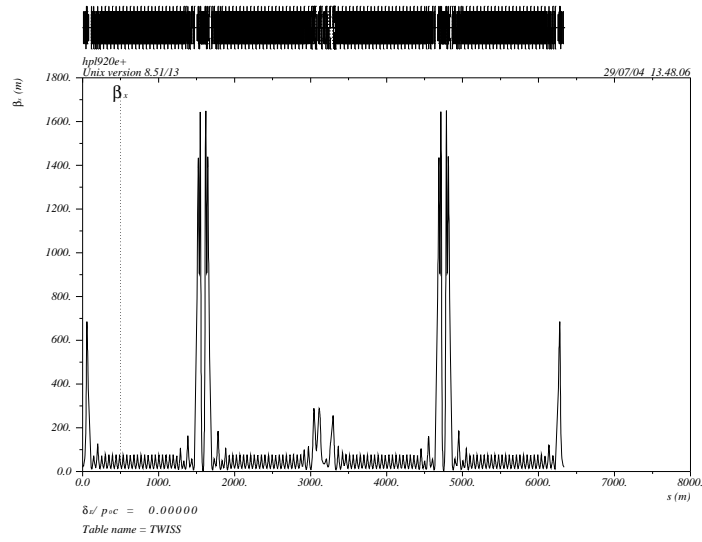
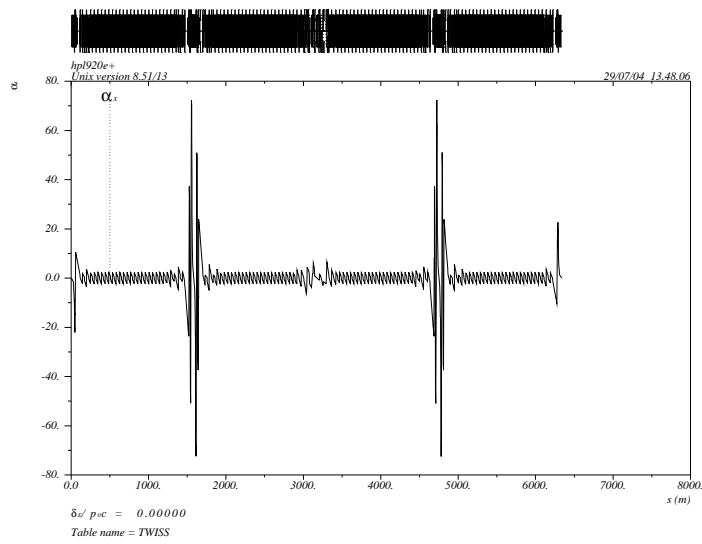
(a) β_x (b) α_x

Figure A.2: Synchrotron motion with 1 RF system

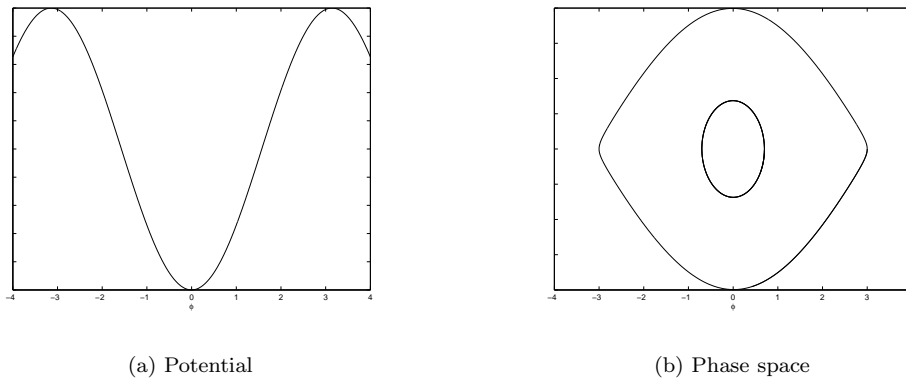
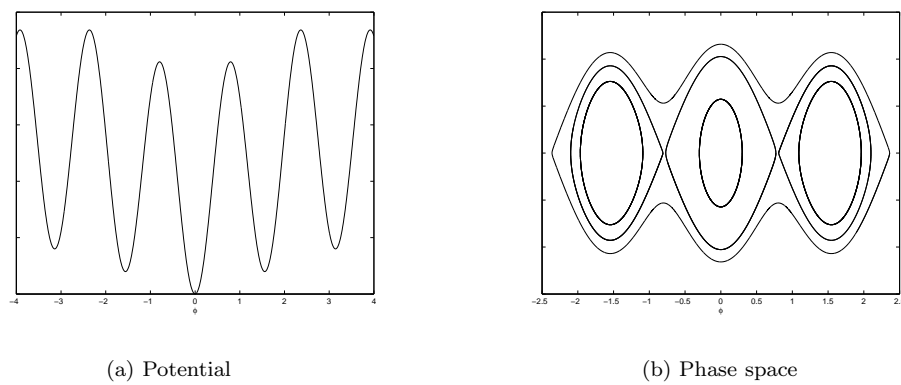


Figure A.3: Synchrotron motion with 2 RF systems



Appendix B

Sketch of the proof of proposition 1

One needs to show that an integral of a random function along a trajectory of the solution of the differential equation can be under certain conditions approximated on $[0, T_0]$ by an Ito's integral

$$\int_0^\tau f_\varepsilon(p(\varepsilon^{-2}s), \phi(\varepsilon^{-2}s), s)ds + \frac{1}{\varepsilon} \int_0^\tau g_\varepsilon(p(\varepsilon^{-2}s), \phi(\varepsilon^{-2}s), s)ds \approx \int_0^\tau a(H(s))ds + \int_0^\tau b(H(s))dW_s$$

Let $p(t)$ and $\phi(t)$ be represented as functions of the invariant H and t , the problem can be restated as

$$\int_0^\tau f_\varepsilon(H(\varepsilon^{-2}s), \varepsilon^{-2}s)ds + \frac{1}{\varepsilon} \int_0^\tau g_\varepsilon(H(\varepsilon^{-2}s), \varepsilon^{-2}s)ds \approx \int_0^\tau a(H(s))ds + \int_0^\tau b(H(s))dW_s \quad (\text{B.1})$$

The idea of the proof is that one can find such Δ that is much greater than the correlation time of the random function so that the integral over $[0, \Delta]$ becomes a sum of some large number of integrals that are approximately independent random variables, but the change of H on such an interval is small. Then the increment of the process on this interval becomes approximately a Gaussian random variable. Its moments define the drift and diffusion coefficients of the diffusion process sought. Such Δ can always be found for processes with finite correlation time and sufficiently small ε . Let the partition of $[0, T_0]$ on such intervals be constructed. First consider the term of second order in ε and develop it in power series to the second order around the starting point

$$\int_0^\Delta f_\varepsilon(H(\varepsilon^{-2}\tau), \varepsilon^{-2}\tau)d\tau = \frac{\Delta}{\Delta\varepsilon^{-2}} \int_0^{\Delta\varepsilon^{-2}} f_\varepsilon(H(\tau), \tau)d\tau = \quad (\text{B.2})$$

$$\Delta \lim_{T \rightarrow \infty} \frac{1}{T} \int_0^T f_\varepsilon(H(0), \tau)d\tau + O(\Delta^2) \quad (\text{B.3})$$

The variation of the last integral is of order Δ^2 and the first moment of order Δ . This means that its contribution reduces to drift

$$\lim_{T \rightarrow \infty} \frac{1}{T} \int_0^T \langle f_\varepsilon(H(0), \tau) \rangle d\tau \quad (\text{B.4})$$

Extending this procedure to the whole interval one arrives at the drift coefficient

$$a(H) = \lim_{T \rightarrow \infty} \frac{1}{T} \int_0^T \langle f_\varepsilon(H, \tau) \rangle d\tau \quad (\text{B.5})$$

Now consider the term of order ε

$$\begin{aligned} & \frac{1}{\varepsilon} \int_0^1 g_\varepsilon(H(\varepsilon^{-2}\tau), \varepsilon^{-2}\tau) d\tau = \frac{\Delta}{\varepsilon \cdot \varepsilon^{-2}} \int_0^{\Delta\varepsilon^{-2}} g_\varepsilon(H(\tau), \tau) d\tau = \\ & \frac{\Delta}{\varepsilon \cdot \varepsilon^{-2}} \int_0^{\Delta\varepsilon^{-2}} \left[g_\varepsilon(H(0), \tau) + \frac{\partial g_\varepsilon}{\partial H}(H(0), \tau) \int_0^\tau g_\varepsilon(H(0), s) ds \right] d\tau + O(\Delta^2) \end{aligned}$$

The first moment of the last integral is

$$\frac{\Delta}{\varepsilon} \lim_{T \rightarrow \infty} \frac{1}{T} \int_0^T \langle g_\varepsilon(H(0), \tau) d\tau \rangle + \frac{\Delta}{\varepsilon} \lim_{T \rightarrow \infty} \frac{1}{T} \int_0^T d\tau \int_0^\tau \left\langle \frac{\partial g_\varepsilon}{\partial H}(H(0), \tau) g_\varepsilon(H(0), \varepsilon^{-2}s) ds \right\rangle + O(\Delta^2) \quad (\text{B.6})$$

The first integral is large and contributes to the drift on faster time scales than ε^{-2} , namely ε^{-1} . To treat the diffusion on time scale of ε^{-2} one first needs to transform the equation to variables in which it vanishes. However in our case (for the synchrotron motion) it turns out to be zero due to fast oscillations in g_ε with zero mean and this is not required. So the drift comes from the second term. It can be rewritten as

$$\begin{aligned} & \Delta \lim_{T \rightarrow \infty} \frac{1}{T} \int_0^T d\tau \int_0^\tau \left\langle \frac{\partial g_\varepsilon}{\partial H}(H(0), \tau) g_\varepsilon(H(0), \varepsilon^{-1}s) ds \right\rangle + O(\Delta^2) = \\ & \Delta \lim_{T \rightarrow \infty} \frac{1}{T} \int_0^T d\tau \int_0^\tau \left\langle \frac{\partial g_\varepsilon}{\partial H}(H(0), \tau) g_\varepsilon(H(0), s) \right\rangle ds + O(\Delta^2) \end{aligned}$$

When extending the integration procedure to the whole interval in the last expression the correlations from the past have also to be taken into account. Neglecting terms of order Δ^2 the drift becomes

$$\lim_{T \rightarrow \infty} \frac{1}{T} \int_0^T d\tau \int_{-T}^\tau \left\langle \frac{\partial g_\varepsilon}{\partial H}(H, \tau) g_\varepsilon(H, s) \right\rangle ds \quad (\text{B.7})$$

The second variation of B.6 is

$$\begin{aligned} & \left\langle \frac{\Delta \cdot \Delta}{\varepsilon^2 \cdot \Delta\varepsilon^{-2} \cdot \Delta\varepsilon^{-2}} \int_0^{\Delta\varepsilon^{-2}} g_\varepsilon(H(0), \tau_1) d\tau_1 \int_0^{\Delta\varepsilon^{-2}} g_\varepsilon(H(0), \tau_2) d\tau_2 \right\rangle + O(\Delta^2) = \\ & \Delta \left\langle \frac{1}{\Delta\varepsilon^{-2}} \int_0^{\Delta\varepsilon^{-2}} g_\varepsilon(H(0), \tau_1) d\tau_1 \int_0^{\Delta\varepsilon^{-2}} g_\varepsilon(H(0), \tau_2) d\tau_2 \right\rangle + O(\Delta^2) = \end{aligned} \quad (\text{B.8})$$

and the diffusion coefficient

$$\lim_{T \rightarrow \infty} \frac{1}{T} \int_0^T \int_0^T \langle g_\varepsilon(H, \tau_1) g_\varepsilon(H, \tau_2) \rangle d\tau_1 d\tau_2 \quad (\text{B.9})$$

To complete the proof one needs to show that the correlation between consequent subintervals is small compared to the first moments of the process and that on each interval the random perturbation

satisfies the central limit theorem with desired precision. It turns out that one should choose $\Delta \sim \varepsilon\sqrt{\varepsilon}$ to satisfy these conditions. The magnitude of Δ determines the precision of the approximation $\sqrt{\varepsilon}$. Precise conditions under which the procedure is applicable can be found in [37], [28]. These conditions are met for sufficiently small ε and a random process of second order with finite correlation time.

Note that for moderate noise amplitude it may turn out that such an averaging procedure may give only a poor approximation due to the square root convergence. In that case the non-Markovian nature of noise is essential and one has to deal with the system of Ito's equation in the extended phase space [55].

The behavior of random oscillating systems on long time scales was also studied in [3], [4], [22], [38].

Appendix C

On the precision of the 'self-consistent chains' method

The chain dynamics can be represented by a series of mappings (multiplications)

$$\begin{aligned}
 x_\tau &= x_0^T P(x_0, \tau), & 0 \leq \tau \leq h_1 \\
 x_\tau &= x_{h_1}^T P(x_{h_1}, \tau), & h_1 \leq \tau \leq h_2 \\
 \dots & \dots & \dots \\
 x_\tau &= x_{h_i}^T P(x_{h_i}, \tau), & h_i \leq \tau \leq h_{i+1} \\
 \dots & \dots & \dots
 \end{aligned} \tag{C.1}$$

where x_τ are distribution vectors belonging to \mathbb{R}^n , the transition probability matrix $P(x, t)$ is some function from $\mathbb{R}^n \times \mathbb{R}$ to $\mathbb{R}^{n \times n}$, $P(x, 0) = E$, and $\{h_i\}$ is a partition of the time interval $[0, T]$ with the points representing the moments of time at which the distribution is recalculated.

Let $h_i = \Delta \cdot i = \frac{i}{m}$, the case of an arbitrary partition is analogous. For this partition the system is truncated at $i = \lfloor \frac{1}{\Delta} \rfloor$. Here we show some convergence estimates for such dynamical system.

Lemma 2 *Let $P(x, \tau)$ possess smooth derivatives up to second order and bounded derivatives of higher orders. Then for distributions x_τ and y_τ starting at initial distributions x_0 and y_0 there exists a constant C not depending on Δ such that $\|x_\tau - y_\tau\| < C\varepsilon$ on $\tau \in [0, T]$ whenever $\|x_0 - y_0\| < \varepsilon$.*

Proof

Without loss of generality we may assume $T = 1$. Consider a partition with $\Delta = \frac{1}{m}$. Consider some interval of the partition $[h_i, h_{i+1}]$ and the evolution of the system with distributions at h_i equal to x_i and y_i .

$$\begin{aligned}
 \|x_{i+1} - y_{i+1}\| &= \left\| x_i^T P(x_i, \frac{1}{m}) - y_i^T P(y_i, \frac{1}{m}) \right\| = \\
 &= \left\| x_i^T P(x_i, \frac{1}{m}) - y_i^T P(x_i, \frac{1}{m}) + y_i^T P(x_i, \frac{1}{m}) - y_i^T P(y_i, \frac{1}{m}) \right\| \leq \\
 &\leq \|x_i - y_i\| \left\| P(x_i, \frac{1}{m}) \right\| + \|y_i\| \left\| P(x_i, \frac{1}{m}) - P(y_i, \frac{1}{m}) \right\|
 \end{aligned}$$

For all finite dimensional distributions $\|x\| \leq 1$ (in C or p norm), $x^T P$ is again a distribution and thus

$\|P\| = \sup_{\|x\|=1} \frac{\|x^T P\|}{\|x\|} \leq \|x^T P\| \leq 1$. The previous inequality turns now to

$$\|x_{i+1} - y_{i+1}\| \leq \|x_i - y_i\| + \left\| P(x_i, \frac{1}{m}) - P(y_i, \frac{1}{m}) \right\|$$

Develop $P(y_i, \tau)$ in power series around $\tau = 0$, then

$$\begin{aligned} \|P(x_i, \tau) - P(y_i, \tau)\| & \|E + \tau P_\tau(x_i, 0) + \frac{\tau^2}{2} P_{\tau^2}(x_i, 0) + \dots - \\ & - (E + \tau P_\tau(y_i, 0) + \frac{\tau^2}{2} P_{\tau^2}(y_i, 0) + \dots)\| \end{aligned} \quad (C.2)$$

If P_τ is Lipschitz-continuous at zero, i.e. when

$$\|P_\tau(x, 0) - P_\tau(y, 0)\| \leq L \|x - y\|$$

the last expression is of order $\tau \|x - y\|$ and for some bounded \hat{L}

$$\|x_{i+1} - y_{i+1}\| \leq \|x_i - y_i\| \left(1 + \hat{L} \frac{1}{m} \right)$$

From this follows that

$$\|x_k - y_k\| \leq \|x_0 - y_0\| \left(1 + \frac{\hat{L}}{m} \right)^k \leq \|x_0 - y_0\| \left(1 + \frac{\hat{L}}{m} \right)^m \leq \|x_0 - y_0\| e^{\hat{L}}$$

for all $k \leq m$. \square

Lemma 3 For fixed n the sequence of functions x_τ converges to some limit x_τ^* , which is a solution of the system of nonlinear equations

$$\dot{x}^* = A(x^*)$$

where

$$A(x) = \lim_{\tau \rightarrow 0} \frac{P(x, \tau) - E}{\tau}$$

and $\|x - x^*\| \leq \frac{C}{m}$

Proof. Consider the evolution of x_τ over interval $[h_i, h_{i+1}]$

$$x_{i+1} = x_i^T P(x_i, \tau), \quad \tau = h_{i+1} - h_i$$

then

$$\frac{x_{i+1} - x_i}{\tau} = x_i^T \frac{P(x_i, \tau) - E}{\tau}$$

and going to the limit

$$\dot{x}^* = x^{*T} A(x^*)$$

which is equivalent to

$$x^*(t) = x_0^* + \int_{t_0}^t x^{*T}(\tau) A(x^*(\tau)) d\tau$$

$$x_{i+1} = x_i^T P(x_i, \tau) = x_i^T (E + P_\tau(x_i, 0) + O(\tau^2)) = x_i^T (E + \tau A(x_i) + O(\tau^2))$$

$$x^*(h_{i+1}) - x_{i+1} = x^*(h_i) + \int_{h_i}^{h_{i+1}} x^*(\tau)P(x^*(\tau), \tau)d\tau - x_i - \tau x_i^T A(x_i) + O(\tau^2)$$

$$x(\tau) = x_i + \tau \frac{d}{d\tau} x(\tau)_{\tau=h_i} + O(\tau^2)$$

$$A(x(\tau)) = A(x^*(h_i) + \tau x^*(h_i) \frac{d}{dx} A(x^*(h_i)) + O(\tau^2)) = A(x_i) + \tau A(\hat{x}_i) + O(\tau^2)$$

$$\int_{h_i}^{h_{i+1}} x(\tau)A(x(\tau))d\tau = x_i A(x_i)(h_{i+1} - h_i) + O(h_{i+1} - h_i)^2 + O((h_{i+1} - h_i) \|x_i - x^* h_i\|)$$

$$\|x_{i+1} - x^*(h_{i+1})\| \leq \|x_i - x^*(h_i)\| + M_1(h_{i+1} - h_i) \|x_i - x^*(h_i)\| + M_2(h_{i+1} - h_i)^2$$

or

$$\|x_{i+1} - x^*(h_{i+1})\| \leq \|x_i - x^*(h_i)\| \left(1 + \frac{M_1}{m}\right) + \frac{M_2}{m^2}$$

From this it follows that the upper bound of the error at point h_{i+1} must satisfy

$$\delta_{i+1} = \delta_i \left(1 + \frac{M_1}{m}\right) + \frac{M_2}{m^2}, \quad i = 1, \dots, m$$

Since δ_i is an increasing function of i it is sufficient to estimate δ_m . Obviously δ_m cannot be smaller than $\frac{M_2}{m}$. This means that we should expect no better than a linear bound on δ_m . Choose some M' and choose k so that $\delta_{k-1} < \frac{M'}{m}$ and $\delta_k \geq \frac{M'}{m}$. Such k exists for all $M' \leq M$. Then $\frac{M_2}{m^2} \leq \delta \frac{M_2}{M'}$ and

$$\delta_{i+1} \leq \delta_i \left(1 + \frac{M_1 + M_2/M'}{m}\right)$$

for all $i > k$.

$$\delta_m \leq \delta_{k+1} \left(1 + \frac{M_1 + M_2/M'}{m}\right)^{m-k-1} \leq \delta_{k+1} \left(1 + \frac{M_1 + M_2/M'}{m}\right)^m \leq \delta_{k+1} e^{M_1 + M_2/M'}$$

$$\text{Since } \delta_k < \frac{M'}{m} \quad \delta_{k+1} \leq \frac{M'}{m} \left(1 + \frac{M_2}{m}\right) + \frac{M_2}{m^2}$$

$$\delta_m \leq \frac{M'}{m} \left(1 + \frac{M_2}{m}\right) + \frac{M_2}{m^2} e^{M_1 + M_2/M'}$$

The last expression attains a minimum at $M' = M_2$. Altogether, the error can be majorated by $\frac{C_1}{m} + \frac{C_2}{m^2}$ or by $\frac{C}{m}$. \square

We now have to show convergence of x_τ^n as $n \rightarrow \infty$. To do that observe that the probability density of a Markov jump process having sufficient regularity satisfies a linear integral equation

$$\frac{\partial p(x, t)}{\partial t} = \int_{-\infty}^{\infty} K(x, y)p(y)dy \quad (\text{C.3})$$

where $K(x, y)$ tells about the probability of a jump from point y to a neighbourhood of point x . Suppose there exists a finite or countable set Ω such that both initial distribution and the kernel of the integral operator are concentrated at these points, then the solution of equation C.3 will be also concentrated in these points. Then we can search for solutions in the form

$$p(x, t) = \sum_{\omega \in \Omega} c_{\omega}(t) \delta(x_{\omega}) \quad (\text{C.4})$$

the kernel is of the form

$$K(x, y) = \sum_{\omega, \omega' \in \Omega} a_{\omega\omega'} \delta(x_{\omega}) \quad (\text{C.5})$$

After substituting this into C.3 it splits into a system of ordinary differential equations for the coefficients c_n which is exactly the Kolmogorov system for a corresponding Markov chain.

$$\dot{c}_{\omega}(t) = \sum_{\omega' \in \Omega} a_{\omega, \omega'} c_{\omega'}(t) \quad (\text{C.6})$$

Suppose that the sequence of kernels K_n converges (weakly) to a kernel \hat{K} , which now doesn't need to be a combination of delta-functions. Suppose that $p_n(x, t)$ and $\hat{p}(x, t)$ are solutions of eq. C.3 corresponding to kernels K_n and \hat{K} . then they satisfy integral equations

$$p_n(x, t) = p_n(x, 0) + \int_0^t \int_{-\infty}^{\infty} K_n(x, y) p_n(y) dy dt$$

and

$$\hat{p}(x, t) = \hat{p}(x, 0) + \int_0^t \int_{-\infty}^{\infty} \hat{K}(x, y) \hat{p}(y) dy dt$$

$$\begin{aligned} & \|p_n(x, t) - \hat{p}(x, t)\| = \\ & = \left\| p_n(x, 0) - \hat{p}(x, 0) + \int_0^t \int_{-\infty}^{\infty} (K_n(x, y) p_n(x, \tau) - \hat{K}(x, y) \hat{p}(y, \tau)) dy d\tau \right\| \leq \\ & \leq \|p_n(x, 0) - \hat{p}(x, 0)\| + \\ & \left\| \int_0^t \int_{-\infty}^{\infty} (K_n(x, y) p_n(x, \tau) - K_n(x, y) \hat{p}(y, \tau) + K_n(x, y) \hat{p}(y, \tau) - \hat{K}(x, y) \hat{p}(y, \tau)) dy d\tau \right\| \leq \\ & \leq \|p_n(x, 0) - \hat{p}(x, 0)\| + \int_0^t (\|K_n\| \|p_n(x, \tau) - \hat{p}(x, \tau)\| + \|K_n - \hat{K}\| \|\hat{p}(x, \tau)\|) d\tau \end{aligned} \quad (\text{C.7})$$

$$\|p_n(x, t) - \hat{p}(x, t)\| \leq \|K_n\| \int_0^t \|p_n(x, \tau) - \hat{p}(x, \tau)\| d\tau + \|\hat{p}(x, t)\| \|K_n - \hat{K}\| t + \|p_n(x, 0) - \hat{p}(x, 0)\|$$

and noticing that $\|\hat{p}\|$ and $\|K_n\|$ are bounded by 1

$$\|p_n(x, t) - \hat{p}(x, t)\| \leq \int_0^t \|p_n(x, \tau) - \hat{p}(x, \tau)\| d\tau + \|K_n - \hat{K}\| t + \|p_n(x, 0) - \hat{p}(x, 0)\|$$

The Gronwall inequality says that whenever $z(t) \geq 0$ and satisfies

$$z(t) \leq c \int_0^t z(\tau) d\tau + b$$

then

$$z(t) \leq be^{ct}$$

Applying this to the previous estimate with $z(t) = \|p_n(x, t) - \hat{p}(x, t)\| + \|K_n - \hat{K}\|$ we arrive at

$$\|p_n(x, t) - \hat{p}(x, t)\| \leq \|p_n(x, 0) - \hat{p}(x, 0)\| e^t + \|K_n - \hat{K}\| (e^t - 1)$$

the estimate is valid for $t < h_1$, i.e. in the interval when the process is Markov. The same reasoning can be applied to consequent intervals. For a time partition with $\Delta = \frac{1}{m}$ the deviation δ_i between \hat{p} and p_n at point $t = h_i$ will satisfy recurrent relation

$$\delta_{i+1} = \delta_i e^{\frac{1}{m}} + \|K_n - \hat{K}\| (e^{\frac{1}{m}} - 1)$$

In analogy with Lemma 2.2 it can be shown that $\delta_m = O(\|K_n - \hat{K}\|)$.

So we see that the deviation between our 'piecewise-Markov' chain and its limiting process, which should correspond to the true physical situation is $O(\frac{1}{m}, \|K_n - \hat{K}\|)$. The rate of convergence of the operator K_n is however hard to estimate analytically, thus the required number of states of the chain should be understood from the numerical experience.

Bibliography

- [1] I. Agapov, G. Hoffstätter, E. Vogel, Bunched beam echo in HERA-p , proc. EPAC 2002
- [2] I. Agapov, F. Willeke, A more accurate approach to calculating proton bunch evolution under influence of intrabeam scattering in proton rings, proc. EPAC 2004
- [3] S. Albeverio, A. Klar, Longtime Behaviour of Nonlinear Stochastic Oscillators *J. Math. Phys.* 35(8), 4005-4027, 1994
- [4] S. Albeverio, A. Klar, Longtime Behaviour of Stochastic Hamiltonian Systems *Potential Analysis* 12, 281-297, 2000
- [5] V. Arnold, *Mathematical methods of classical mechanics*, Nauka 1979
- [6] R. Bellman et al., *Numerical inversion of the Laplace transform: applications to biology, economics, engineering, and physics*. American Elsevier, 1966.
- [7] C. Bernardini et. al., *Phys. Rev. Lett.* 10 (1963), p. 407
- [8] D. Boussard, G. Dome, C. Graziani, The influence of RF noise on the lifetime of proton bunched beams, Geneva 1980, *Proceedings, High energy Accelerators* pp 620-626
- [9] J. Bjorken, S. Mtingwa, *Intrabeam Scattering, Particle Accelerators* 1983 13, pp 115-143
- [10] K. Chang, F. Howes , *Nonlinear Singular perturbation Phenomena: Theory and Application*. Springer, 1984.
- [11] A. Chao, M. Tigner, *Handbook of Accelerator Physics and Engineering*, World Scientific 1999
- [12] B. Chirikov, A universal instability of many-dimensional oscillator systems, *Phys. Rep.* 52, 263 1979
- [13] P. Ciarlet, J. Lions, *Handbook of numerical analysis*, vol. 1,2, North-Holland 1991
- [14] I. Cornfeld, S. Fomin, Y. Sinai, *Ergodic theory*, Springer, 1982
- [15] R. Courant, D. Hilbert, *Methodods of mathematical physics*, Interscience Publishers, 1953
- [16] E. Courant and H. Snyder, Theory of Alternating-Gradient synchrotron, *Annals of Physics* 1958 3, pp 11-48
- [17] G. Dome, Theory of RF Acceleration and RF noise, CERN SPS/84-14
- [18] J. Le Duff, Single and multiple Touschek effect, CERN Accelerator School 1987.
- [19] K. Ehret et. al., Observation of coasting beam at the HERA proton ring, *Nuclear Instruments A* 456 (2001), pp 206-216

-
- [20] L. Evans, B. Zotter, Intrabeam scattering in the SPS, CERN/SPS/80-15
- [21] W. Feller, An Introduction to Probability Theory and Its Applications, vol. 1, 2, Wiley, 1957-1968.
- [22] M. Freidlin, A. Wentzell, Random perturbations to dynamical systems, Springer 1984
- [23] L. Gammaitoni et. al., Stochastic resonance, Reviews of modern Physics v. 70 1, 1998
- [24] W. Gardiner, Handbook of stochastic methods for physics, chemistry and the natural sciences. 2nd ed. Springer, 1985.
- [25] A. Gerasimov, Phase convection and distribution tails in periodically driven brownian motion, Physica D 41 1990, 89-131
- [26] A. Gerasimov, Random driving of nonlinear oscillator, Phys. Rev. E 49 5 1994, 3881-3887
- [27] G. Giacaglia, Perturbation methods in non-linear systems. Springer, 1972.
- [28] M. Gihman, A. Skorohod, Asymptotic methods in stochastic differential equations, Nauka
- [29] M. Gihman, A. Skorohod, The Theory of random processes, v. 1,2, Springer 1974-1975
- [30] K. Hirata, K. Yokoya, Non-Gaussian distribution of electron beams due to incoherent stochastic processes, Particle Accelerators 1992 39, pp. 147-158
- [31] A. Hofmann, S. Myers, Beam dynamics in a double RF system, CERN ISR-TH-RF/80-26
- [32] S. Ivanov, O. Lebedev, Coasting beam in HERA-p ring, DESY HERA 01-03
- [33] S. Ivanov, O. Lebedev, Noise performance studies at the HERA-p Ring, DESY HERA 03-02
- [34] E. Kamke, Differentialgleichungen: Gewoehnliche Differentialgleichungen , Geest & Portig 1962
- [35] I. Karatzas, S. Shreve. Brownian motion and stochastic calculus. Springer, 1988
- [36] T. Kato, Perturbation theory for linear operators. Springer, 1966.
- [37] R. Khasminskii, A limit theorem for the solutions of differential equations with random right-hand sides, Theory of probability and its applications , 1966, XI pp 390-406
- [38] R. Khasminskii, On stochastic processes defined by differential equations with a small parameter, Theory of probability and its applications, 1966, XI pp 390-406
- [39] A. Kolomensky, A. Lebedev, The theory of cyclic Accelerators, North-Holland 1966
- [40] S. Krinsky, J. Wang, Bunch diffusion due to RF noise, Part. Accel. 12 1982, pp 107-117
- [41] L. Landau, E. Lifshitz, Mechanics, Pergamon 1960
- [42] L. Landau, E. Lifshitz, The classical theory of fields, Pergamon
- [43] E. Lifshitz, L. Pitaevskii, Physical kinetics, Pergamon 1981
- [44] V. Lebedev, S. Nagaitsev, Particle diffusion due to Coulomb Scattering, proc. EPAC 2002.
- [45] A. Lichtenberg, M. Lieberman, Regular and stochastic motion, Springer 1983.
- [46] Y. Mori, Intrabeam scattering in stochastic approach, KEK Report 90-14

-
- [47] Y. Mizumachi, Partial linearization of the RF voltage of a storage ring to reduce bunch diffusion, KEK Preprint 80-20
- [48] A. Pauluhn, Stochastic beam dynamics in storage rings, DESY 93-198
- [49] A. Piwinski, Intra-beam scattering, proc 9th Conf. on High Energy Accelerators 1974, p. 405
- [50] A. Piwinski, Intra-beam scattering in presence of linear coupling, DESY 90-113
- [51] A. Piwinski, The Touschek effect in strong focusing storage rings, DESY 98-179.
- [52] H. Risken, The Fokker-Planck equation: Methods of solution and applications, Springer, 1996.
- [53] M. Sands, The physics of electron storage rings, an introduction, SLAC-121 UC-28
- [54] M. Seidel, The proton collimation system of HERA, PhD thesis, DESY 94-103
- [55] R. Stratanovich, Topics in the theory of random noise, v. 1,2, Gordon and Breach 1963-1967
- [56] G. Stupakov, S. Kauffmann, Echo Effect in Accelerators, SSCL-587 (1992)
- [57] J. Tennyson, Resonance transport in near-integrable systems with many degrees of freedom, Physica D, 1982, 123-135
- [58] M. Zorzano, R. Wanzenberg, Intrabeam scattering and the coasting beam in the HERA proton ring, DESY HERA 00-06
- [59] H. Wiedemann, Particle Accelerators v. 1,2, Springer 2003
- [60] K. Wille, The Physics of Particle Accelerators, Oxford University Press 2000
- [61] F. Willeke, Beam dilution in proton storage rings, proc. JAS 2000.
- [62] F. Willeke, G. Ripken, Methods of beam optics, DESY 88-114
- [63] M. Venturini, Intrabeam scattering and wake fields in low emittance electron rings, SLAC-PUB-9355
- [64] Jie Wei, private communications
- [65] E. Vogel, Fast Longitudinal diagnostics for the HERA proton Ring, PhD thesis, DESY 2001
- [66] E. Vogel, RF amplitude modulation to suppress longitudinal coupled bunch instabilities in the SPS, proc. EPAC 2004
- [67] C. Zhou, J. Kurths, Resonant patterns in noisy active media, Phys. Rev. E 69 2004, 056210
- [68] www.desy.de/f/hera/, Travelling to the heart of matter with HERA

Acknowledgements

I want to thank Ferdinand Willeke, George Hoffstätter and Ursula van Rienen for supervising my PhD work. I am grateful to Vladimir Balandin, Helmut Mais, Nina Golubeva, Mathias Vogt, Elmar Vogel, Desmond Barber, Markus Hoffmann, Michiko Minty, Rainer Wanzenberg, Susan Wipf, Mark Lomperski, Bernard Holzer, Jie Wei, Valery Lebedev, Sergei Ivanov and some other people whom I might have forgotten for valuable discussions and support. Special thanks go to my family.